California Environmental Protection Agency

Air Resources Board

Air Quality Impacts of the Use of Ethanol in California Reformulated Gasoline

Appendix B

Photochemical Modeling

December 1999

Table of Contents

List of Tables

List of Figures

B-1. Introduction

This appendix describes the air quality simulations performed in support of the analysis of the potential impact on air quality caused by the phase-out of gasoline containing methyl *tertiary*-butyl ether (MTBE) and replacement by ethanol-based or non-oxygenated fuels. It is important to bear in mind that the model results for this study are being used in a relative, rather than absolute sense. That is, the model was used to estimate the change from 1997 MTBE gasoline to ethanol-containing and non-oxygenated gasolines in 2003, rather than to predict absolute values in 2003. The estimated changes were then used to adjust the base year (1997) air quality measurements to future (2003) concentrations, as described in Appendix C. The modeling community is in general agreement that models are best used in a relative sense.

In the sections that follow a brief description of the air quality model is presented together with the photochemical mechanism chosen. A description of the input files necessary to run each of the scenarios considered is presented, together with a summary of the results. A discussion of sensitivity simulations and model performance is included. An analysis of the sensitivity of ozone, PAN, and PPN under a wide variety of conditions was conducted with a box model.

B-2. Photochemical Model Description

Photochemical air quality modeling is a primary tool for understanding the complex interrelationships among pollutants emitted and transported in a given area. Photochemical air quality models are computer models that represent the state-of–the-science understanding of how ozone and other secondary pollutants are formed and the relationship to the primary pollutants emitted by different source categories. They have been used to assess the effectiveness of air pollution control strategies to achieve the air quality standards. The Flexible Chemical Mechanism Version of the Urban Airshed Model (UAM-FCM) is an air quality model that has been used by ARB since 1995.

The UAM-FCM is an adaptation of the Urban Airshed Model (UAM) to provide flexibility in incorporating different Carbon Bond IV or SAPRC-type photochemical mechanisms into the UAM (Kumar *et al.,* 1995). The UAM has been the primary air quality regulatory model for ozone control strategy development. However, it has a hard-coded a version of the Carbon Bond IV photochemical mechanism, together with a unique algorithm to solve the set of differential equations representing the chemical transformations that is accurate, robust and fast. The algorithm was designed to take maximum advantage of the Carbon Bond IV features. The treatment of photolytic reactions in the UAM is also unique. All values for the photolytic reaction rates are hard-coded, and depend on the value of the NO_2 photolytic reaction rate. The hard-coded approach in the UAM makes it very difficult to study recent and more updated mechanisms, such as those developed by Dr. W.P.L. Carter at the University of Riverside. Any change or update in the Carbon Bond IV mechanism, photolytic rates, or the implementation of a different chemical mechanism requires changes to the UAM

code that need to be done by hand. However, the UAM-FCM can read a text file version of a mechanism and create program subroutines that are readily integrated with the model (Kumar *et al.*, 1995). Below we briefly describe the main aspects of the UAM and the UAM-FCM.

B-2.1. Urban Airshed Model

Morris and Meyers (1990) provide a detailed description of the UAM. Only a brief summary is provided here. The UAM is a gridded 3-dimensional air quality model that can simulate the atmospheric physical and chemical processes that cause air pollution. The basic advection-diffusion equation is:

$$\frac{\partial C_i}{\partial t} + \frac{\partial (uC_i)}{\partial x} + \frac{\partial (vC_i)}{\partial y} + \frac{\partial (wC_i)}{\partial z} = \frac{\partial}{\partial x}(K_H \frac{\partial C_i}{\partial x}) + \frac{\partial}{\partial y}(K_H \frac{\partial C_i}{\partial y}) + \frac{\partial}{\partial z}(K_V \frac{\partial C_i}{\partial z})$$

$$+ R_i + S_i + L_i \qquad \text{(B-1)}$$

The first term on the left-hand side of Equation (1) represents the time-varying concentration of pollutant i, and the last three terms on the left-hand side of Equation (1) represent advection. The first three terms on the right-hand side of Equation (1) represent turbulent diffusion, R_i are chemical reaction processes, S_i are emission source processes, and L_i correspond to losses by deposition. The other terms in Equation (1) are the horizontal and vertical wind speed components -- u, v, and w -- and the horizontal and vertical diffusivity coefficients, K_H and K_V . Equation (1) is solved for each pollutant and grid cell at each time step in the simulation. As designed, the UAM has hard-coded a version of the Carbon Bond IV (CB4) chemical mechanism. The CB4 version implemented in the UAM was last updated in 1993 by adding radical-radical interactions. The hard-coded approach to the atmospheric chemical mechanism used in the UAM prevents the implementation of newer and more up-to-date chemical mechanisms.

B-2.2. Flexible Chemical Mechanism Version of the Urban Airshed Model

The UAM-FCM was developed under contract for ARB (Kumar *et al.*, 1995). The UAM-FCM has a software package (the FCM) that reads a text file describing the photochemical mechanism, and creates a set of mechanism-specific programs that are then integrated into the UAM. The FCM allows the user to incorporate reaction-specific photolytic rates, by providing a file for each photolytic reaction, with data on cross-section and quantum yield for each wavelength of interest. The UAM-FCM has a generalized technique to solve the set of differential equations that is not mechanism specific, but is accurate and robust. The current version of the UAM-FCM can handle up to 220 chemical reactions (including up to 20 photolytic reactions), and up to 140 chemical species.

B-2.3. SAPRC97 Chemical Mechanism

Carter (1993, 1997) developed the atmospheric chemical mechanism designated as SAPRC97 (version D), which is readily processed by the UAM-FCM software. To save computing time in solving the set of differential equations that represent the reaction mechanism, only a small number of hydrocarbon species are treated explicitly in this mechanism. In the SAPRC series of mechanisms, hydrocarbons are grouped together using the lumped-molecule approach. In this approach the reactions of many alkanes, alkenes, and aromatic species that are present in the emission inventory are represented by lumped reaction mechanisms (Carter, 1990). The computer software calculates the kinetic rates and product yield parameters for the lumped species that best represent the unique hydrocarbon mixture in the emission inventory (Carter, 1988; Carter 1990). For this study the one-product mechanism is used to represent the reactions of isoprene (Carter, 1996). In addition, explicit reaction mechanisms (as opposed to a lumped representation) for several compounds of interest (such as benzene, 1,3-butadiene, ethanol, and methyl *tertiary*-butyl ether) were added to the original version of the SAPRC97. It was also desired to distinguish between acetaldehyde and formaldehyde formed as by-products of photochemical reactions (secondary), from those emitted directly from sources (primary). The explicit reactions for the additional species were obtained from Dr. Carter's ftp site (ftp://cert.ucr.edu/pub/carter/mech/saprc97).

A complete listing of this photochemical mechanism is provided in the Attachment B-1. The list of hydrocarbon species that are treated explicitly is given in Table 2.1. Note that in the SAPRC97 chemical mechanism, PPN is used to lump peroxypropionyl nitrate and higher molecular weight acyl peroxy nitrates. Thus, modeled PPN cannot be compared directly with measured PPN. In addition to the species listed in Table 2.1, the photochemical mechanism includes a large number of species that are generated by the oxidation of hydrocarbons, as well as a set of chemical reactions that represents the inorganic reactions that take place in air. The mechanism used in our simulations has a total of 99 species and 204 reactions, of which 20 are photolytic. Of the 99 species, 29 are treated as steady state, 4 species are held constant, and hourly average concentrations are generated by the UAM-FCM for the other 66 species.

Table 2.1 List of Hydrocarbon Species Treated Explicitly in SAPRC97

Name	Symbol
Formaldehyde (secondary)	**HCHO**
Formaldehyde (primary)	**FORM**
Acetaldehyde (secondary)	**CCHO**
Acetaldehyde (primary)	**ALD**
Acetone	**ACET**
Methyl ethyl ketone	**MEK**
Peroxyacetyl nitrate	**PAN**
Peroxypropionyl nitrate and higher molecular weight acyl peroxy nitrates	**PPN**
Methane	**CH4**
Ethene	**ETHE**
Isoprene	**ISOP**
Benzene	**C6H6**
1,3-Butadiene	**BUTD**
***p*-Dichlorobenzene**	**PDCB**
Perchloroethylene	**PERC**
Dichloromethylene	**DICM**
Ethanol	**ETOH**
Methyl *tertiary*-butyl ether	**MTBE**
Glyoxal	**GLY**
Methyl Glyoxal	**MGLY**
Benzaldehyde	**BALD**
Cresols	**CRES**
Phenols	**PHEN**

B-2.4. Computer

The executable UAM-FCM files were prepared and compiled according to the recommended procedure by Kumar *et al.* (1995). The emission inventory corresponding to each year and case under study were used to calculate the reaction rates and product yields of the lumped species. All simulations were run on a Unix workstation. The time to run a 24-hour episode simulation was about 2 hours and twenty minutes.

Figure 2.1 Modeling Domain

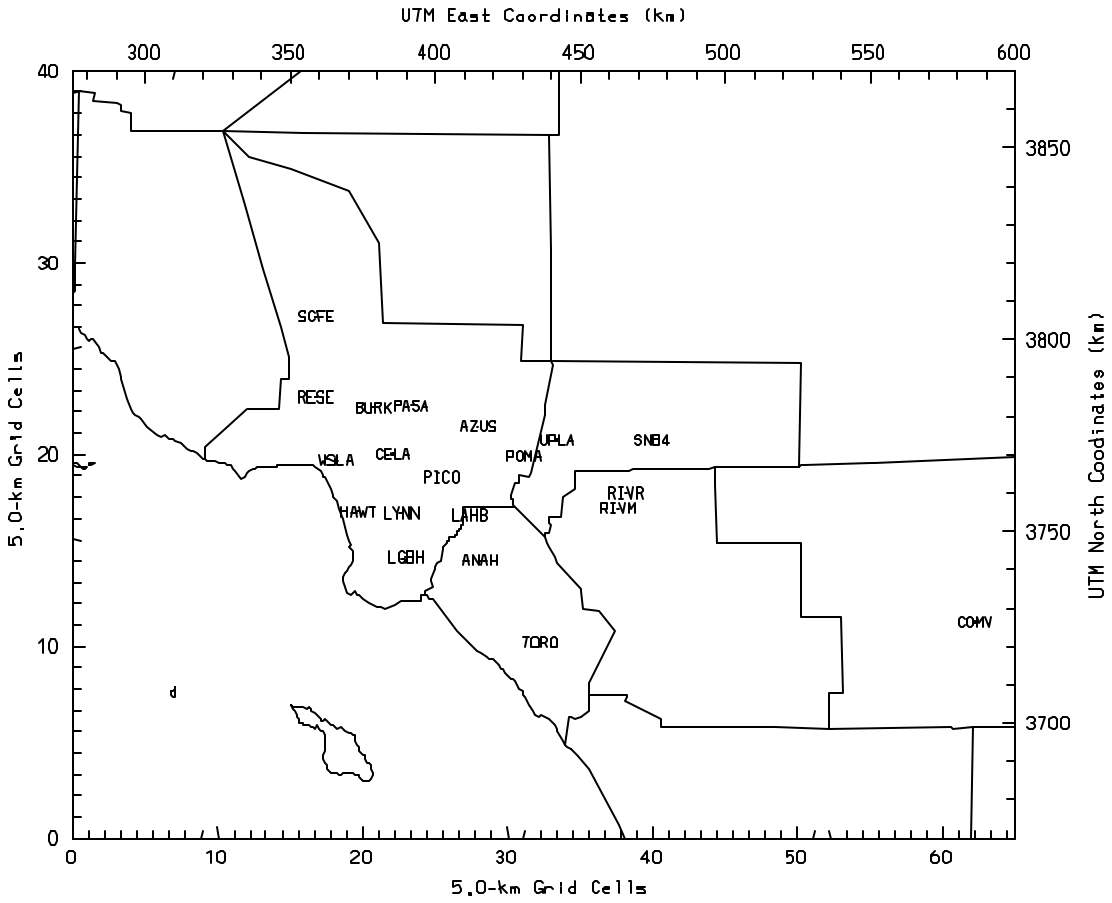

B-3. Model Input Description

B-3.1. Episode and Domain

The UAM-FCM was applied to a three-day summer ozone episode in the South Coast, the August 26-28, 1987 Southern California Air Quality Study (SCAQS) episode (Lawson, 1990). The SCAQS domain has been gridded into 65 x 40 x 5 cells. Each horizontal square cell is 5 x 5 km^2, with varying vertical height. The origin of the domain is at (275, 3670) in UTM coordinates (Zone 11). The domain is shown in Figure 2.1. It includes the counties of Los Angeles, Orange, and Kern, and portions of Riverside, San Diego, San Bernardino, and Ventura counties.

The August 26-28, 1987 SCAQS episode corresponds to an episode with very high observed ozone concentrations. We believe that the meteorological conditions of the episode represent close to worst-case conditions conducive to high pollutant concentrations. The SCAQS domain also contains a large fraction of the population in the State. Therefore, this episode and domain also represent worst-case conditions for exposure analysis of photochemically generated pollutants (e.g., ozone, NO_2, acetaldehyde, formaldehyde, PAN and PPN). For these reasons we believe that modeling of this single episode is sufficient for our study. Therefore, the meteorology of the August 26-28, 1987 SCAQS episode will be used in conjunction with the VOC and NO_x emissions appropriate for the year 1997, and 2003 scenarios described in Table 3.2. Worst-case conditions for directly emitted pollutants (e.g., CO, benzene, 1,3-butadiene, ethanol, and MTBE) are more readily inferred from air quality measurement (see Appendix C).

B-3.2. Basic Input Files

The UAM-FCM requires 13 input files that provide information on the initial and boundary conditions of the domain, temperature, wind direction, wind speed, terrain, photolytic rates, reaction rate constants, and product yields, and emissions from area and point sources. Mobile sources and biogenic emissions are included in the area source file. The files used in our simulations, (except for the initial and boundary conditions, and area and point source emissions) were prepared by the South Coast Air Quality Management District for the 1994 State Implementation Plan (SCAQMD, 1994). The same diffusion break, region top, metscalars, terrain, temperature, and meteorological input files were used in all simulations, since these characterize the meteorological conditions for the episode and terrain. Table 3.1 provides a description of these files. Other files, such as initial and boundary conditions, point sources and area emissions were created for each specific simulation.

Table 3.1 List of the Meteorological and Terrain Files for the SCAQS August 26-28, 1987 Episode

Input File Identification	Description
ms238d11.b, ms239d11.b, ms240d11.b	Metscalar file
sim238bl, sim239bl, sim240bl	Control file
df238d11.b	Diffusion break file
tm238d11.b, tm239d11.b, tm240d11.b	Temperature file
rt238d11.b	Region top file
tr238d11.b	Terrain file
wd238d11.b, wd239d11.b, wd240d11.b	Wind file

B-3.3. Region Top and Boundary Conditions

The region top and boundary conditions (together with the point and area sources) are specific to each of the different scenarios considered in this modeling study. The scenarios considered include the years 1997 and 2003 with different types of gasoline. These scenarios are listed in Table 3.2.

Table 3.2 Scenarios Considered for the Photochemical Modeling

Scenario	Description of Motor Vehicle Fuel Used
1997 MTBE	Current MTBE-based California Phase 2 Reformulated Gasoline (CaRFG)
2003 MTBE	Year 2003 MTBE-based CaRFG
2003 Et2.0%	Year 2003 Ethanol-based fully complying fuel (with oxygen content of 2.0 wt%)
2003 Et3.5%	Year 2003 Ethanol-based fully complying fuel (with oxygen content of 3.5 wt%)
2003 NonOxy	Year 2003 Non-oxygenated fully complying fuel

The region top and boundary condition files describe the air quality at the boundaries of the domain under study. These two files specify hourly ambient levels of each of the species in the SAPRC mechanism. For these simulations the region top and boundary conditions were treated as constant for all species throughout the episode. Region top concentrations were essentially the same as those used for the boundary conditions. Table 3.3 and Table 3.4 show the pollutant concentrations used for the boundary and region top, respectively.

Table 3.3 Baseline Boundary Concentration (ppb)

Species	1997 MTBE	2003 MTBE	2003 Et2.0%	2003 Et3.5%	2003 NonOxy
O3	40.0	40.0	40.0	40.0	40.0
NO	0.9095	0.8285	0.8285	0.8285	0.8285
NO2	1.6832	1.4	1.4	1.4	1.4
N2O5	1.0	1.0	1.0	1.0	1.0
HONO	0.08371	0.06913	0.06913	0.06913	0.06913
CO	200.0	200.0	200.0	200.0	200.0
CO2	1000.0	1000.0	1000.0	1000.0	1000.0
CCHO	0.5	0.53	0.53	0.53	0.53
HCHO	0.5	0.5	0.5	0.5	0.5
RCHO	0.98	0.98	0.98	0.98	0.98
ETHE	0.829	0.7626	0.7626	0.7626	0.7626
CH4	1720.0	1720.0	1720.0	1720.0	1720.0
ALK1	0.49	0.49	0.49	0.49	0.49
ALK2	1.01	1.01	1.01	1.01	1.01
ARO1	0.4273	0.3962	0.3962	0.3962	0.3962
ARO2	0.14507	0.13538	0.13538	0.13538	0.13538
OLE1	0.7048	0.69056	0.69056	0.69056	0.69056
OLE2	0.01	0.01	0.01	0.01	0.01
C6H6	0.08	0.08	0.08	0.08	0.08
NO3	1.0	1.0	1.0	1.0	1.0
HO2	0.1	0.1	0.1	0.1	0.1
MTBE	0.1	0.1	0.01	0.01	0.01
ETOH	0.01	0.01	0.3	0.41	0.01
All other species	0.01	0.01	0.01	0.01	0.01

Table 3.4 Region Top Concentrations (ppb)

Species	1997 MTBE	2003 MTBE	2003 Et2.0%	2003 Et3.5%	2003 NonOxy
O3	40.0	40.0	40.0	40.0	40.0
NO	0.9095	0.8285	0.8285	0.8285	0.8285
NO2	1.6832	1.4	1.4	1.4	1.4
N2O5	1.0	1.0	1.0	1.0	1.0
HONO	0.08371	0.06913	0.06913	0.06913	0.06913
CO	200.0	200.0	200.0	200.0	200.0
CO2	1000.0	1000.0	1000.0	1000.0	1000.0
CCHO	0.5	0.53	0.53	0.53	0.53
HCHO	0.5	0.5	0.5	0.5	0.5
RCHO	0.98	0.98	0.98	0.98	0.98
ETHE	0.829	0.7626	0.7626	0.7626	0.7626
CH4	1720.0	1720.0	1720.0	1720.0	1720.0
ALK1	0.49	0.49	0.49	0.49	0.49
ALK2	1.0	1.0	1.0	1.0	1.0
ARO1	0.4218	0.3912	0.3912	0.3912	0.3912
ARO2	0.14507	0.13538	0.13538	0.13538	0.13538
OLE1	0.7048	0.69056	0.69056	0.69056	0.69056
OLE2	0.01	0. 01	0.01	0. 01	0. 01
C6H6	0.08	0. 08	0. 08	0. 08	0. 08
NO3	1.0	1.0	1.0	1.0	1.0
HO2	0.1	0.1	0.1	0.1	0.1
MTBE	0.1	0.1	0.01	0.01	0.01
ETOH	0.01	0.01	0.3	0.41	0.01
All other species	0.01	0.01	0.01	0.01	0.01

B-3.4. Initial Conditions

All simulations were started with the same initial conditions given in Table 3.5. Because of this, only the results of the last simulation day, August 28, are used in the analysis. The results of the last simulation day, based on our past experience, are insensitive to the initial conditions.

Table 3.5 Initial Species Concentrations (ppb)

Species	Concentration
O3	70.0
NO	1.0
NO2	2.0
HNO3	0.1
HONO	0.1
CO	200.0
CO2	0.1
H2O2	0.1
CCHO	1.1
HCHO	5.8
RCHO	0.98
ETHE	1.4
CH4	1720.0
ALK1	0.49
ALK2	1.01
ARO1	0.7
ARO2	0.23
OLE1	0.83
OLE2	0.23
OLE3	0.00
C6H6	0.16
All other species	0.01

B-3.5. Point and Area Sources

Point source emission and area source emission files were prepared for each specific scenario studied. The preparation of each file is discussed in Appendix A.

B-3.6. Air Quality Monitoring Sites

Table 3.6 lists the 20 air quality monitoring sites in the South Coast modeling domain used to analyze the results of each different scenario studied. In addition to these sites, the domain maximum was also used. Table 3.6 shows the site locations in the domain.

Table 3.6 Sites in the Modeling Domain Used to Study the Impact of Each of the Scenarios Studied

Site Name	Id
Anaheim	ANAH
Azusa	AZUS
Burbank	BURK
Los Angeles North Main	CELA
Costa Mesa - Mesa Verde Drive	COMV
Hawthorne	HAWT
La Habra	LABH
North Long Beach	LGBH
Lynwood	LYNN
Pasadena - S. Wilson Avenue	PASA
Pico Rivera	PICO
Pomona	POMA
Reseda	RESE
Riverside - Rubidoux	RIVR
Riverside - Magnolia	RIVM
Santa Clarita - County Fire Station	SCFE
San Bernardino - 4th Street	SNB4
El Toro	TORO
Upland	UPLA
West Los Angeles - VA Hospital	WSLA

B-4. Results

As indicated above, only the results of the third day of the episode simulated (August 28) were used in the analysis to avoid dependence on the initial conditions.

B-4.1. Domain Maximum 1-Hour-Average Concentrations

Table 4.1 shows the domain maximum concentration of the pollutants of interest for each scenario simulated. As shown in Table 4.1, the domain maximum ozone decreases (6 - 8%) from 1997 to 2003 because of reductions in overall emissions. CO shows a more significant decrease (25 - 35%). Nitric acid and ethanol both decrease by up to 9%. The maximum 1-hour-average ethanol concentration is dominated by a non-motor vehicle emission source. Although total ethanol emissions increase from 1997 to the

2003 ethanol-containing fuel scenarios, emissions from a single stationary source (which dominates the magnitude of the maximum ethanol concentration) have decreased. In general the predicted concentrations do not show a large change from 1997 to 2003 for most of the pollutants, except for NO, NO_2, CO, benzene, ethanol, and nitric acid.

Maximum ozone concentrations among the year 2003 simulations are very similar, within 1-2%. CO concentration is higher for the NonOxy scenario among the 2003 simulations, and is lowest for the Et3.5% scenario.

Table 4.1 Domain Maximum 1-Hour-Average Concentrations for Each Scenario

	Domain Maximum 1-Hour-Average Concentration (ppb)												
Simulation	**O_3**	**NO**	**NO_2**	**CO**	**Formaldehyde**	**Acetaldehyde**	**C_6H_6**	**BUTD**	**MTBE**	**ETOH**	**PAN**	**PPN**	**HNO_3**
1997 MTBE	**235.9**	**214.3**	**105.3**	**3,023.6**	**22.7**	**9.2**	**3.4**	**3.0**	**6.1**	**45.6**	**4.4**	**1.4**	**57.7**
2003 MTBE	**222.2**	**190.7**	**97.2**	**2,189.1**	**23.0**	**8.7**	**1.9**	**3.0**	**3.9**	**41.4**	**4.2**	**1.4**	**52.3**
2003 Et2.0%	**220.2**	**190.6**	**97.0**	**2,189.1**	**22.7**	**8.8**	**1.9**	**3.0**	**0.0**	**42.3**	**4.1**	**1.4**	**52.3**
2003 Et3.5%	**221.0**	**190.6**	**97.1**	**2,083.3**	**22.9**	**8.9**	**2.0**	**3.0**	**0.0**	**42.8**	**4.2**	**1.4**	**52.2**
2003 NonOxy	**220.4**	**190.6**	**97.0**	**2,262.6**	**22.7**	**8.8**	**1.9**	**3.0**	**0.0**	**41.4**	**4.0**	**1.4**	**52.4**

[a] **Formaldehyde and acetaldehyde refer to total concentrations from primary emissions and secondary formation, C_6H_6 is benzene, BUTD is 1,3-butadiene, MTBE is methyl *tertiary*-butyl ether, ETOH is ethanol, PAN is peroxyacetyl nitrate, PPN represents peroxypropionyl nitrate and higher molecular weight acyl peroxy nitrates, and HNO_3 is nitric acid.**

The model predicts a domain maximum 1-hour PAN concentration of 4.2 ppb and 4.1 ppb for the 2003 MTBE, and 2003 Et2.0% scenarios, respectively. The differences in predicted PAN concentrations for each scenario are due to differences in the emissions of various VOCs with higher PAN formation potentials than ethanol. From Table 4.9 in Appendix A, it is clear that the 2003 Et2.0% scenario has higher ethanol emissions than the 2003 MTBE. However, the 2003 MTBE has higher emissions of alkanes, aromatics, and olefins compared to the 2003 Et2.0%. Figure 7.3 and Figure 7.4 in later in the appendix suggest that the lumped species ALK2, ARO2, OLE1, OLE2, and OLE3 can have (depending on the environmental conditions) higher PAN formation potentials than ethanol. Another factor is that although ethanol emissions are higher in the 2003 Et2.0% scenario, they only represent 8% of the nonmethane VOC emissions. For comparison, ALK2, ARO2, OLE1, OLE2, and OLE3 comprise about 31% of the nonmethane VOC emissions in 2003 Et2.0%. Hence, PAN formation is primarily governed by the differences in alkane, aromatic, and olefinic emissions between scenarios, rather than the emissions of ethanol.

Figure 4.1 through Figure 4.5 show hourly the 1997 and 2003 scenarios for ozone, NO, and NO_2, at Anaheim (ANAH), Burbank (BURK), downtown Los Angeles (CELA), Riverside-Rubidoux (RIVR), and at the grid cell with the domain maximum (GMX). The time plots clearly show that the 1997 and 2003 scenarios have very similar predicted

ozone concentrations during the last day of the simulation. There are significant differences in predicted NO_2 concentrations between 1997 and 2003, as expected. All 2003 scenarios have the essentially the same predicted NO and NO_2 hourly concentrations.

Figure 4.6 through Figure 4.10 show ethanol, MTBE, and CO time series plots for Anaheim, Burbank, downtown Los Angeles, Riverside-Rubidoux, and at the grid with the domain maximum. The plots are only for the 2003 scenarios (Et2.0%, Et3.5%, NonOxy, and MTBE). As expected, the 2003 Et3.5% scenario has highest predicted ethanol concentrations, while the 2003 MTBE is the only scenario with significant MTBE hourly concentrations among all the 2003 scenarios.

Figure 4.11 through Figure 4.15 show time series plots of hourly PAN (and higher molecular weight acyl peroxy nitrates), and nitric acid concentrations for the 1997 and 2003 scenarios, at Anaheim, Burbank, downtown Los Angeles, Riverside-Rubidoux, and at the domain maximum. Predicted PAN, PPN, and nitric acid concentrations are the same for all 2003 scenarios. Both PAN and PPN show a large maximum on the second day of the episode that has significantly decreased by the third day of the episode simulated.

From Figure 4.1 through Figure 4.5, it is clear that although hydrocarbon and NO_X emissions decreased from 1997 to 2003, the reduction did not significantly impact the O_3, NO, and NO_2 levels predicted by the photochemical mechanism. This is confirmed by the small impact on the predicted maximum ozone concentrations. In addition, the NO_X-to-hydrocarbon ratio may not have significantly changed from 1997 to 2003, which may explain the essentially similar PAN, PPN (and higher molecular weight acyl peroxy nitrates), and nitric acid predicted concentrations for these years (see Figure 4.11 through Figure 4.15).

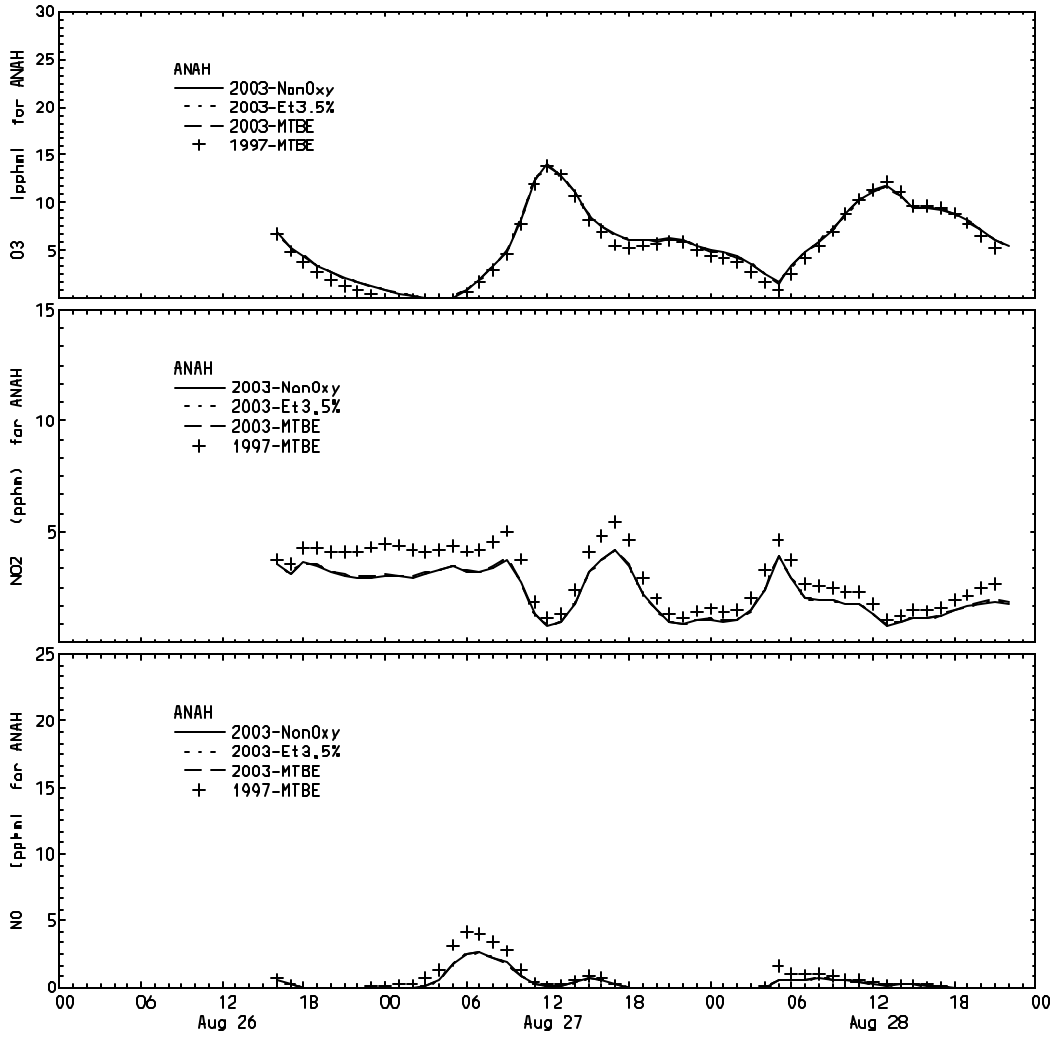

Figure 4.1 Time Series for Ozone, NO_2, and NO at Anaheim for 1997 and 2003 Scenarios

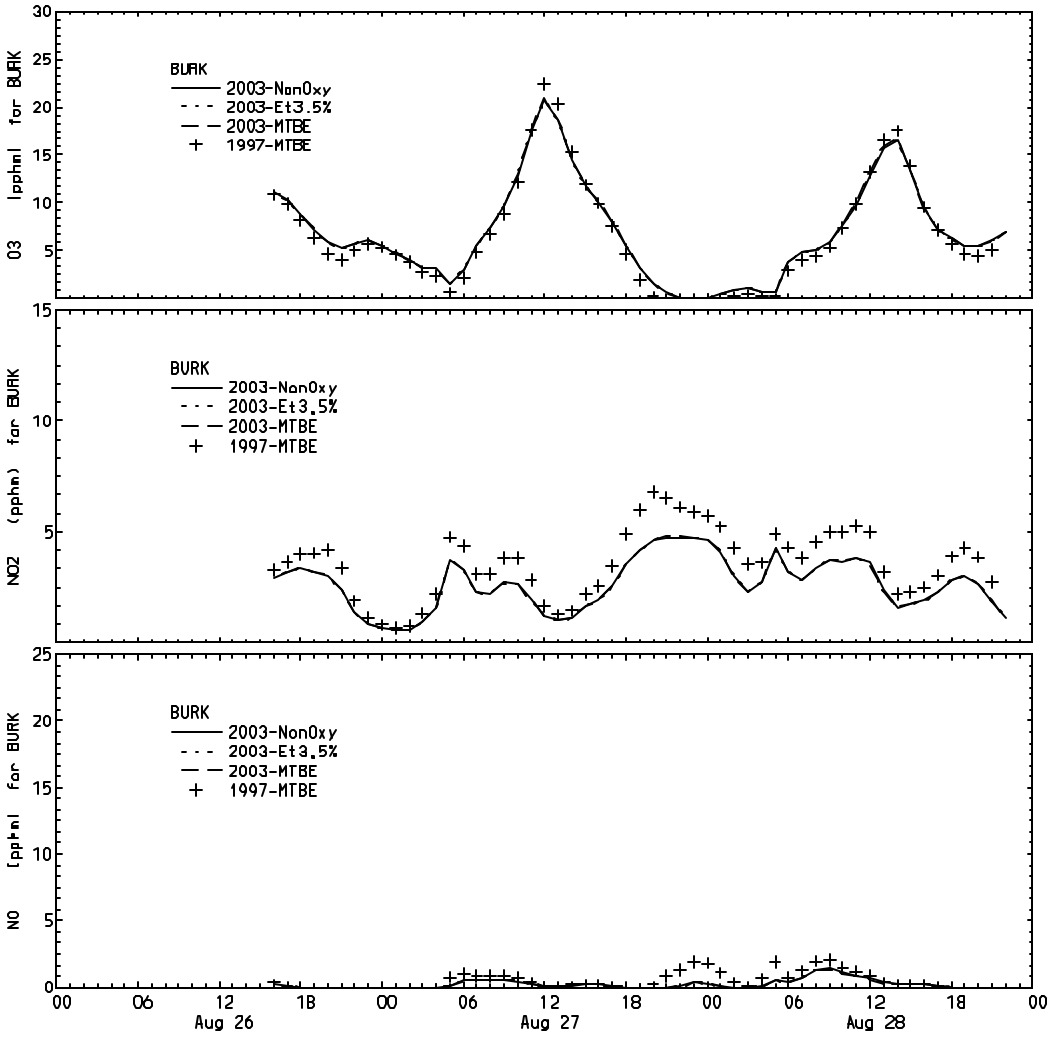

Figure 4.2 Time Series for Ozone, NO_2, and NO at Burbank for 1997 and 2003 Scenarios

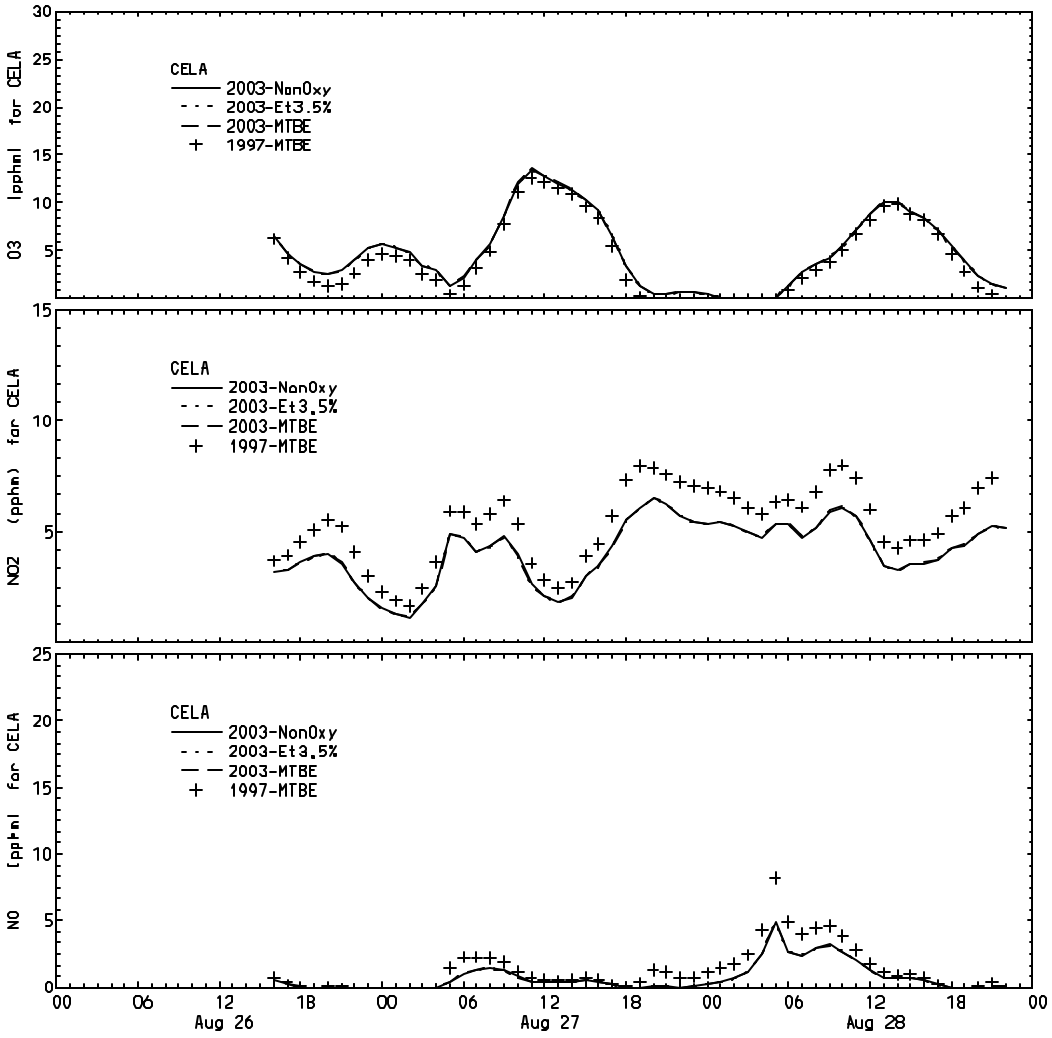

Figure 4.3 Time Series for Ozone, NO_2, and NO at Los Angeles for 1997 and 2003 Scenarios

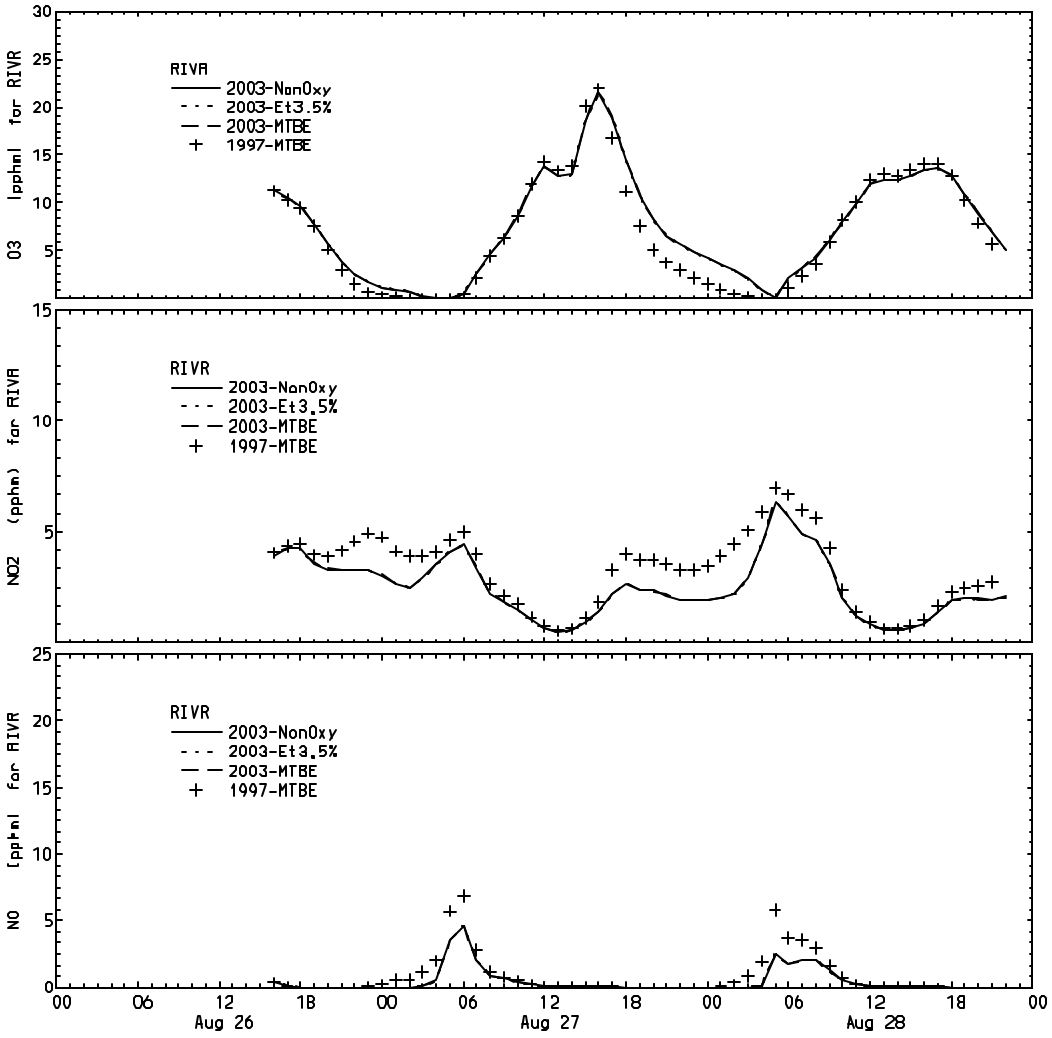

Figure 4.4 Time Series for Ozone, NO_2, and NO at Riverside for 1997 and 2003 Scenarios

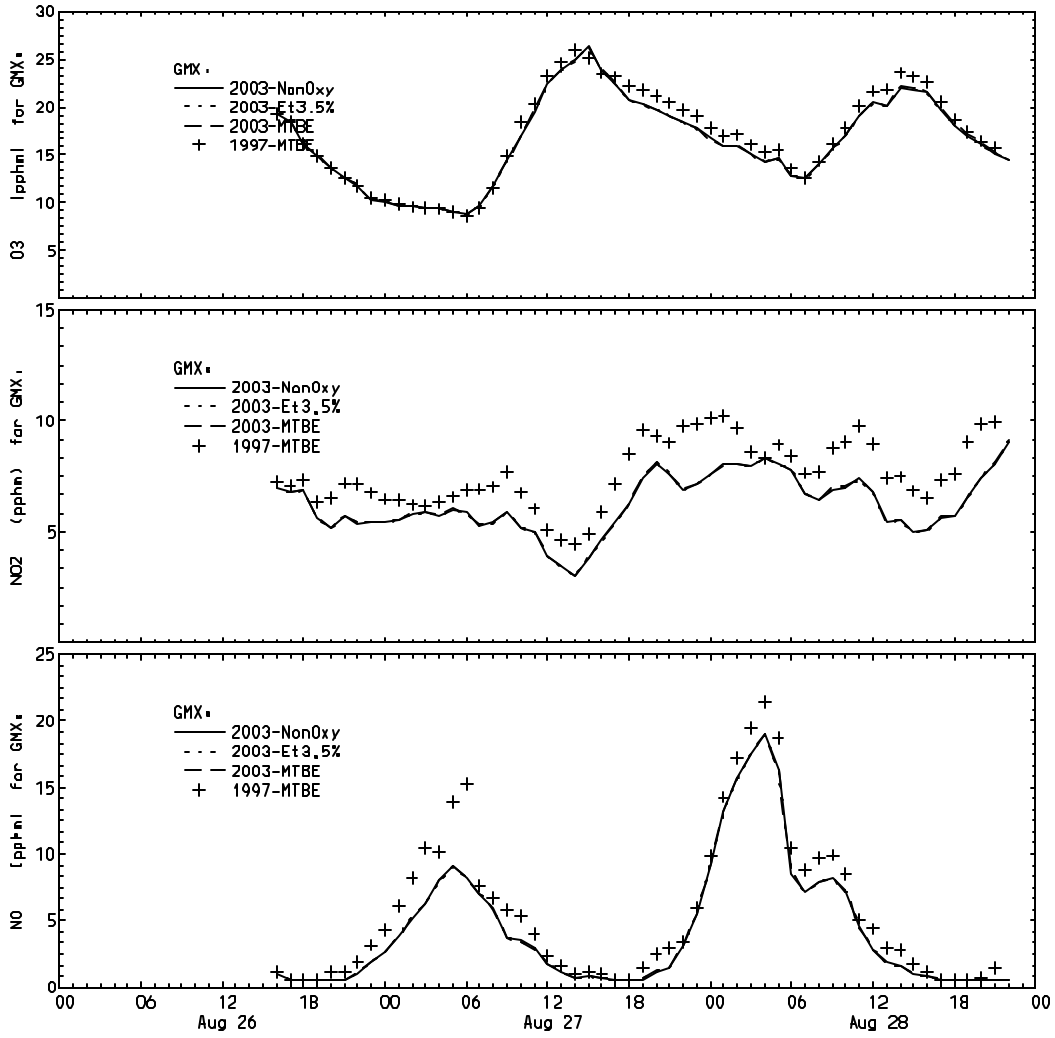

Figure 4.5 Time Series for Ozone, NO_2, and NO at Grid with Domain Maximum for 1997 and 2003 Scenarios

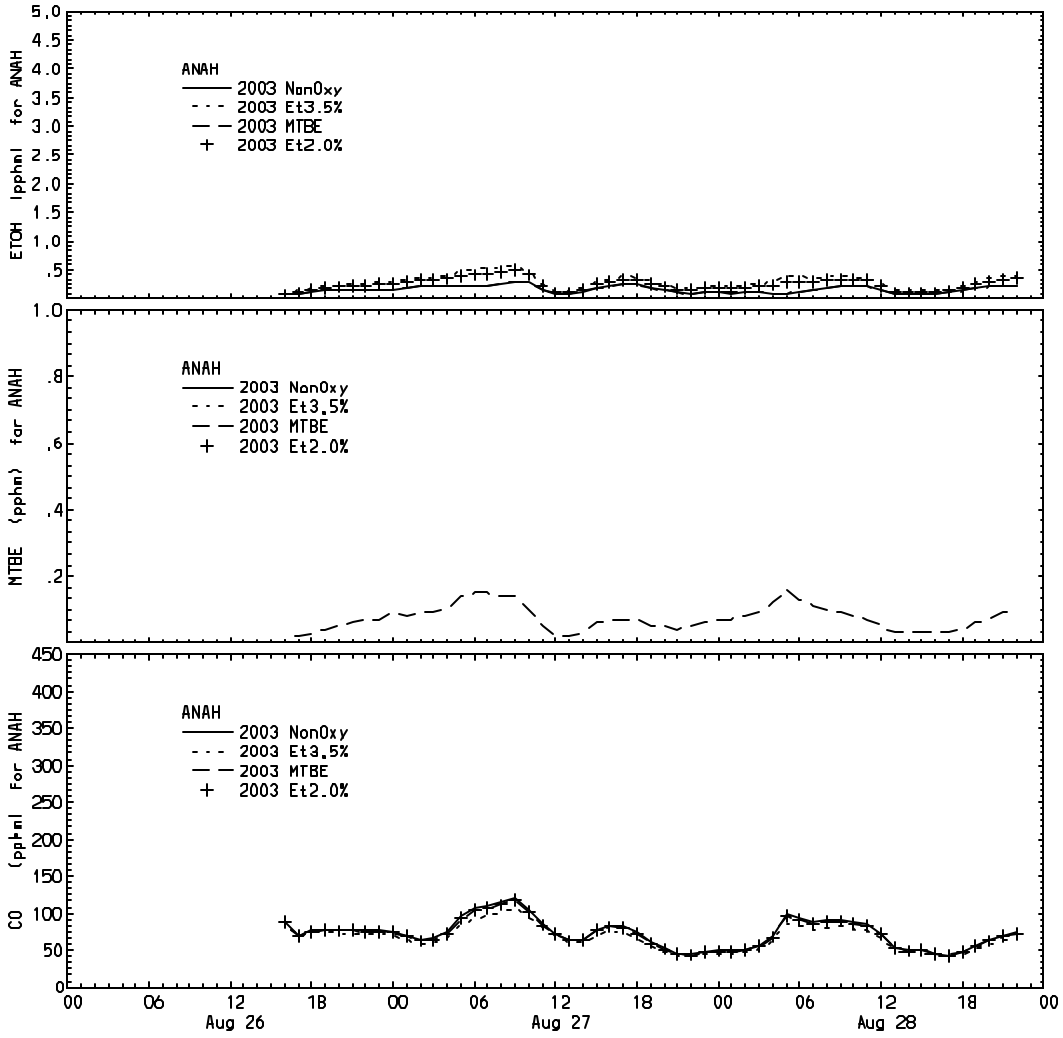

Figure 4.6 Time Series for MTBE, Ethanol, and CO at Anaheim for 2003 Scenarios

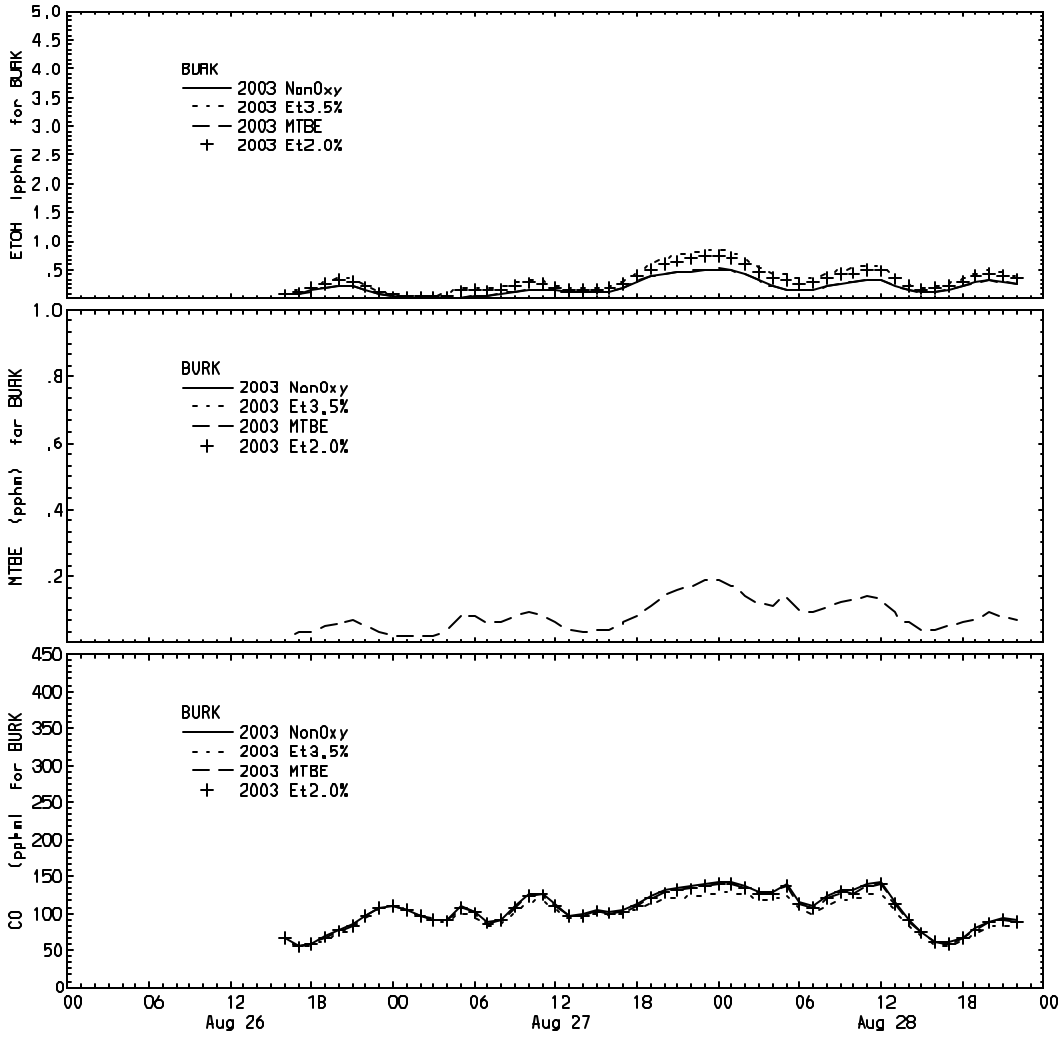

Figure 4.7 Time Series for MTBE, Ethanol, and CO at Burbank for 2003 Scenarios

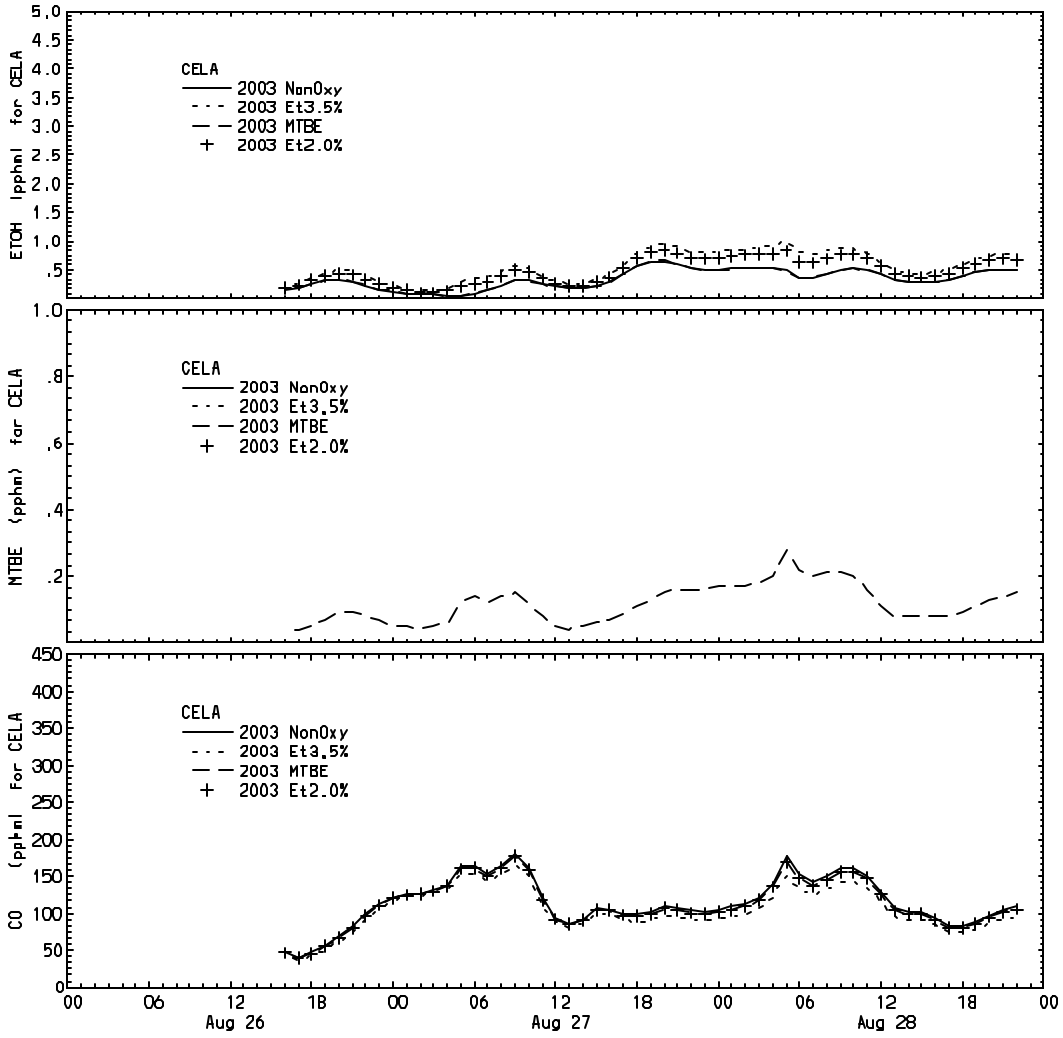

Figure 4.8 Time Series for MTBE, Ethanol, and CO at Los Angeles for 2003 Scenarios

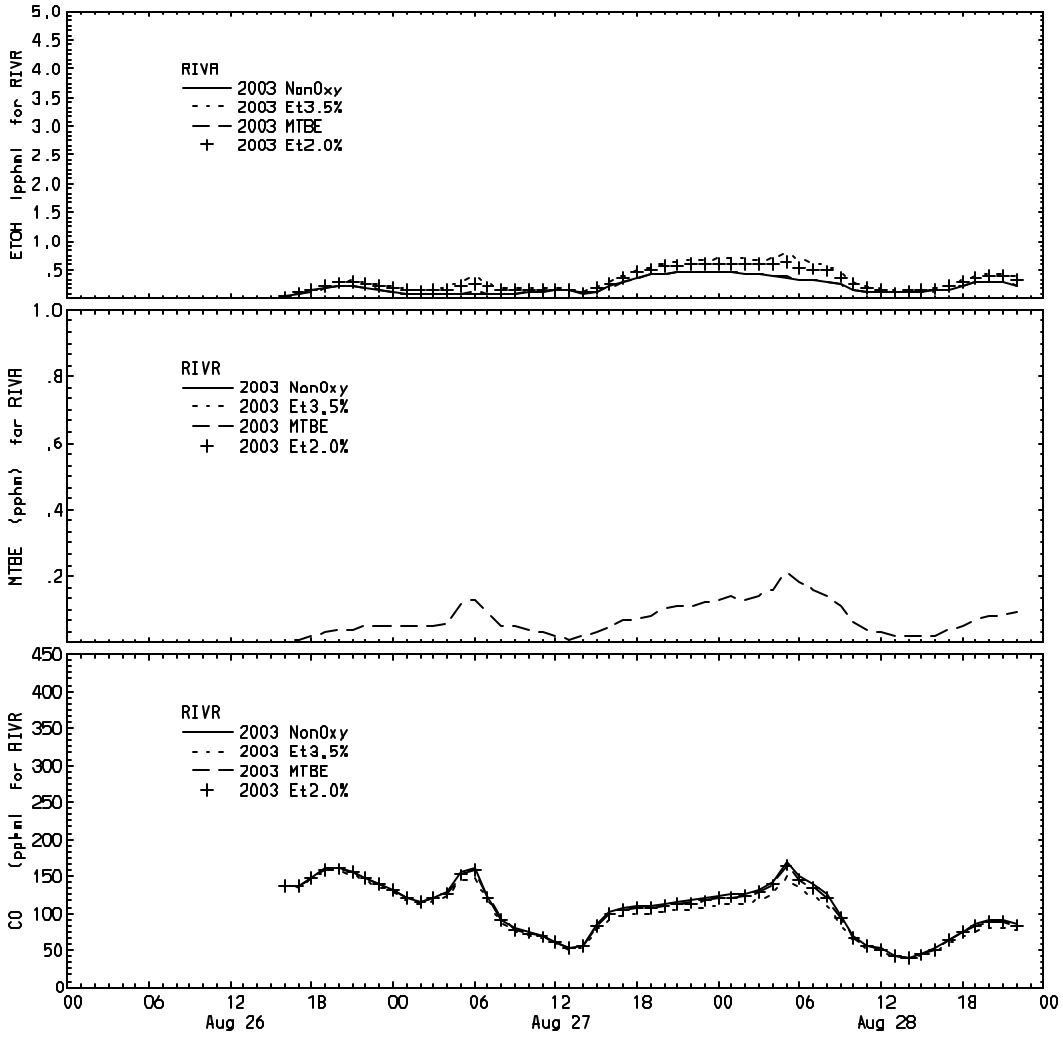

Figure 4.9 Time Series for MTBE, Ethanol, and CO at Riverside for 2003 Scenarios

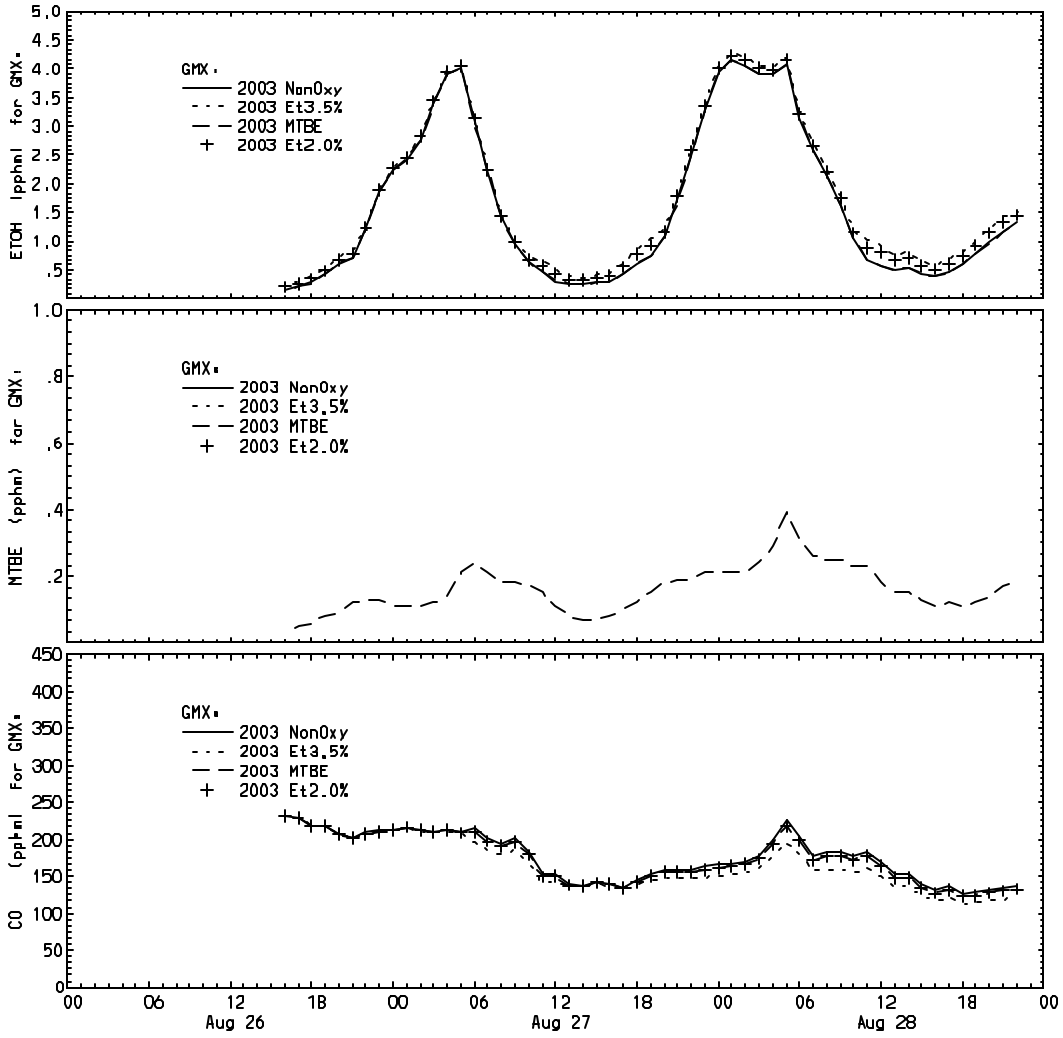

Figure 4.10 Time Series for MTBE, Ethanol, and CO at Grid with Domain Maximum for 2003 Scenarios

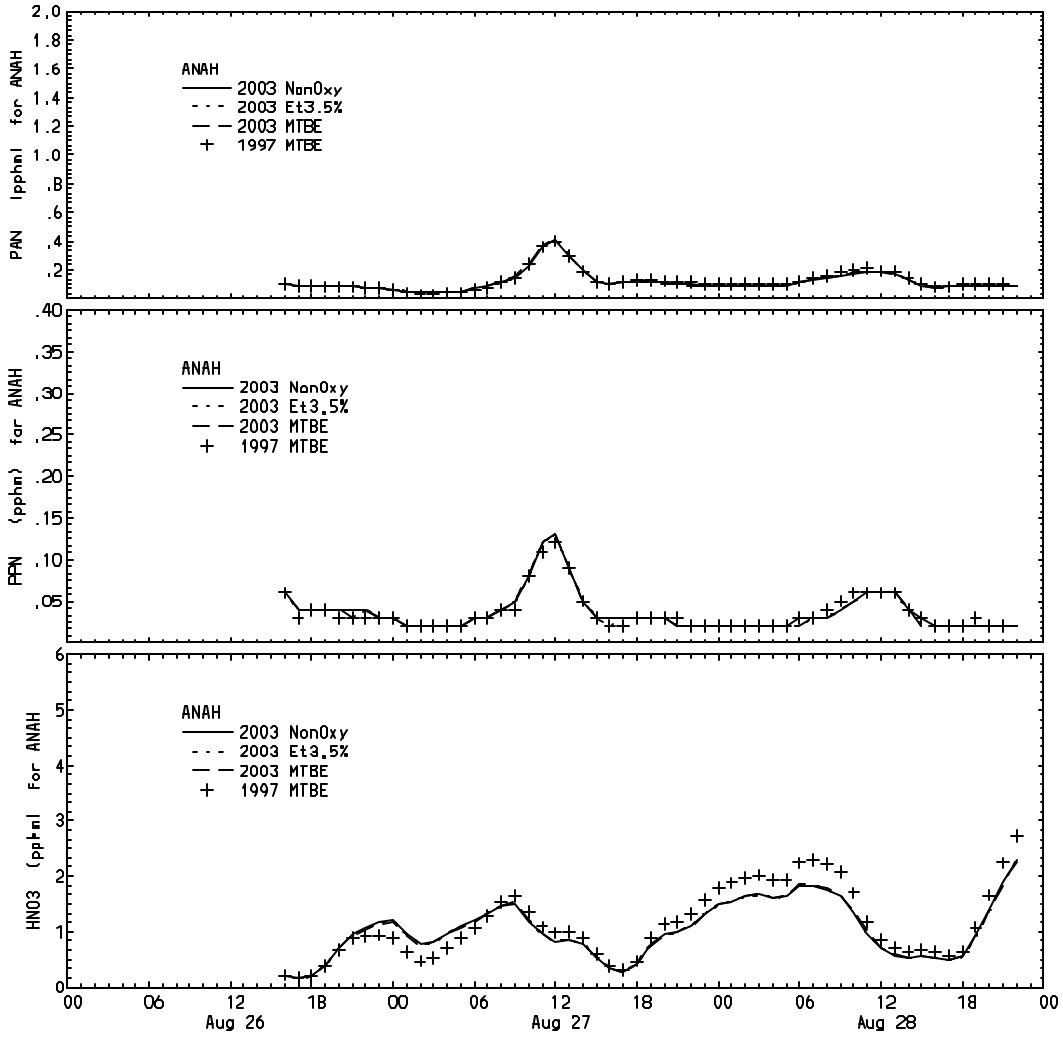

Figure 4.11 Time Series for PAN, PPN, and Nitric Acid at Anaheim for 1997 and 2003 Scenarios

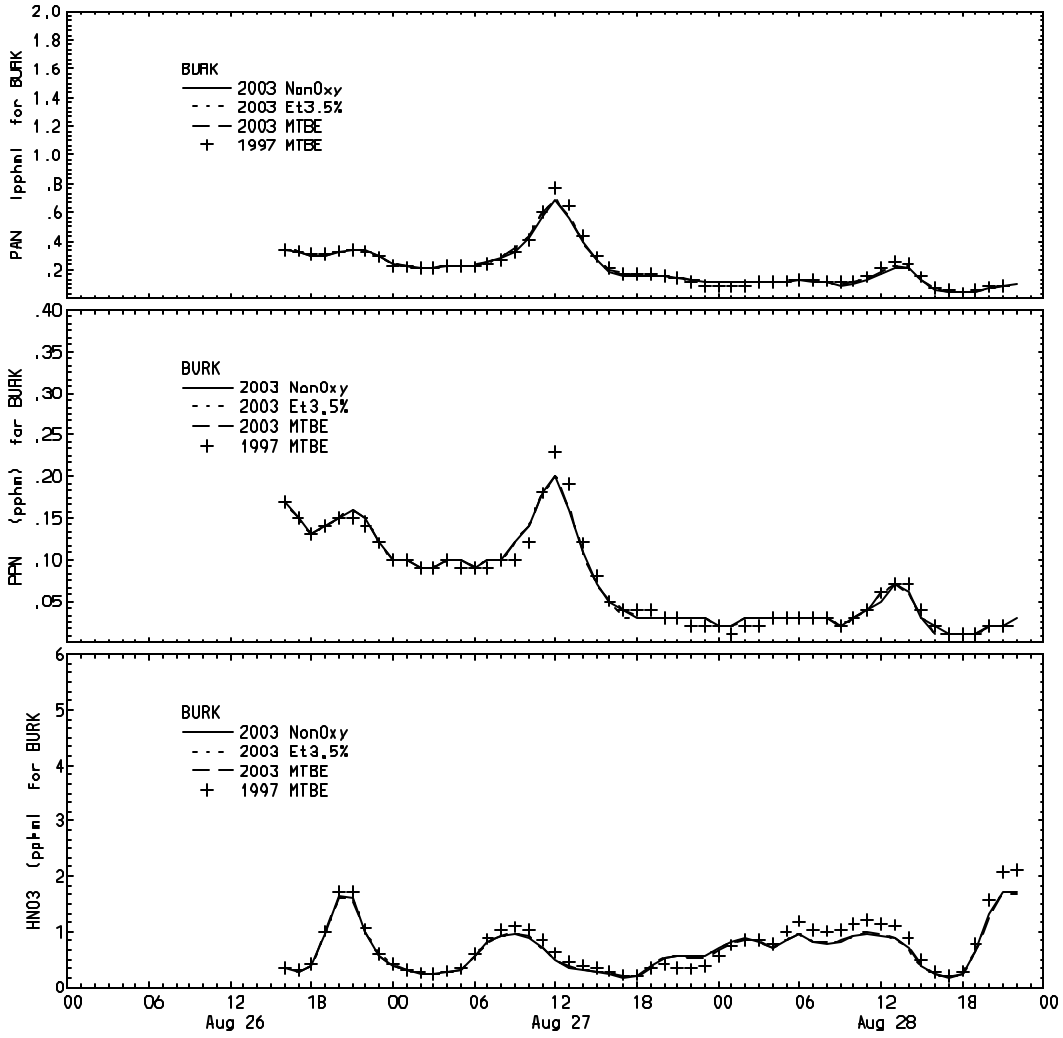

Figure 4.12 Time Series for PAN, PPN, and Nitric Acid at Burbank for 1997 and 2003 Scenarios

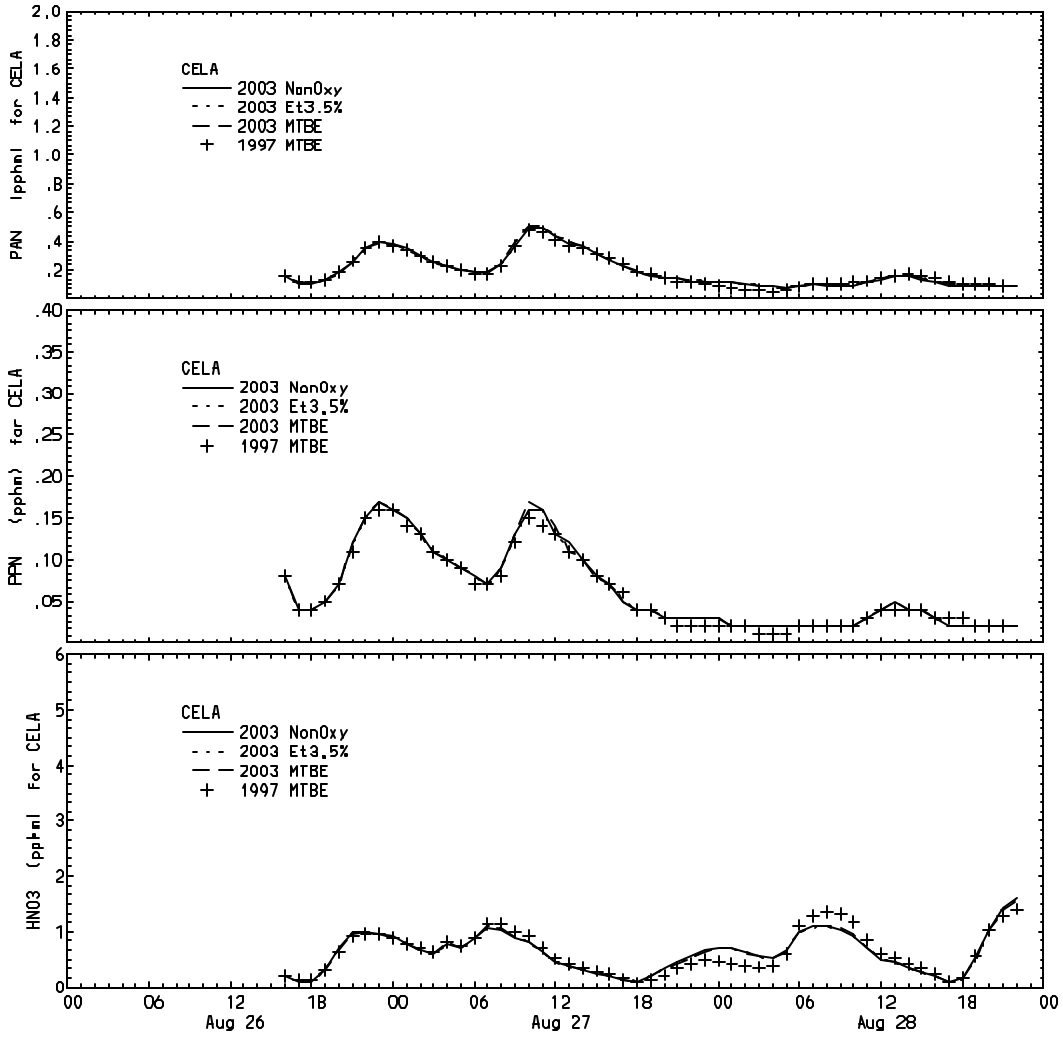

Figure 4.13 Time Series for PAN, PPN, and Nitric Acid at Los Angeles for 1997 and 2003 Scenarios

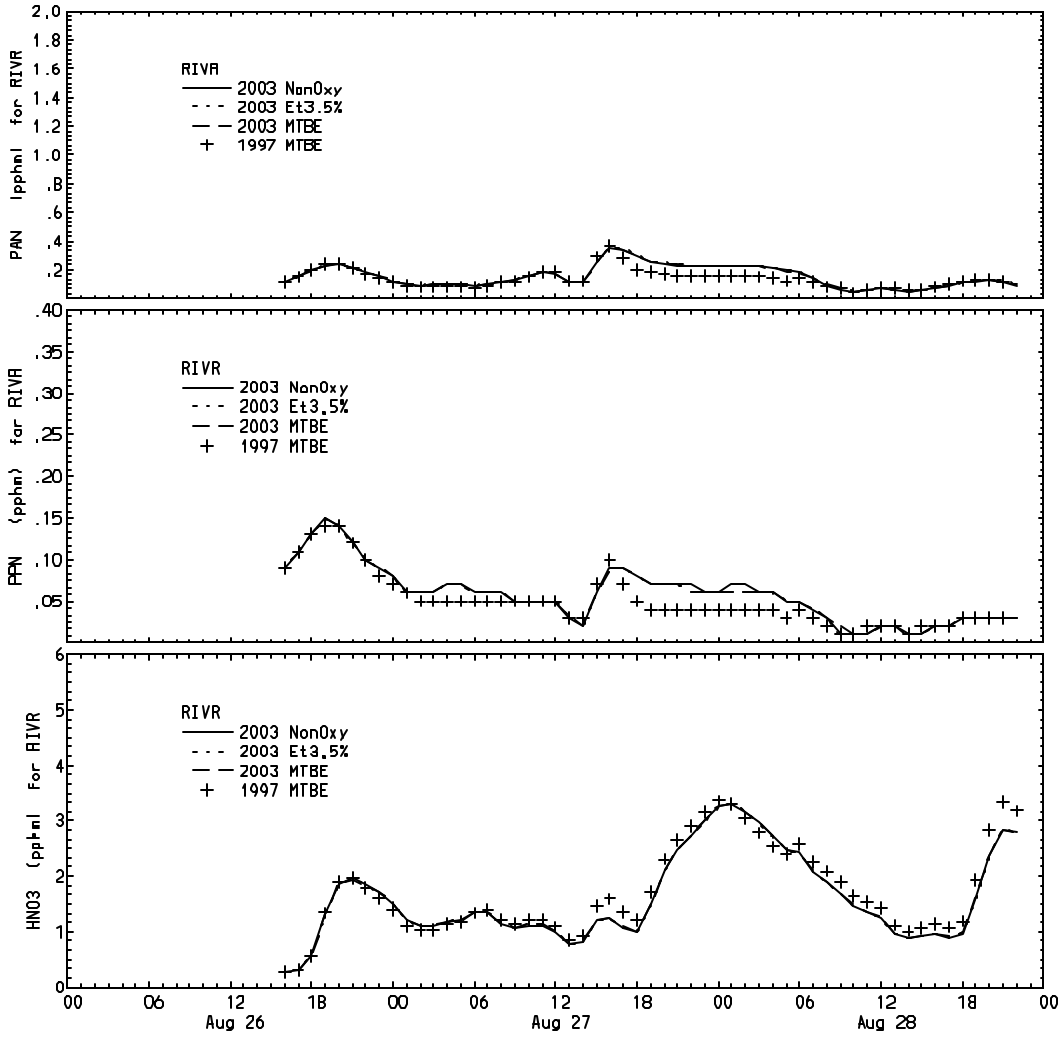

Figure 4.14 Time Series for PAN, PPN, and Nitric Acid at Riverside for 1997 and 2003 Scenarios

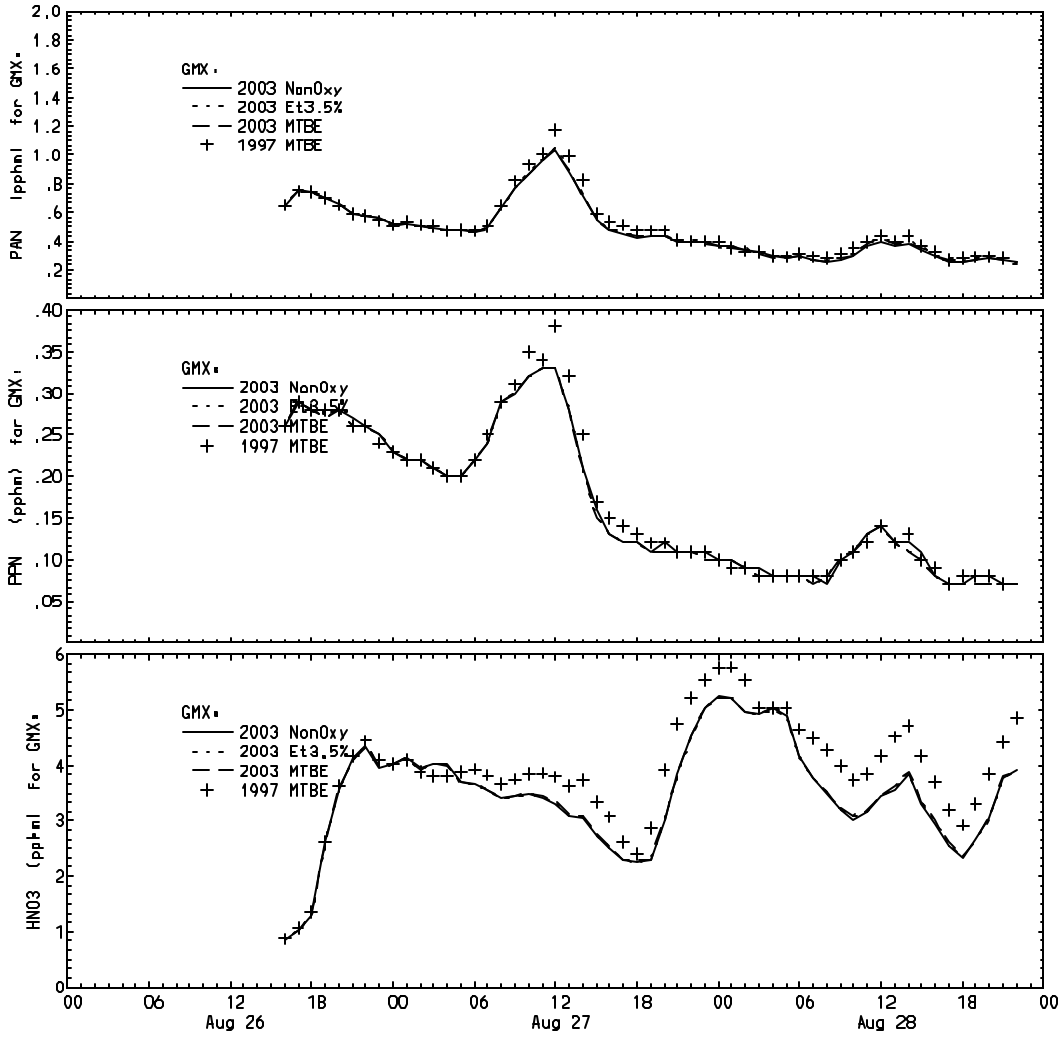

Figure 4.15 Time Series for PAN, PPN, and Nitric Acid at Grid with Domain Maximum for 1997 and 2003 Scenarios

B-4.2. Domain Maximum 8-Hour-Average Concentrations

Table 4.2 shows domain maximum 8-hour-average concentrations for selected pollutants. As shown, the 8-hour-average ozone concentration decreases by up to 5% from 1997 to 2003. CO is reduced by up to 32% for the Et3.5% scenario. Similarly, the 8-hour benzene concentration is reduced by 37% between 1997 and 2003. The 8-hour-average formaldehyde is reduced by 4%, but the 8-hour-average acetaldehyde decreases by up to 13% from 1997. The 8-hour nitric acid predicted concentration is seen to decrease by 5% from 1997 to 2003, while 8-hour PPN and BUTD are essentially unchanged. PAN and ethanol 8-hour-average concentrations decrease by up to 9% from 1997 baseline. As discussed in Section B-4.1, the predicted ethanol concentrations are dominated by non-motor vehicle sources, which may explain the predicted decrease in ethanol 8-hour-average concentrations

Table 4.2 Domain Maximum 8-Hour-Average Concentrations for Each Scenario

	Domain Maximum 8-Hour-Average Concentration[a] (ppb)												
Simulation	**O_3**	**NO**	**NO_2**	**CO**	**Formaldehyde**	**Acetaldehyde**	**C_6H_6**	**BUTD**	**MTBE**	**ETOH**	**PAN**	**PPN**	**HNO_3**
1997 MTBE	**187.3**	**150.3**	**86.4**	**2,432**	**16.8**	**7.7**	**2.46**	**2.08**	**4.1**	**40.9**	**3.25**	**0.99**	**47.9**
2003 MTBE	**177.9**	**133.4**	**75.0**	**1,816**	**16.3**	**6.7**	**1.60**	**2.05**	**2.7**	**37.2**	**2.98**	**0.94**	**45.6**
2003 Et2.0%	**178.0**	**133.2**	**74.9**	**1,816**	**16.1**	**6.8**	**1.59**	**2.05**	**0.0**	**38.0**	**2.98**	**0.94**	**45.5**
2003 Et3.5%	**178.1**	**133.2**	**74.9**	**1,741**	**16.2**	**6.8**	**1.61**	**2.05**	**0.0**	**38.5**	**3.01**	**0.94**	**45.5**
2003 NonOxy	**178.3**	**133.2**	**75.0**	**1,872**	**16.1**	**6.8**	**1.56**	**2.05**	**0.0**	**37.2**	**2.96**	**0.95**	**45.6**

[a] **Formaldehyde and acetaldehyde refer to total concentrations from primary emissions and secondary formation, C_6H_6 is benzene, BUTD is 1,3-butadiene, MTBE is methyl *tertiary*-butyl ether, ETOH is ethanol, PAN is peroxyacetyl nitrate, PPN represents peroxypropionyl nitrate and higher molecular weight acyl peroxy nitrates, and HNO_3 is nitric acid.**

B-4.3. Domain Maximum 24-Hour-Average Concentrations

Table 4.3 shows maximum 24-hour-average concentrations in the domain for selected pollutants. As shown, the 24-hour-average ozone concentration decreases by up to 4% from 1997 to 2003. CO is reduced by up to 29% for the 2003 Et3.5% scenario. Similarly, the 24-hour benzene concentration is reduced by almost 37% between 1997 and 2003. The 24-hour-average formaldehyde is reduced by up to 16%, but the 24-hour-average acetaldehyde is unchanged. The 24-hour nitric acid concentration is seen to decrease by 12% from 1997 to 2003, while PPN decreases by 2% for the 2003 Et3.5%, increases by 3% for the 2003 NonOxy, and is unchanged for the 2003 MTBE ands 2003 Et2.0%. The impact on 24-hour PAN concentration is also modest, with a decrease of up to 6% for the 2003 NonOxy scenario. The 24-hour-average ethanol concentration is reduced up to 9% for the 2003 NonOxy case. As discussed in Section B-4.1, the

predicted ethanol concentrations are dominated by non-motor vehicle sources, which may explain the predicted decrease in ethanol 24-hour-average concentrations.

Table 4.3 Domain Maximum 24-Hour-Average Concentrations For Each Scenario

	Domain Maximum 24-Hour-Average Concentration[a] (ppb)												
Simulation	**O_3**	**NO**	**NO_2**	**CO**	**Formaldehyde**	**Acetaldehyde**	**C_6H_6**	**BUTD**	**MTBE**	**ETOH**	**PAN**	**PPN**	**HNO_3**
1997 MTBE	**148.0**	**66.2**	**72.8**	**1,614**	**11.35**	**6.2**	**1.72**	**0.88**	**2.63**	**19.05**	**2.12**	**0.58**	**36.73**
2003 MTBE	**142.7**	**57.8**	**60.7**	**1,252**	**9.90**	**6.2**	**1.10**	**0.88**	**1.67**	**17.35**	**2.03**	**0.58**	**32.41**
2003 Et2.0%	**142.7**	**57.7**	**60.4**	**1,252**	**9.57**	**6.2**	**1.09**	**0.87**	**0.00**	**17.89**	**2.02**	**0.58**	**32.28**
2003 Et3.5%	**142.8**	**57.7**	**60.5**	**1,206**	**9.78**	**6.2**	**1.10**	**0.88**	**0.00**	**18.14**	**2.06**	**0.58**	**32.27**
2003 NonOxy	**142.9**	**57.7**	**60.5**	**1,286**	**9.49**	**6.2**	**1.06**	**0.87**	**0.00**	**17.36**	**2.00**	**0.60**	**32.28**

[a] **Formaldehyde and acetaldehyde refer to total concentrations from primary emissions and secondary formation, C_6H_6 is benzene, BUTD is 1,3-butadiene, MTBE is methyl *tertiary*-butyl ether, ETOH is ethanol, PAN is peroxyacetyl nitrate, PPN represents peroxypropionyl nitrate and higher molecular weight acyl peroxy nitrates, and HNO_3 is nitric acid.**

B-5. Sensitivity Simulations

Sensitivity analysis is an evaluation of the model response to variations in one or more of the model inputs. The sensitivity simulations performed in our study represent the cumulative effect of 1) use of EMFAC2000 instead of EMFAC7G, 2) consideration of chlorine radical chemistry, 3) use of updated rate constants for the reactions of hydroxyl radical with ethanol and MTBE, and 4) revised boundary conditions. The sensitivity simulations considered for this study are listed in Table 5.1, and a brief description of the each of the effects considered in the sensitivity simulations is provided below.

B-5.1. Increasing Motor Vehicle Hydrocarbon and CO Emissions

The on-road motor vehicle emissions were increased to evaluate the potential impact of using EMFAC2000 (ARB, 1999) instead of EMFAC7G. EMFAC2000 was not available at the time of this study, but emissions from motor vehicles increase substantially with EMFAC2000. A large increase in hydrocarbon emissions will change the NO_X-to-hydrocarbon ratio and potentially impact the radical flux. This may increase the photochemical oxidation of ethanol and lead to increase acetaldehyde and PAN impacts. For this purpose, hydrocarbon emissions were multiplied by a factor of three to place an upper-limit to the impact of using EMFAC2000, which at one time proposed multiplication factors of 2.34 and 1.84 for the 2000 on-road motor vehicle emission

inventory in the South Coast Air Basin for hydrocarbons and NO_X, respectively. The factor of three is also consistent with an independent fuel-based inventory for the South Coast Air Basin in 1997 which proposes a multiplication factor of 3.5±0.6 for on-road motor vehicle hydrocarbon emissions of stabilized exhaust (Singer and Harley, 2000). The Singer and Harley (2000) fuel-based inventory is for stabilized exhaust emissions and does not include cold start or evaporative emissions, so it is not necessarily inconsistent with draft versions of EMFAC2000. We also have some concerns with Singer and Harley's methodology (primarily lack of freeway measurements where gm/gallon emission rates are likely to be lower) and view it as an upper-bound estimate. The motor vehicle CO emissions were also increased by a factor of three to represent the impact of using EMFAC2000, which proposes a significant (a factor of about three) increase of motor vehicle CO emissions.

Table 5.1 Sensitivity Scenarios

Scenario	Description
1997 MTBE Sens	**Increased on-road motor vehicle ROG and motor vehicle CO by factor of 3 for the 1997 MTBE fuel, added of chlorine + ethanol reaction, updated OH radical rate constant for OH + ethanol, and OH + MTBE, and used revised boundary conditions**
2003 MTBE Sens	**Increased on-road motor vehicle ROG and motor vehicle CO by factor of 3 for the 2003 MTBE fuel, added of chlorine + ethanol reaction, updated OH radical rate constant for OH + ethanol, and OH + MTBE, and used revised boundary conditions**
2003 Et2.0% Sens	**Increased on-road motor vehicle ROG and motor vehicle CO by factor of 3 for the 2003 Et2.0% fuel, added of chlorine + ethanol reaction, updated OH radical rate constant for OH + ethanol, and OH + MTBE, and used revised boundary conditions**
2003 Et3.5% Sens	**Increased on-road motor vehicle ROG and motor vehicle CO by factor of 3 for the 2003 Et3.5% fuel, added of chlorine + ethanol reaction, updated OH radical rate constant for OH + ethanol, and OH + MTBE, and used revised boundary conditions**
2003 NonOxy Sens	**Increased on-road motor vehicle ROG and motor vehicle CO by factor of 3 for the 2003 NonOxy fuel, added of chlorine + ethanol reaction, updated OH radical rate constant for OH + ethanol, and OH + MTBE, and used revised boundary conditions**

B-5.2. Potential Impact of the Chlorine Radical Reaction With Ethanol

In addition to the increase in on-road motor vehicle emissions described above, the chemical mechanism used was modified in response to concerns on the impact of including chlorine radical reactions in the atmospheric chemical mechanism (Finlayson-Pitts, 1999). Reactions of chlorine radical with hydrocarbons are not part of SAPRC97 mechanism used in our study (see Attachment B1).

The chlorine (Cl) radical behaves similarly to the hydroxyl radical on its reaction with hydrocarbons. Cl radicals can be generated during daylight through photolysis of Cl_2 present in the air (Spicer *et al.*, 1998; Seinfeld and Pandis, 1998). Other sources of Cl radical are sea salt interaction with nitrogen oxides, and the hydroxyl radical reaction with the gaseous HCl produced by the acidification of sea salt with sulfuric acid or nitric acid (Fantechi *et al.*, 1998, and references cited therein). The Cl radical is known to have a key role on the reactions that cause stratospheric ozone depletion (Seinfeld and Pandis, 1998). In addition, it has been recognized that it can also play a role in the tropospheric oxidation of hydrocarbons near coastal areas (Finlayson-Pitts, 1999; de Haan *et al.*, 1999; Hov, 1985). Other reactive halogenated species, such as bromine and iodide, can also play a role in the tropospheric ozone budget in some areas (Platt *et al.*, 1999; Stutz *et al.*, 1999), but are not believed to be of relevance to the South Coast Air Basin.

A proper treatment of the Cl radical reactions in an atmospheric chemical mechanism should include reactions of Cl radical with all hydrocarbons, including methane, 1,3-butadiene, isoprene, MTBE, ethanol, benzene, and their reaction products (for example, see Fantechi *et al.*, 1998), including reactions with other inorganic species. However, there are significant uncertainties in the reliability of models on chlorine chemistry, because there are limited smog chamber data to test mechanisms for chlorine radical reactions (Carter, 1999a). Hence, the addition of Cl radical reactions will require a revision of the atmospheric chemical mechanism, which is outside the scope of this study. A way to address, the potential impact of adding Cl radical reactions is to focus on its effect on ethanol. We added a Cl radical reaction with ethanol, assuming the same lumped products as with the OH reaction with ethanol in the SAPRC97 chemical mechanism (see Attachment B3), and using a constant reaction rate of 9.4×10^{11} $cm^3molecule^{-1}s^{-1}$ (Finlayson-Pitts, 1999):

ETOH + CL = #.1 RO2-R + #.9 HO2 + #.156 HCHO + #.922 CCHO + #.1 RO2

The above reaction is a coarse approximation, since the reaction products and product yields could be very different from the real reaction (for example, HCl is not included as a byproduct of the Cl radical reaction with ethanol). Two additional assumptions were made to place an upper-limit on the potential effect of including the Cl radical reaction with ethanol. First, the reaction was not restricted to daylight hours only; and, second, we assumed a constant Cl radical concentration of $1x10^4$ atoms per cm^3 (Finlayson-Pitts, 1999; Fantechi *et al.*, 1998) throughout the domain. The impact of adding the above reaction is to greatly increase the oxidation of ethanol and lead to increased acetaldehyde and PAN impacts. It is expected that the maximum impact will be for the 2003 Et3.5% scenario, because of the higher ethanol emission rates in the inventory, relative to the other scenarios.

B-5.3. Updated Rate Constants

In response to comments received (Atkinson, 1999a), we also revised, for the sensitivity simulations, the rate constants used in our chemical mechanism so that the OH + ETOH reaction will have a rate constant given by $k=5.56\times10^{13}(T/300)^{2}\exp(532/T)$ $cm^{3}molecule^{-1}s^{-1}$, and the OH + MTBE reaction the rate constant was updated to be $k=5.89\times10^{-13}(T/300)^{2}\exp(483/T)$ $cm^{3}molecule^{-1}s^{-1}$ (Atkinson, 1999b). These changes increased the OH + ethanol rate constant by only 0.03%, and the OH + MTBE rate constant by 3.8%, with respect to the values originally used (see Attachment B.3). The use of the revised kinetic rate constants will increase slightly the photochemical oxidation of ethanol and MTBE.

B-5.4. Revised Boundary Conditions

In response to comments received (Atkinson, 1999a), we also revised the HONO, N_2O_5, and NO_3 concentrations used in the boundaries and top concentration when performing the sensitivity simulations. The revised concentrations are shown in Table 5.2. The HONO boundary and top concentrations used in the sensitivity simulations are larger by a factor of 9 for the 1997 MTBE sens, and by a factor of 8 for the 2003 scenarios than those used in the baseline simulations (see Table 3.3 and Table 3.4). The N_2O_5 and NO_3 concentrations used in the boundaries and top concentration are lower by a factor of three for the 1997 MTBE sens, and by a factor of 50 for the 2003 scenarios than those used in the baseline simulations (see Table 3.3 and Table 3.4). The reason for using higher N_2O_5 and NO_3 in the boundaries and top concentrations for the 1997 MTBE sens was dictated by the model's ability to resolve the set of non-linear simultaneous equations represented by the chemical reactions. Use of lower N_2O_5 and NO_3 concentrations in the 1997 MTBE sens scenario will cause the model to not to converge on a solution due to very stiff conditions. We do not believe that the different N_2O_5 and NO_3 boundary and top concentrations used for the 1997 and 2003 sensitivity scenarios will affect any of the conclusions derived from the results of these simulations.

Table 5.2 Boundary and Top Concentrations Used in the Sensitivity Simulations (ppb)

Sensitivity Simulation	HONO	N_2O_5	NO_3
1997 MTBE Sens	0.784	0.307	0.307
2003 MTBE Sens	0.660	0.020	0.020
2003 Et2.0% Sens	0.660	0.020	0.020
2003 Et3.5% Sens	0.660	0.020	0.020
2003 NonOxy Sens	0.660	0.020	0.020

B-5.5. Sensitivity Results

The predicted domain maximum 1–hour-average concentrations from the sensitivity simulations are given in Table 5.3. The results in Table 5.3 reflect the factor of three increase in on-road motor vehicle hydrocarbon and CO emissions, the use of revised rate constants for the OH + ethanol and OH + MTBE reactions, the effect of the Cl + ethanol reaction, and the revised top concentrations and boundaries, as described above. By comparing Table 4.1 and Table 5.3, it is clear that the predicted domain maximum 1-hour-average concentrations increased significantly for many species when the motor vehicle hydrocarbon emissions were increased by a factor of three. Ethanol, 1,3-butadiene, and nitric acid are notable exceptions. As discussed in Section B-4.1, the maximum 1-hour-average ethanol concentration is dominated by a non-motor vehicle emission source. The 1,3-butadiene domain maximum 1-hour concentration occurs at 0400 over the same location in Ventura County (upwind from the Los Angeles urban area) for all the sensitivity scenarios. At this hour, only nighttime reactions of 1,3-butadiene with NO_3 radical and O_3 are important. Assuming a nighttime O_3 concentration of 100 ppb, and a NO_3 radical concentration of 0.02 ppb, the NO_3 radical reaction is a factor of 3 faster than the O_3 reaction. The lack of sensitivity of 1,3-butadiene domain maximum 1-hour concentration to hydrocarbon emission increases is then presumably due to a local source. Nitric acid is formed by reaction of NO_2 with the hydroxyl radical. Hydroxyl radical concentrations increase as ozone increases, so nitric acid concentrations appear to be limited by NO_X emissions for this summertime episode, especially for the 2003 scenarios.

Table 5.3 Domain Maximum 1-Hour-Average Concentrations for Sensitivity Simulations

	Domain Maximum 1-Hour-Average Concentration (ppb)												
Simulation	**O_3**	**NO**	**NO_2**	**CO**	**Formaldehyde**	**Acetaldehyde**	**C_6H_6**	**BUTD**	**MTBE**	**ETOH**	**PAN**	**PPN**	**HNO_3**
1997 MTBE Sens	**425**	**214**	**120**	**7,448**	**37.4**	**19.1**	**9.1**	**3.1**	**16.5**	**45.2**	**18.1**	**5.7**	**69.8**
2003 MTBE Sens	**331**	**191**	**97**	**4,982**	**26.2**	**13.4**	**4.7**	**3.1**	**9.9**	**41.1**	**11.4**	**3.7**	**54.4**
2003 Et2.0% Sens	**318**	**191**	**97**	**4,982**	**24.8**	**13.7**	**4.6**	**3.1**	**0.0**	**43.1**	**10.9**	**3.7**	**54.2**
2003 Et3.5% Sens	**323**	**191**	**97**	**4,670**	**25.6**	**14.7**	**4.7**	**3.1**	**0.0**	**44.2**	**11.7**	**3.6**	**54.1**
2003 NonOxy Sens	**317**	**191**	**97**	**5,193**	**24.6**	**13.3**	**4.3**	**3.1**	**0.0**	**41.1**	**10.4**	**3.8**	**54.4**

[a] **Formaldehyde and acetaldehyde refer to total concentrations from primary emissions and secondary formation, C_6H_6 is benzene, BUTD is 1,3-butadiene, PAN is peroxyacetyl nitrate, PPN represents peroxypropionyl nitrate and higher molecular weight acyl peroxy nitrates, and HNO_3 is nitric acid**

The 1997 MTBE sensitivity scenario shows a larger increase in maximum concentrations for many species than the 2003 sensitivity scenarios. For example, the predicted maximum 1-hour-average ozone concentration increases by a factor of 1.8 from the 1997 MTBE base case to the 1997 MTBE sensitivity simulation, whereas it only increases by an average factor of 1.46 for the 2003 scenarios. Acetaldehyde increases by a factor of 2.1 in 1997 when motor vehicle hydrocarbon emissions are tripled, but it only increases by a factor of 1.51 for the 2003 NonOxy scenario. Similarly, formaldehyde increases by factor of 1.65 for the 1997 MTBE scenario, but only a factor of 1.08 for the 2003 NonOxy scenario. This difference also occurs for benzene, PAN, and PPN. Presumably, these differences are because the motor vehicle emissions are a larger fraction of the total inventory in 1997 as compared to 2003 (42% of ROG in 1997 versus 30% in 2003).

The major finding is that the predicted maximum 1-hour-average concentrations for acetaldehyde and PAN from the ethanol-containing gasoline (Et3.5%) are now 1.4 ppb and 1.3 ppb, respectively, greater than the maximum predicted for the non-oxygenated gasoline (NonOxy). These acetaldehyde and PAN impacts from the ethanol-containing gasoline represent an upper limit because the factor of three increase in all on-road hydrocarbon emissions is larger than expected from EMFAC2000 when it becomes final and the ozone episode modeled here is an extreme ozone event.

B-6. Model Performance

A performance evaluation is the process of establishing that the air quality model is adequately reproducing the chemical and physical processes that generate ozone and other pollutants. One aspect of model performance includes the sensitivity simulations described in Section B-5. In this section we test the model's ability to reproduce measured air quality data. For this purpose, an area and point emission inventory was prepared for a 1987 baseline simulation. Differences and ratios of observed and simulated maximum concentrations were calculated for each day of the August 26-28, 1987 episode in the SCAQS domain. Historical model performance evaluations have focused on ozone, and to a lesser extent, NO_2. Results are presented for other pollutants under study, including CO, NO, PAN, acetaldehyde, benzene, 1,3-butadiene, and formaldehyde. Although nitric acid data is available from the 1987 SCAQS field program, UAM-FCM does consider the thermodynamic equilibrium of nitric acid with ammonia and ammonium nitrate. We were also unable to conduct a model performance evaluation for ethanol, MTBE, or PPN, as there are no air quality measurements available for these pollutants for the 1987 episode.

B-6.1. Model Performance Statistics

Several statistical measures were used (ARB, 1992), including the Mean Absolute Gross Error (MAGE):

$$MAGE = \sum \frac{|C_s - C_o|}{N} \quad \text{(B-2)}$$

where N is the number of observations, C_s is the simulated concentration and C_o is the observed concentration.

Mean Absolute Normalized Gross Error (MANGE):

$$MANGE = \frac{1}{N} \sum \frac{|C_s - C_o|}{C_o} \quad \text{(B-3)}$$

Mean Bias (MBIAS):

$$MBIAS = \sum \frac{C_s - C_o}{N} \quad \text{(B-4)}$$

Normalized Mean Bias (NBIAS):

$$NBIAS = \frac{1}{N} \sum \frac{C_s - C_o}{C_o} \quad \text{(B-5)}$$

and the Unpaired Peak Estimation Accuracy (UPEA):

$$UPEA = \frac{C_s^{max} - C_o^{max}}{C_o^{max}} \quad \text{(B-6)}$$

Where C_s^{max} is the maximum estimated 1-hour concentration at any site in the domain, and C_o^{max} is the maximum observed 1-hour concentration at any site in the domain.

B-6.2. Ozone, CO, NO, and NO_2

The average statistics for all sites in the domain are given in Table 6.1 for August 28, 1987 (the last day of the 3-day simulation). The UAM-FCM SAPRC97 tends to over-predict maximum ozone by only 4%. The predicted maximum NO_2 is within 10% of the observed maximum, but the model significantly under-predicts maximum CO and NO, as is typical for grid-based predictions of directly emitted compounds.

Table 6.1 UAM-FCM with SAPRC97 Model Performance Evaluation

	O_3[a]	CO[b]	NO[c]	NO_2[d]
UPEA (%)	**4**	**-21**	**-56**	**7**
MBIAS (ppb)	**28**	**-142**	**-49**	**-14**
MAGE (ppb)	**38**	**771**	**51**	**31**
NBIAS (%)	**32**	**7**	**-71**	**-14**
MANGE (%)	**38**	**48**	**76**	**60**

[a] **Only ozone concentrations over 61 ppb were used.**

[b] **Only CO concentrations over 201 ppb were used.**

[c] **Only NO concentrations over 21 ppb were used.**

[d] **Only NO_2 concentrations over 11 ppb were used.**

Although the UAM has been widely applied to a number of episodes (see for example, Morris and Meyers, 1990), the UAM-FCM, on the other hand, has had limited application since its development in 1995. Therefore it was considered appropriate to examine the model performance of the UAM-FCM when using a different chemical mechanism, such as the Carbon-Bond IV (CB-IV).

The CB-IV chemical mechanism uses the lumped structure approach to represent the atmospheric oxidation of hydrocarbons in ambient air (Gery *et al.*, 1989). Carbon-bond surrogates are used to represent the chemistry of the three most common type of carbon bonds (single: PAR, double: OLE, and the CHO- group: ALD2), and two molecular surrogates represent the chemistry of aromatic compounds (monoalkylbenzenes: TOL based on toluene; dialkylbenzenes and trialkylbenzenes: XYL based on *m*-xylene). Ethene, isoprene, ethanol, methanol, formaldehyde, methylglyoxal, glyoxal, and PAN are treated explicitly.

Carbon-Bond IV (version 6.21) was implemented into the UAM-FCM. We speciated area and point source emission files, together with initial and boundary conditions for the August 26-28, 1987, for the CB-IV mechanism. Table 6.2 summarizes the performance of the UAM-FCM with CBIV. Compared to the performance of the SAPRC97 mechanism in Table 6.1, CB-IV tends to under-predict maximum ozone concentration by 11% on the last day of the episode. However, both SAPRC97 and CB-IV have similar average performance for CO, NO, and NO_2. Overall, the UAM-FCM has similar model performance with either SAPRC97 or CB-IV. Figure 6.1 through Figure 6.5 show a comparison of ozone, NO and NO_2, as predicted by SAPRC97 and CB-IV (together with the measured concentrations), for Anaheim, Burbank, Downtown Los Angeles, and Riverside. Figure 6.5 shows a comparison of ozone, NO, and NO_2, as predicted by SAPRC97 and CB-IV, for the cell with the maximum pollutant concentration in the domain (no measured data are shown, since there is no monitoring station at this location).

Table 6.2 UAM-FCM with CB4 Model Performance Evaluation

	O_3[a]	CO[b]	NO[c]	NO_2[d]
UPEA (%)	**-11**	**-23**	**-42**	**0**
MBIAS (ppb)	**-1**	**-251**	**-38**	**-13**
MAGE (ppb)	**27**	**771**	**45**	**28**
NBIAS (%)	**5**	**0**	**-50**	**-12**
MANGE (%)	**24**	**46**	**67**	**56**

a Only ozone concentrations over 61 ppb were used.

b Only CO concentrations over 201 ppb were used.

c Only NO concentrations over 21 ppb were used.

d Only NO_2 concentrations over 11 ppb were used.

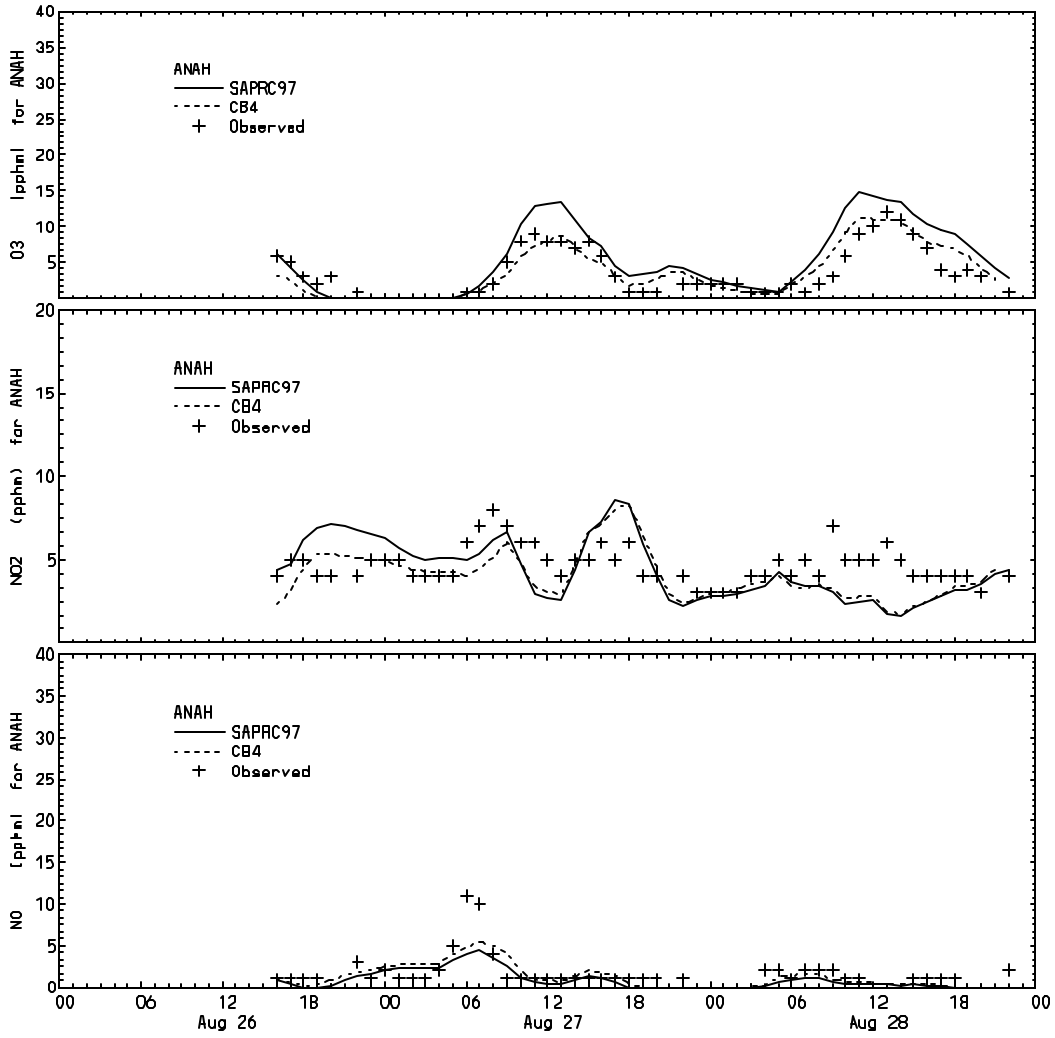

Figure 6.1 Comparison of Predicted Ozone, NO, and NO_2 by SAPRC97 and CB-IV Against Ambient Data at Anaheim (1987 SCAQS)

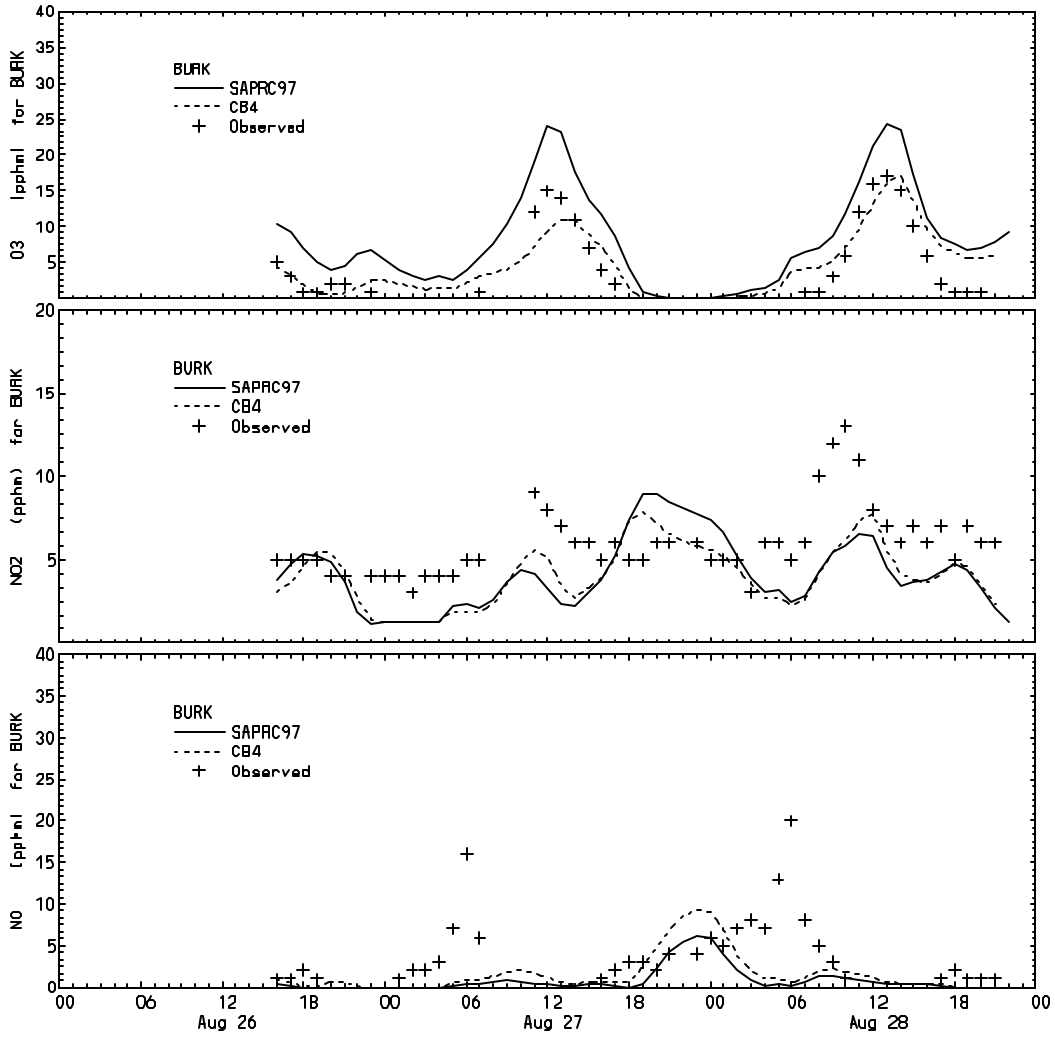

Figure 6.2 Comparison of Predicted Ozone, NO, and NO_2 by SAPRC97 and CB-IV Against Ambient Data at Burbank (1987 SCAQS)

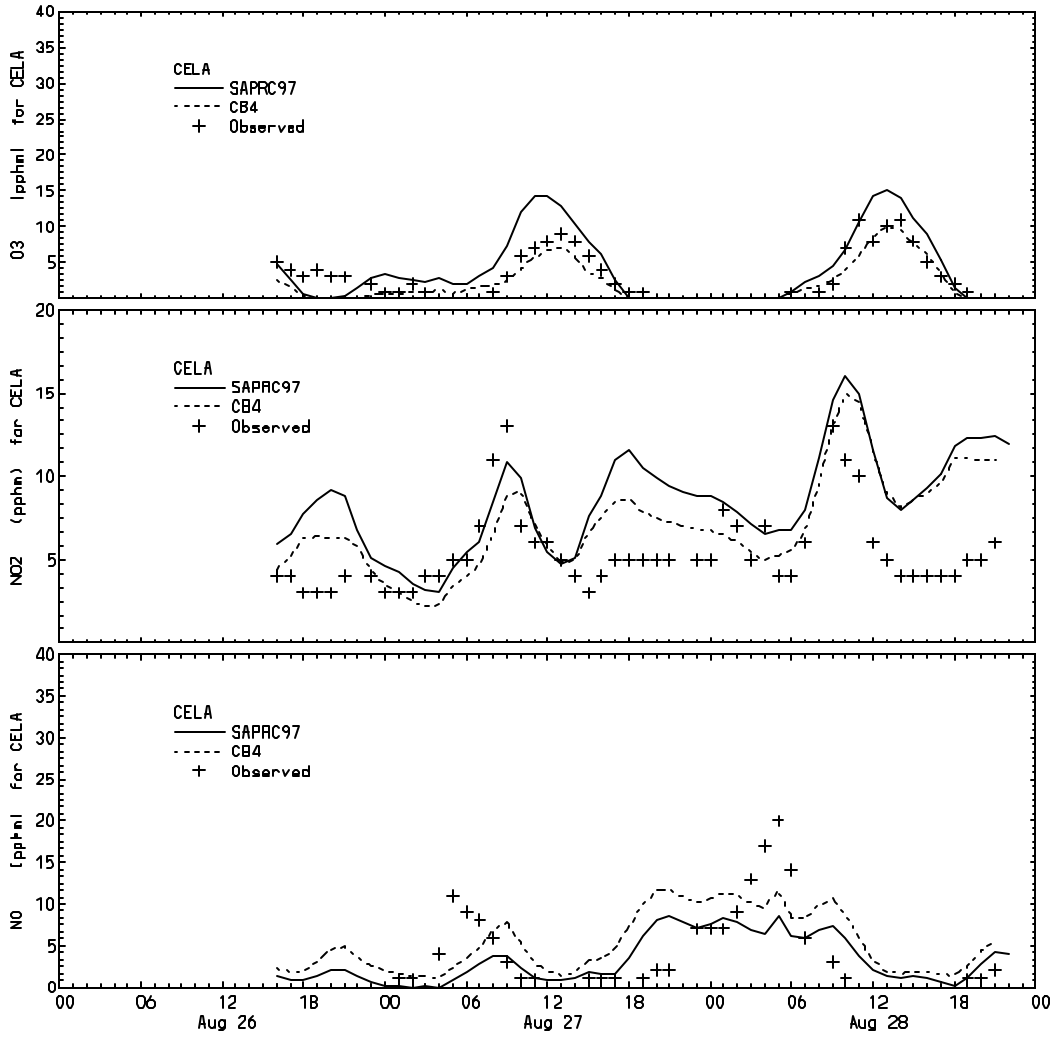

Figure 6.3 Comparison of Predicted Ozone, NO, and NO_2 by SAPRC97 and CB-IV Against Ambient Data at Los Angeles (1987 SCAQS)

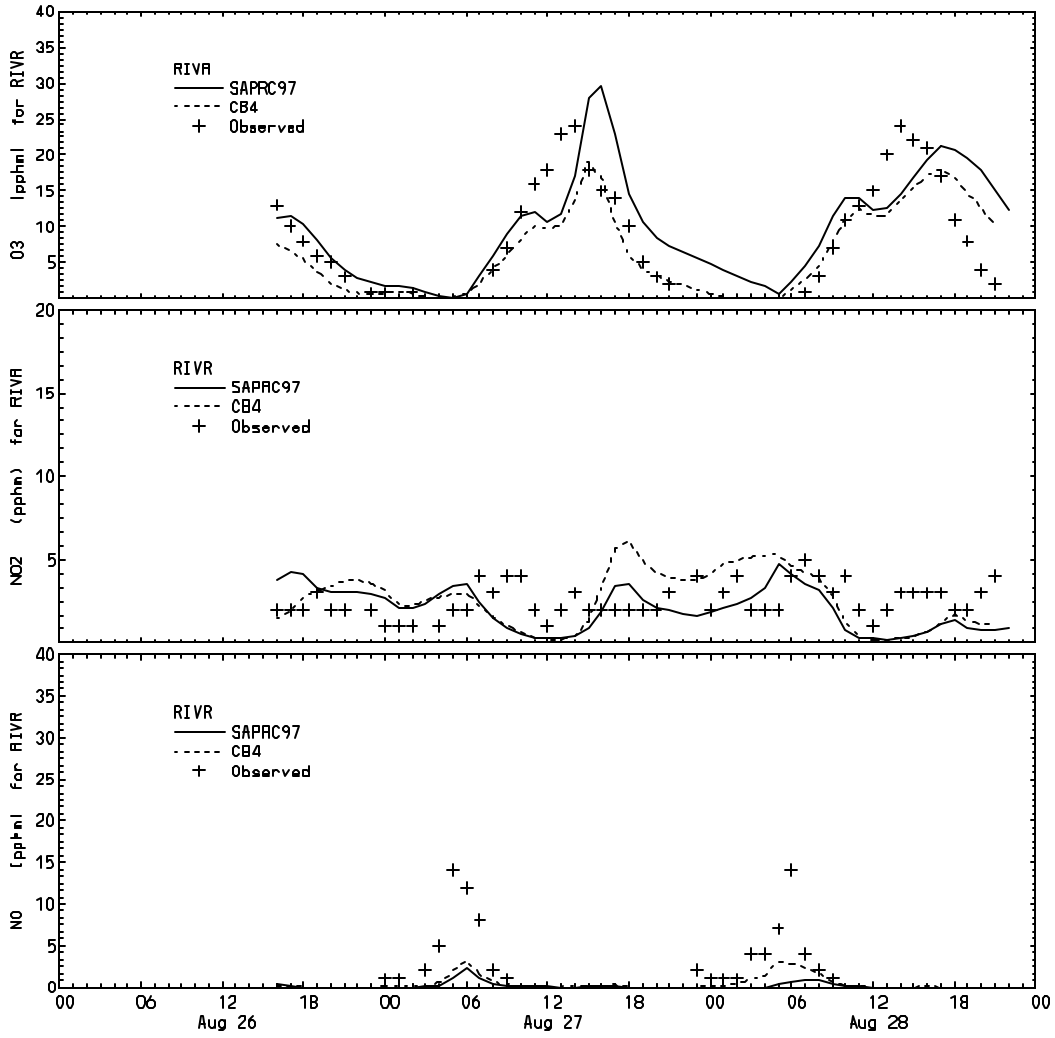

Figure 6.4 Comparison of Predicted Ozone, NO, and NO_2 by SAPRC97 and CB-IV Against Ambient Data at Riverside (1987 SCAQS)

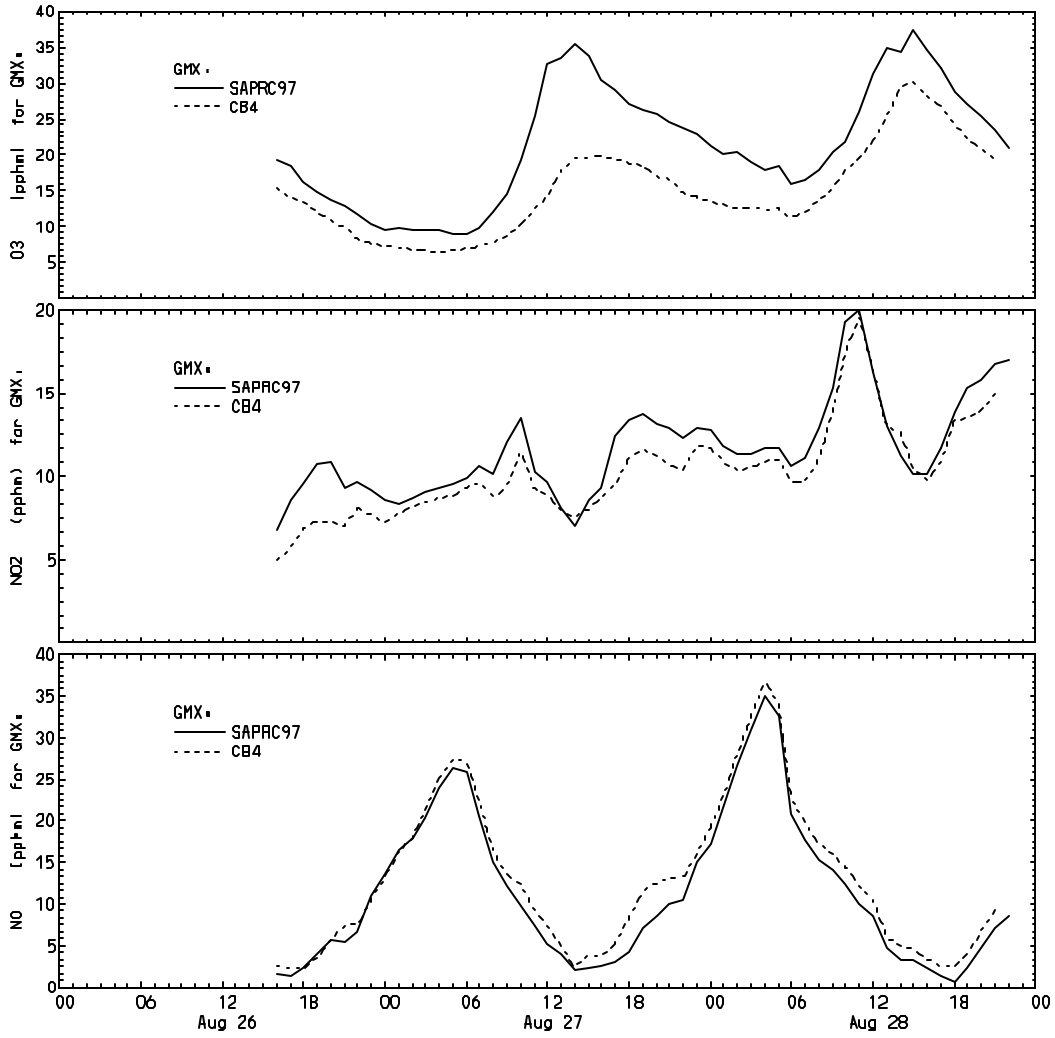

Figure 6.5 Comparison of Predicted Ozone, NO, and NO_2 by SAPRC97 and CB-IV at the Domain Maximum

B-6.3. PAN

PAN measurements are available at six sites in the SCAQS domain during August 27-28, 1987. Comparisons of hourly PAN concentrations against observations for each site are shown in Figure 6.6 and Figure 6.7. These figures show that, on the last day of the episode, the model underpredicts PAN concentrations at Burbank, Los Angeles, and, especially, at Claremont and Riverside. However, the model overestimates PAN at Anaheim. Table 6.3 shows the maximum observed and predicted 1-hour-average PAN concentrations. PAN concentrations are sensitive to local variations in the NO to NO_2 ratio and temperature, microscale features that cannot be simulated by gridded models like UAM-FCM.

Table 6.3 Observed and Predicted Maximum 1-Hour-Average PAN Concentrations for August 28, 1987

Site	Observed (ppb)	Predicted (ppb)
Anaheim	**1.1**	**5.0**
Azusa	**12**	**8.0**
Burbank	**12**	**6.6**
Claremont	**30**	**6.1**
Los Angeles	**10**	**6.0**
Riverside	**13**	**5.2**

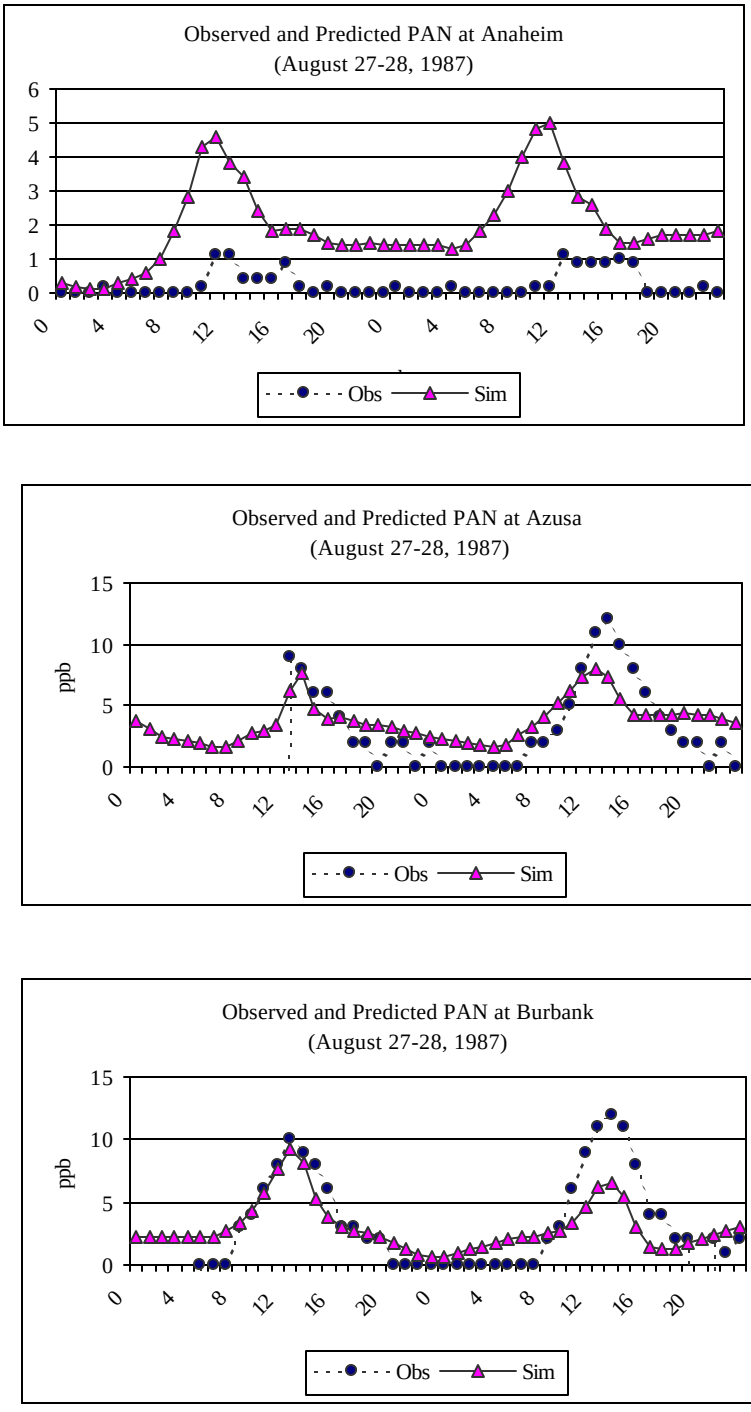

Figure 6.6 Comparison of Observed and Predicted PAN at Anaheim, Azusa, and Burbank

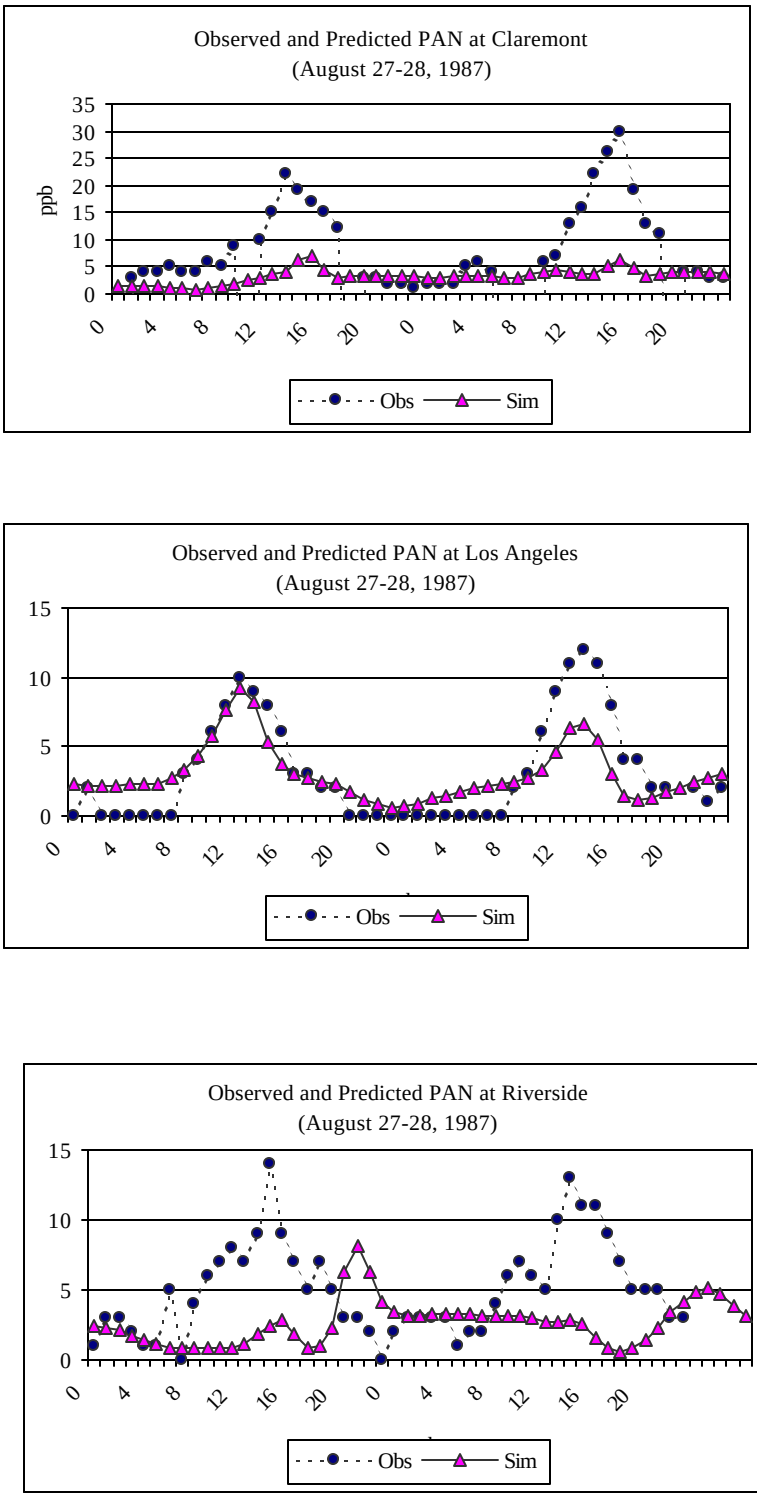

Figure 6.7 Comparison of Observed and Predicted PAN at Claremont, Los Angeles, and Riverside

B-6.4. Acetaldehyde, Benzene, 1,3-Butadiene, and Formaldehyde

As an additional evaluation of the air quality model performance, we compare in Table 6.4 the predicted and measured 3-hour-average concentrations for benzene, 1,3-butadiene, total formaldehyde, and total acetaldehyde. Note that concentrations in Table 6.4 are expressed in ppb, and not in ppbC. There are large discrepancies for all species and times between predicted and observed 3-hour-average concentrations at the Los Angeles and Riverside sites. For the other sites, the air quality model predicts a value comparable to that measured. For example, at start time of 0600, the model predicts good agreement with measured data at Anaheim and Hawthorne (for benzene and acetaldehyde), at Long Beach (all species), and Burbank (acetaldehyde). However, when averaging of all the values for a start time of 0600, the model overpredicts for benzene and 1,3-butadiene, and underpredicts the aldehydes. The comparison between model and measurements does not significantly improve later in the day (start time of 1100). However, on average there is better agreement between model predictions and measured data in the late morning (start time of 1100). Overall, the predicted results for acetaldehyde and formaldehyde are in rough agreement with the measurements, while the model severely under-predicts benzene and 1,3-butadiene concentrations. The instantaneous mixing of emissions into a large grid cell by UAM-FCM is a reasonable approximation for secondary pollutants like ozone, NO_2, acetaldehyde, and formaldehyde, but not for directly emitted pollutants such as benzene and 1,3-butadiene.

Table 6.4 Measured and Predicted 3-Hour-Average Concentrations for Selected VOCs on August 28, 1987 (ppb)

Site	Start Hour	Benzene		1,3-Butadiene		Formaldehyde		Acetaldehyde	
		Measured	Predicted	Measured	Predicted	Measured	Predicted	Measured	Predicted
Anaheim	600	1.8	2.1	0.3	0.2	6.8	9.8	4.7	4.9
Anaheim	1100	2.6	1.7	0.3	0.0	19.0	11.0	17.0	6.1
Azusa	600	6.0	3.0	1.1	0.3	8.7	17.0	5.8	8.4
Azusa	1100	5.1	2.4	0.1	0.0	19.0	17.0	17.0	10.0
Burbank	600	8.9	1.5	1.5	0.1	8.1	13.0	5.3	5.3
Burbank	1100	6.3	2.9	0.3	0.1	17.0	20.0	16.0	12.0
Los Angeles	600	38.0	4.6	2.1	0.8	7.8	15.0	3.5	7.9
Los Angeles	1100	5.9	4.3	0.2	0.1	10.0	26.0	9.9	17.0
Hawthorne	600	1.2	1.6	0.1	0.2	3.0	6.4	3.1	3.6
Hawthorne	1100	0.6	1.6	0.1	0.1	4.9	7.7	4.1	4.7
Long Beach	600	5.0	3.8	0.5	0.6	11.0	10.0	5.5	5.5
Long Beach	1100	2.8	3.4	0.1	0.1	14.0	16.0	13.0	12.0
Riverside	600	5.9	2.6	0.7	0.1	8.5	18.0	5.7	9.1
Riverside	1100	2.5	0.7	0.1	0.0	13.0	6.8	13.0	3.2
Average (600)		9.5	2.8	0.9	0.3	7.7	13.0	4.8	6.4
Average (1100)		3.7	2.4	0.2	0.1	14.0	15.0	13.0	9.2
Average (600 & 1100)		6.6	2.6	0.5	0.2	11.0	14.0	8.8	7.8

B-7. Ozone, PAN, and PPN Formation Potentials

In addition to the 3-dimensional airshed model simulations, we also investigated the ozone, PAN, and PPN (which includes higher molecular weight acyl peroxy nitrates) formation potentials for each of the explicit VOCs and lumped species in the SAPRC97 chemical mechanism. This was used to explain the lack of sensitivity of PAN formation to the ethanol content of the gasoline observed in Section B-4.

B-7.1. Description of Formation Potentials

The formation of secondary pollutants in an airshed is a complex process, which involves a series of photochemical reactions driven by the sunlight. It has been recognized that individual organic compounds can contribute differently to the creation of secondary air pollutants in atmosphere. Over decades, a variety of scales of VOC formation potential have been devised to quantify the degree to which different organic compounds affect formation of a given pollutant, such as ozone. More generally, the potential of a given organic compound in atmospheric chemistry refers to the reactivity of that compound to promote formation of products. Among these scales, the incremental reactivity developed by Carter and Atkinson (1989) is the simplest method of calculating the potential of an organic compound to form ozone or any other pollutant.

Given a VOC_i, its ozone incremental reactivity is defined as the ratio of the ozone concentration change to a small perturbation of the VOC_i:

$$\textit{Ozone formation potential} = \lim_{\Delta VOC_i \to 0}\left[\frac{O_3(VOC_i + \Delta VOC_i) - O_3(VOC_i)}{\Delta VOC_i}\right] \qquad \text{(B-7)}$$

where $O_3(VOC_i + \Delta VOC_i)$ and $O_3(VOC_i)$ are the ozone concentrations of the perturbed case and base case of VOC_i, respectively. Yang *et al.* (1995) show that ozone formation potential can be estimated as the local sensitivity of the predicted ozone concentration to the *initial* concentrations of each organic compound in a mixture.

Similarly, the PAN formation potential of a given organic compound, VOC_i, in a mixture or airshed can be calculated by:

$$\textit{PAN formation potential} = \lim_{\Delta VOC_i \to 0}\left[\frac{PAN(VOC_i + \Delta VOC_i) - PAN(VOC_i)}{\Delta VOC_i}\right] \qquad \text{(B-8)}$$

where $PAN(VOC_i + \Delta VOC_i)$ and $PAN(VOC_i)$ are the PAN concentrations of the perturbed case and base case of VOC_i, respectively. The equation, in essence, is a local sensitivity of PAN to the concentration change of an organic compound and can be computed by the partial differentiation of PAN with respect to VOC_i. The PAN sensitivity coefficient, i.e.,

$$\frac{\partial PAN}{\partial VOC_i}$$

is interpreted as the amount of PAN formed per unit amount of VOC_i changed in the mixture and has units of ppm-PAN/ppm-VOC or ppm-PAN/ppm-C. As mentioned above, the PAN formation potential was estimated as the local sensitivity of the predicted ozone concentration to the *initial* concentrations of each organic compound in a mixture (Yang *et al.* (1995).

The total formation potential for ozone, PAN, and PPN (which includes higher molecular weight acyl peroxy nitrates) can be calculated by using a first-order approximation:

$$\textit{Total PAN formation potential} = \sum_i \left(\frac{\partial PAN}{\partial VOC_i} \right) \Delta VOC_i \qquad \text{(B-9)}$$

B-7.2. Model Description and Inputs

The scenario for the ozone, PAN, and PPN (and includes higher molecular weight acyl peroxy nitrates) formation potential calculations is adopted from the average condition of 39 cities across the U.S. designed by Carter (1994) for ozone incremental reactivity. Pollutant formation potential scales are time varying over the 10-hour simulation. The results presented here are the formation potentials of ozone, PAN, and PPN (and includes higher molecular weight acyl peroxy nitrates) estimated at 1800 where the maximum ozone occurs in the simulation period, because the time satisfies the condition of maximum incremental reactivity scale (Yang *et al.*, 1995).

We implemented the SAPRC97 chemical mechanism -- as described in Attachment B1 -- in a box model to evaluate the ozone, PAN, and PPN (and includes higher molecular weight acyl peroxy nitrates) formation potential of selected individual VOCs and lumped VOC categories. Table 7.1 gives the PAN and PPN (and includes higher molecular weight acyl peroxy nitrates) reactions, together with the value of their corresponding kinetic parameters (as used in the box model). Table 7.2 provides the default meteorological inputs for the box-model simulations. Table 7.3 gives the initial conditions for several episodes in the South Coast Air Basin, and Table 7.4 has the initial conditions for episodes representative of two large cities in Brazil.

Table 7.1 PAN and PPN Equilibrium Reaction Rate Constants

Reactions	$CCO\text{-}O_2 + NO_2 = PAN$[a]	PAN[a] $= CCO\text{-}O_2 + NO_2 + RCO_3$	$C_2CO\text{-}O_2 + NO_2 = PPN$[b]	PPN[b] $= C_2CO\text{-}O_2 + NO_2 + RCO_3$
Kinetic	$A_o = 2.57 \times 10^{-28}$	$A_o = 4.9 \times 10^{-3}$	$A = 8.4 \times 10^{-12}$	$A = 1.6 \times 10^{17}$
Parameters	$E_o = 0.0$	$E_o = 23.972$	$E = 0.0$	$E = 27.966$
	$B_o = -7.1$	$B_o = 0.0$	$B = 0.0$	$B = 0.0$
	$A_i = 12.0 \times 10^{-12}$	$A_i = 4.0 \times 10^{16}$		
	$E_i = 0.0$	$E_i = 27.079$		
	$B_i = -0.9$	$B_i = 0.0$		
	$F = 0.3$	$F = 0.3$		
	$N = 1.0$	$N = 1.0$		
$K(298^oK)$	3.3×10^4 $ppm^{-1}min^{-1}$	3.9×10^{-2} min^{-1}	1.2×10^4 $ppm^{-1}min^{-1}$	4.1×10^{-2} min^{-1}

Note: **All kinetic parameters in cm-molecules-sec units. PPN represents peroxypropionyl nitrate and higher molecular weight acyl peroxy nitrates (see Attachment B1).**

[a] rate constant expression given by $k = [k0*M/(1+(K0*M/K1))]*F^Z$, with $Z = 1/[\ 1+\log_{10}(k0*M/k1)/N^2\ ]$. Where, $k0 = A0*[(T/T_{REF})^{B0}]*\exp(-E0/RT)$, and, $k1 = A1*[(T/T_{REF})^{B1}]*\exp(-E1/RT)$

[b] rate constant expression given by $k = A(T/T_{REF})^B\exp(-E/RT)$, where k and A are in cm-molecule-s units, T is temperature in ^oK, R=0.0019872 kcal mol^{-1} ^oK, and E is in kcal mol^{-1}

Table 7.2 Meteorological Inputs[a]

Time	Temperature (^oK)	Mixing Height (m)	Zenith Angle (degrees)[b]
800	**295.5**	**292.9**	**71.6**
900	**297.7**	**595.7**	**59.5**
1000	**299.9**	**998.5**	**47.5**
1100	**301.8**	**1201**	**35.9**
1200	**303.3**	**1503**	**25.9**
1300	**304.5**	**1610**	**20.1**
1400	**305.6**	**1716**	**22.1**
1500	**305.8**	**1823**	**30.4**
1600	**306.1**	**1823.1**	**41.3**
1700	**305.9**	**1823.2**	**53.1**
1800	**305.1**	**1823.3**	**65.2**

[a] **Adopted from the average scenario of 39 cities, Carter (1994).**

[b] **Evaluated at the latitude of 36.22^o and the solar declination of 16.5^o (Los Angeles)**

Table 7.3 Initial Concentrations for South Coast Air Basin Scenarios (ppm)

Initial Concentrations	South Coast[b] 1968	Los Angeles[c] 1968	LARPP[d] 1973	Los Angeles 8/28/87[a]	SCAQS 8/28/87[a]	Los Angeles 12/3/87[a]	Claremont[f] 9/8/93	Azusa[e] 8/6/97	Azusa[e] 10/4/97	Azusa[e] 8/22/97
O_3	0.01	0.01	0.01	0.0067	0.01	0.01	0.04	0.02	0.0043	0.001
NO	0.24	0.341	0.034	0.1	0.04	0.19	0.18	0.031	0.05	0.141
NO_2	0.049	0.069	0.007	0.05	0.05	0.06	0.12	0.104	0.065	0.072
CO	10.3	10.3	1.91	5.4	2.0	6.64	4.0	2.64	2.53	3.1
Methane	3.3	3.3	2.01	2.62	2.6	3.44	2.6	2.82	2.58	2.6
Ethene	0.065	0.076	-	0.0526	0.027	0.036	0.018	0.028	0.026	0.0301
Formaldehyde	0.005	0.005	0.01	0.008	0.005	0.011	-	0.011	0.0074	0.0003
Acetaldehyde	0.005	0.005	0.005	0.0035	0.005	0.0067	-	0.006	0.0028	0.0009
Acetone	-	-	-	0.057	-	0.0083	-	0.016	0.0075	0.0007
MEK	-	-	-	0.0008	-	0.0032	-	0.005	0.001	0.0003
Benzene	-	-	-	0.038	0.0078	0.011	0.0029	-	0.013	0.0025
Isoprene	-	-	-	0.0008	-	0.0005	-	0.000	0.0008	0.0041
Ethanol	-	-	-	-	-	-	-	-	-	-
MTBE	-	-	-	-	-	-	-	-	-	-
1,3 Butadiene	-	0.0028	-	-	-	-	0.0003	-	-	0.00018
Dichloromethane	-	-	-	0.001	-	0.014	0.0004	0.000	-	-
ALK1 (lumped alkanes, $k_{OH}<1.0x10^4$ $ppm^{-1}min^{-1}$)	0.37	0.455	0.286	0.506	0.18	0.245	0.081	0.373	0.24	0.078
ALK2 (lumped alkanes, $k_{OH}\geq1.0x10^4$ $ppm^{-1}min^{-1}$)	0.038	0.039	0.021	0.18	0.018	0.014	0.0094	0.13	0.083	0.014
ARO1 (lumped aromatics, $k_{OH}<2.0x10^4$ $ppm^{-1}min^{-1}$)	0.033	0.06	0.024	0.206	0.06	0.034	0.0068	0.083	0.068	0.011
ARO2 (lumped aromatics)	0.044	0.081	0.02	0.11	0.081	0.019	0.0058	0.089	0.051	0.007
OLE1 (lumped terminal alkenes, $k_{OH}\geq2.0x10^4$ $ppm^{-1}min^{-1}$)	0.016	0.036	0.023	0.094	0.036	0.108	0.004	0.023	0.075	0.0076
OLE2 (lumped internal alkenes)	-	0.02	0.017	0.0098	0.02	0.005	0.0022	0.019	0.01	0.0026
OLE3 (terpenes)	-	-	-	-	-	-	0.00017	-	-	0.0041
ROG/NO_X	8.3	8.3	3.1	44	13.3	6.8	1.6	30.8	25.1	3.05

[a]Lawson, 1990

[b]Lonemann, 1968

[c]Kopczynski, 1968

[d]Calvert, 1976

[e]McCauley, 1999

[f]Pasek, 1999

Note: Other constant concentrations are included in the simulation runs, i.e., CO_2, O_2, Air, and H_2.

Table 7.4 Initial Concentrations for Brazil Scenarios (ppm)

Initial Concentrations	Porto Alegre, Brazil 1998[a]	Avenida Brazil, Rio de Janeiro 1999[b]
O_3	0.01	0.01
NO	0.143	0.22
NO_2	0.029	0.045
CO	3.34	5.1
Methane	1.70	1.90
Ethene	0.036	0.056
Formaldehyde	0.0124	0.0097
Acetaldehyde	0.014	0.0102
Acetone	-	-
MEK	-	-
Benzene	0.038	0.068
Isoprene	0.0042	-
Ethanol	0.012	0.0485
MTBE	0.066	-
1,3 Butadiene	0.062	0.012
Dichloromethane	-	-
ALK1 (lumped alkanes, $k_{OH} < 1.0x10^4$ $ppm^{-1}min^{-1}$)	0.315	1.03
ALK2 (lumped alkanes, $k_{OH} \geq 1.0x10^4$ $ppm^{-1}min^{-1}$)	0.2	0.57
ARO1 (lumped aromatics, $k_{OH} < 2.0x10^4$ $ppm^{-1}min^{-1}$)	0.12	0.245
ARO2 (lumped aromatic)	0.22	0.515
OLE1 (lumped terminal alkenes, $k_{OH} \geq 2.0x10^4$ ppm^{-1} min^{-1})	0.061	0.075
OLE2 (lumped internal alkenes)	0.10	0.164
OLE3 (terpenes)	-	-
ROG/NO_X	44.5	67.0

[a] Grosjean *et al.* (1998)

[b] Grosjean (1999)

Note: Other constant concentrations are included in the simulation runs, i.e., CO_2, O_2, Air, and H_2.

B-7.3. Results

Figure 7.1 and Figure 7.2 present the individual ozone formation potentials for the twelve cases described in Table 7.3 and Table 7.4. Note that all box model simulations were conducted with all VOC and NO_X inputs as initial conditions, i.e., no emissions over the simulation time period. This is a reasonable approach for a Lagrangian model that simulates an air parcel as it travels over a region, but will likely underestimate the contribution from fast-reacting species in comparison to more slowly reacting compounds (e.g., alkanes, ethanol). The ranking has a general consistency with relatively high ozone formation potentials for ethene, 1,3-butadiene, formaldehyde, acetaldehyde, isoprene, ARO2, and the three lumped olefin classes. However, the ozone formation potential for ARO1 is negative for some of the cases. Previous studies have shown that aromatic compounds could have negative ozone reactivity under some high-VOC loading conditions (Carter, 1994; Khan *et al.*, 1998).

For PAN production, 1,3-butadiene, acetaldehyde, isoprene, ARO2, and the three lumped olefin classes have relatively high formation potential compared to other compounds, as shown in Figure 7.3 and Figure 7.4. As with ozone, the ARO1 class was found to have negative formation potential for some cases. For the ten explicit VOC compounds in the figures, the rank of PAN formation potentials estimated here has general agreement with a recent study by Derwent *et al.* (1998). Figure 7.5 and Figure 7.6 show that 1,3-butadiene, isoprene, and the three lumped olefin classes have higher PPN (including higher molecular weight acyl peroxy nitrates) formation potentials. For most simulated cases, ARO1 and ARO2 have negative potential for PPN (and higher molecular weight acyl peroxy nitrates) production.

The total ozone formation potentials for the ten explicit VOCs are given in Table 7.5 and Table 7.6. The total PAN formation potentials are provided in Table 7.7 and Table 7.8, and the total PPN formation potentials are shown in Table 7.9 and Table 7.10. Note that the missing values in Table 7.5 to Table 7.10 denote compounds that were not included in the initial conditions and, hence, do not have calculated formation potentials. For the Los Angeles cases in the last 1960s and early 1970s, the lumped alkane class ALK1 is the main contributor to ozone, PAN, and PPN (and higher molecular weight acyl peroxy nitrates) concentrations. The lumped aromatic class ARO2 also contributes significantly for these historical cases. For the more recent cases in the 1980s and 1990s, ALK1 remains a large contributor, but the role of ARO2 diminishes and the contribution of the lumped olefin classes increase. This shift most likely reflects the effects of a decreasing aromatic content in gasoline and diesel fuel.

In the two Brazilian cases, ALK1 is the major contributor to ozone, and ARO2, OLE1, and OLE2 dominate PAN concentrations. OLE2 is the major contributor to PPN (and higher molecular weight acyl peroxy nitrates). Even though ethanol and acetaldehyde concentrations are relatively high, they are not the major contributors to PAN. Thus, the box model simulations are consistent with the results from the three-dimensional airshed model that ethanol substitution scenarios will not necessarily lead to a substantial in increase in PAN concentrations.

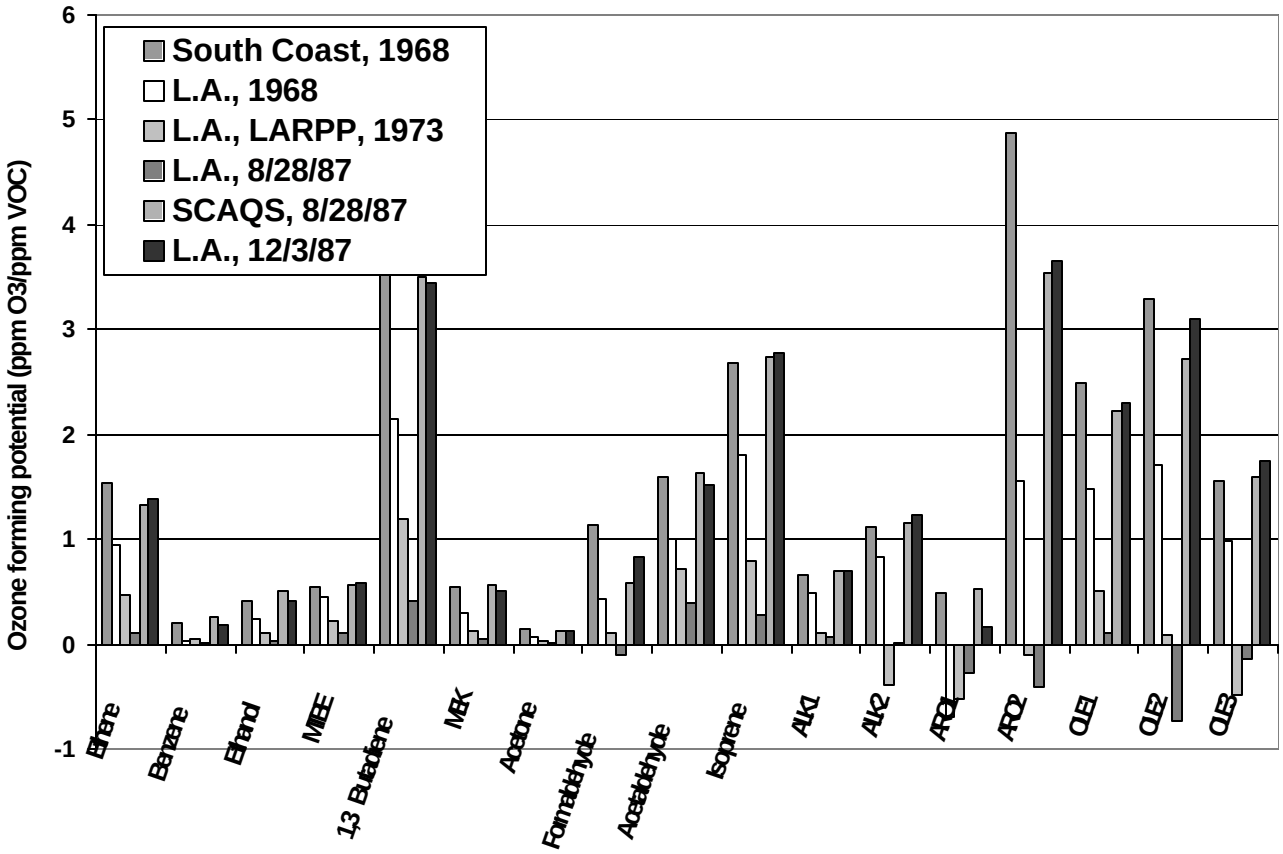

Figure 7.1 Ozone Formation Potentials From Individual VOCs

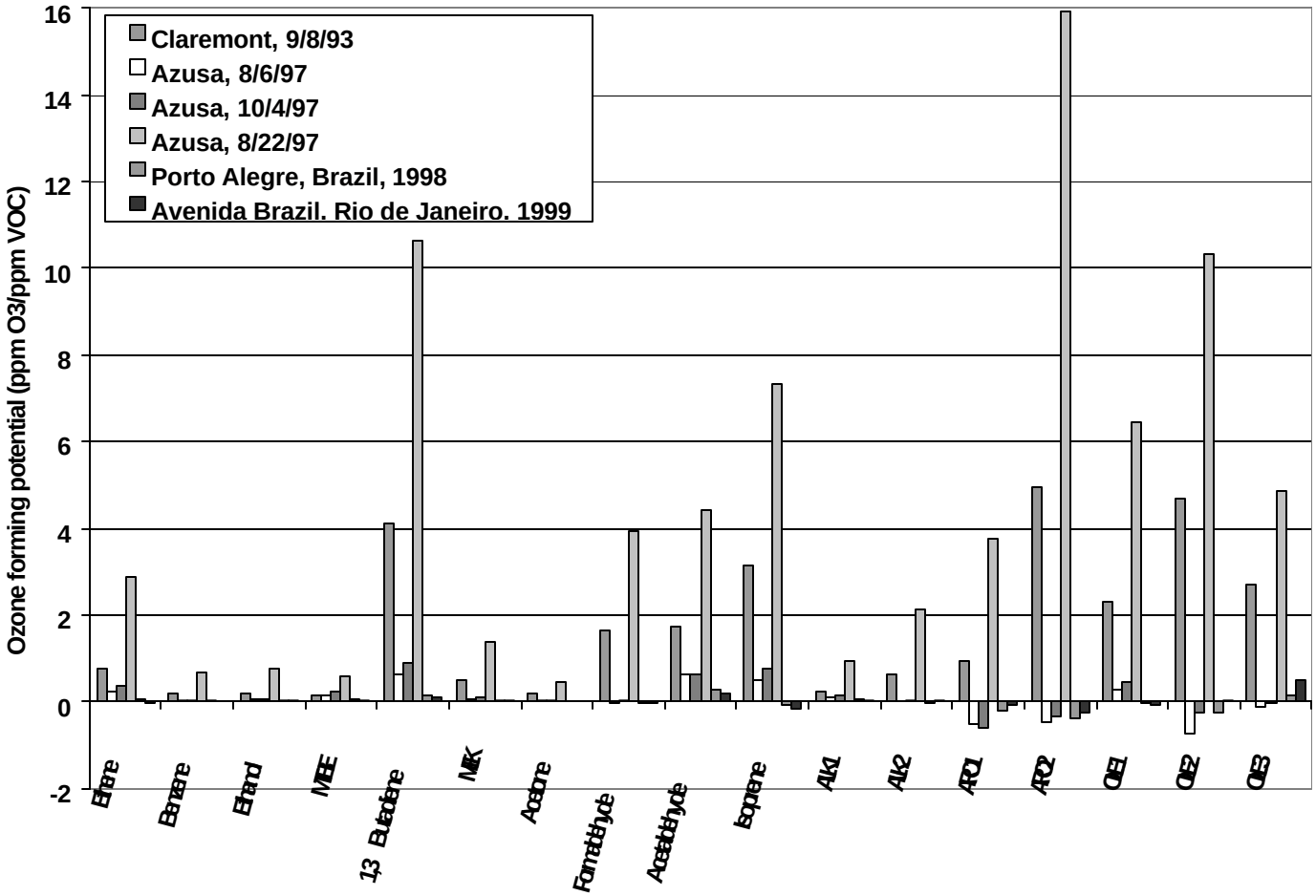

Figure 7.2 Ozone Formation Potentials From Individual VOCs (continued)

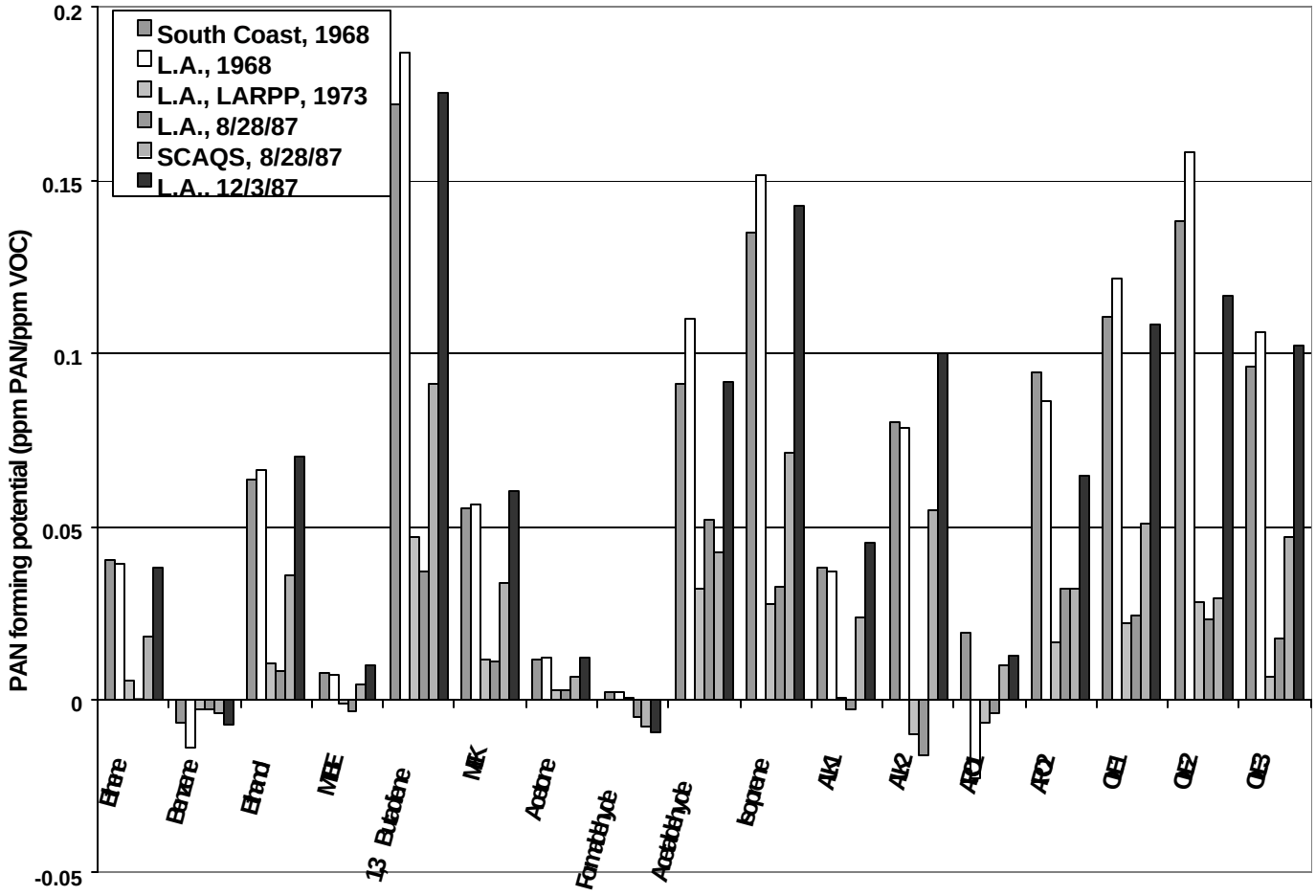

Figure 7.3 PAN Formation Potentials From Individual VOCs

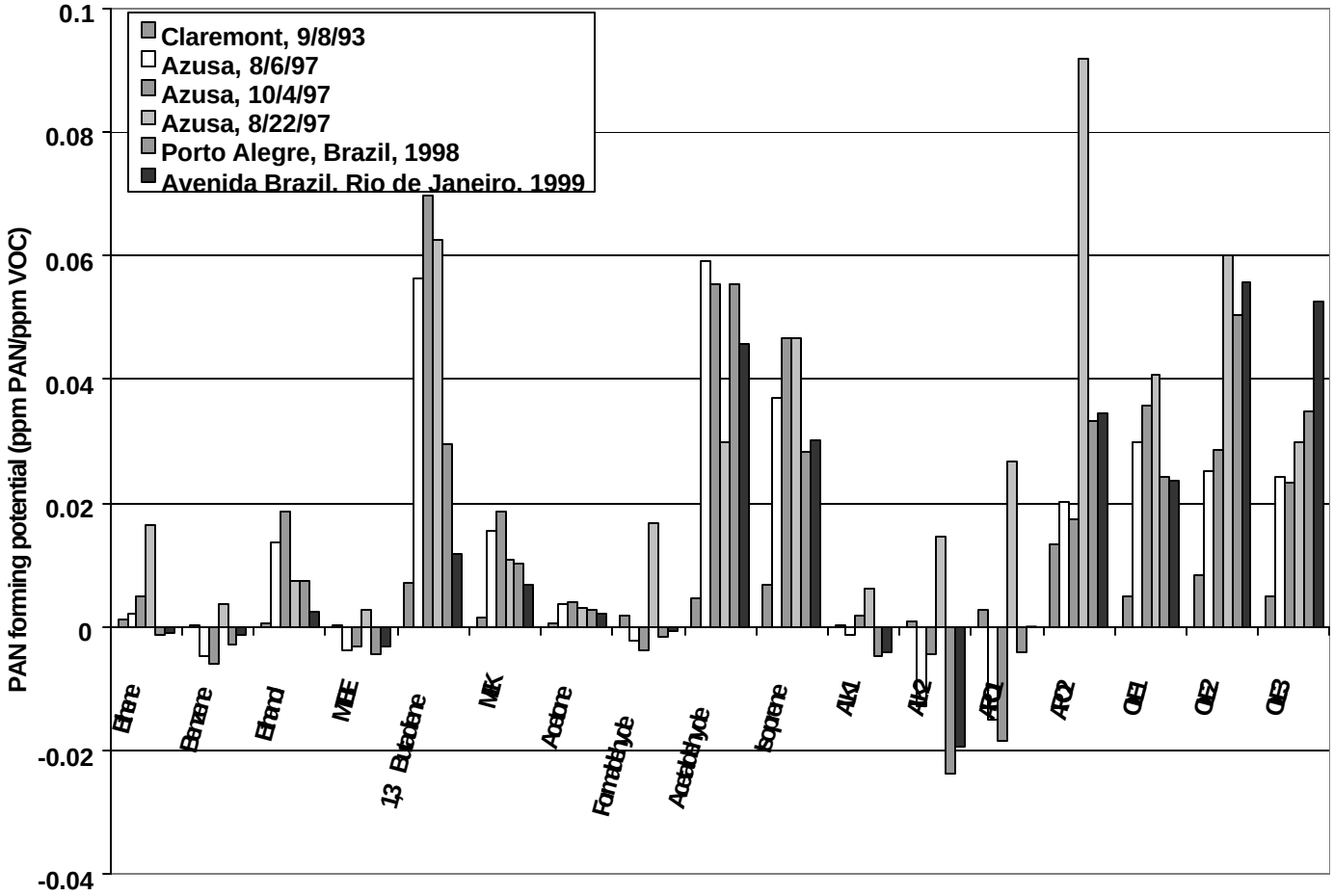

Figure 7.4 PAN Formation Potentials From Individual VOCs (continued)

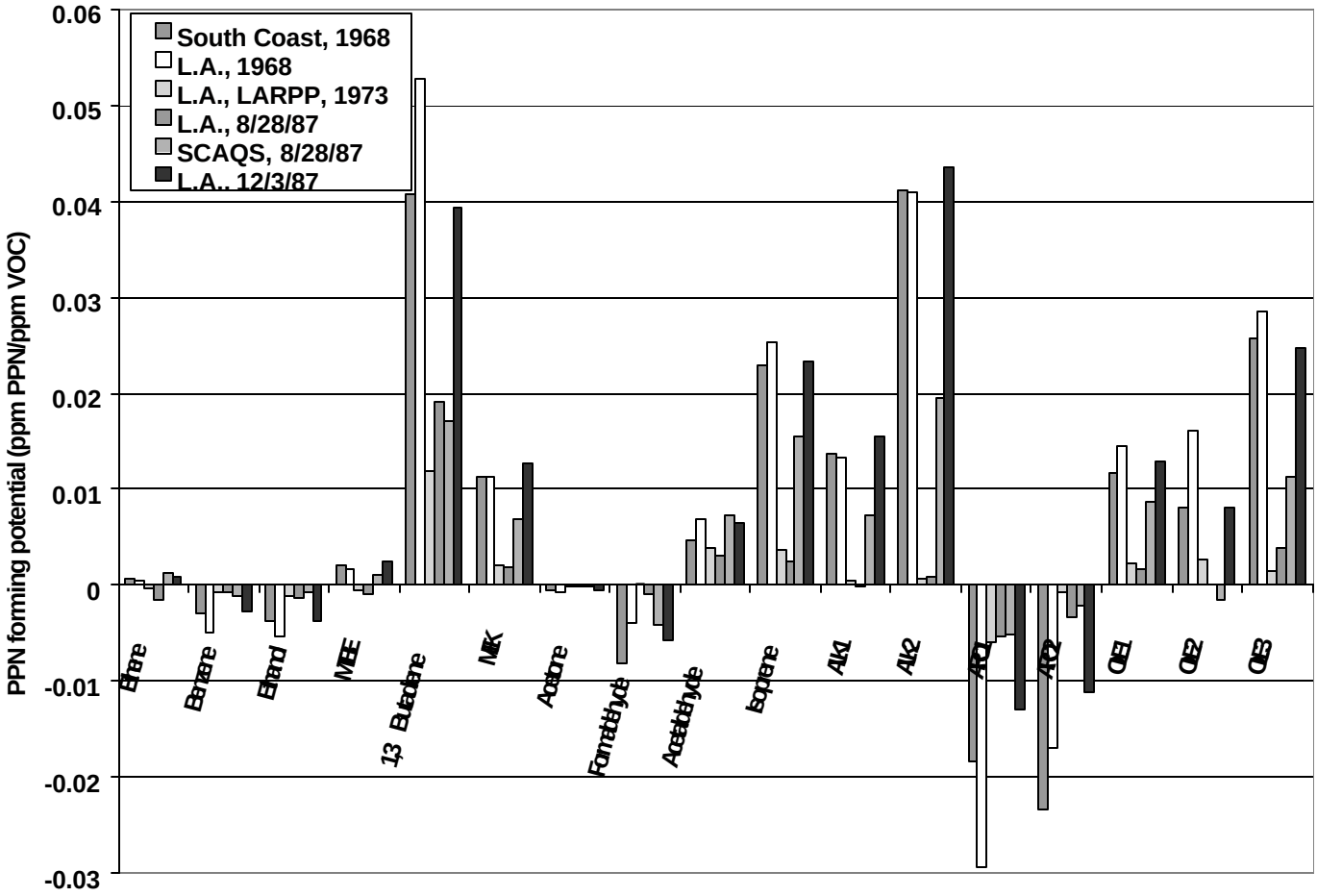

Figure 7.5 PPN Formation Potentials From Individual VOCs

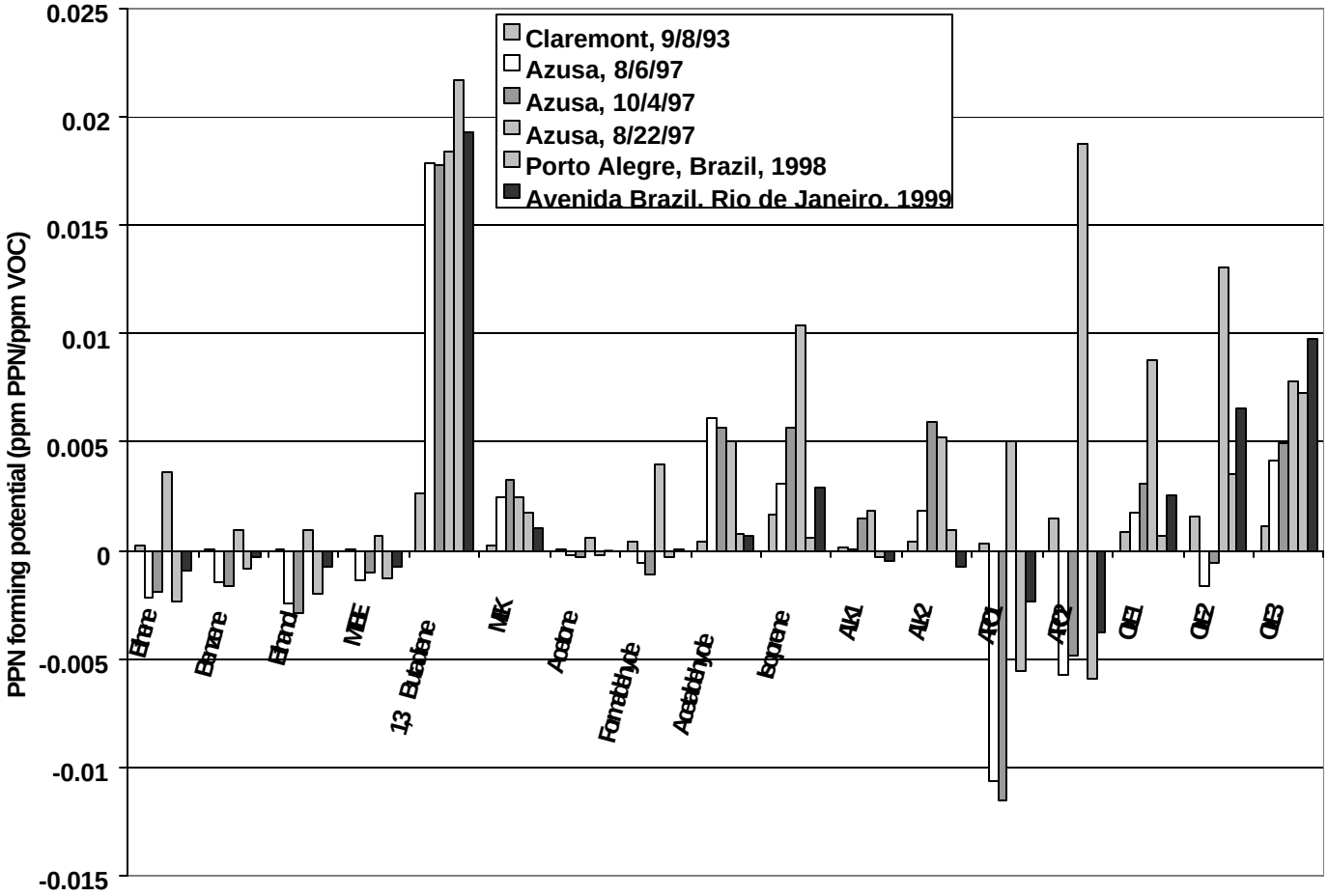

Figure 7.6 PPN Formation Potentials From Individual VOCs (continued)

Table 7.5 Contribution From Individual VOCs to Total Ozone Formation* (ppm)

VOCs	South Coast[b] 1968	Los Angeles[c] 1968	Los Angeles LARPP[d] 1973	Los Angeles 8/28/87[a]	SCAQS 8/28/87[a]	Los Angeles 12/3/87[a]	Claremont[f] 9/8/93	Azusa[e] 8/6/97	Los Angeles[e] 10/4/97	Los Angeles[e] 8/22/97
Ethene	0.09953	0.07193		0.00520	0.03515	0.05048	0.01409	0.00636	0.00939	0.08674
Benzene				0.00043	0.00205	0.00197	0.00049		0.00042	0.00168
Ethanol										
MTBE										
1,3-Butadiene		0.00592					0.00124			0.00186
MEK				0.00004		0.00163		0.00043	0.00010	0.00040
Acetone				0.00004		0.00101		0.00023	0.00014	0.00032
Formaldehyde	0.00569	0.00214	0.00100	-0.00081	0.00290	0.00916		-0.00008	0.00007	0.00113
Acetaldehyde	0.00793	0.00503	0.00362	0.00135	0.00816	0.01019		0.00404	0.00179	0.00414
Isoprene				0.00023		0.00144		0.00044	0.00062	0.03009
ALK1	0.23994	0.22601	0.03184	0.03925	0.12619	0.17033	0.01895	0.04533	0.03887	0.07233
ALK2	0.04231	0.03239	-0.00820	0.00027	0.02027	0.01738	0.00584	0.00011	0.00084	0.02891
ARO1	0.01625	-0.04142	-0.01254	-0.05754	0.00915	0.00557	0.00628	-0.04218	-0.04161	0.04027
ARO2	0.21484	0.12599	-0.00205	-0.04482	0.06570	0.07153	0.02865	-0.04196	-0.01717	0.11135
OLE1	0.04005	0.05394	0.01191	0.01022	0.01559	0.24770	0.00917	0.00613	0.03381	0.04902
OLE2		0.03445	0.00150	-0.00713		0.01561	0.01034	-0.01380	-0.00258	0.02715
OLE3							0.00046			0.01989

*TOFP = $\sum_i (OFP_i)(VOC_i^o)$

[a] Lawson, 1990 [b] Lonemann, 1968 [c] Kopczynski, 1968
[d] Calvert, 1976 [e] McCauley, 1999 [f] Pasek, 1999

Table 7.6 Contribution From Individual VOCs to Ozone Formation* (ppm)

VOCs	Porto Alegre, Brazil 1998[a]	Avenida Brazil, Rio de Janeiro 1999[b]
Ethene	**0.00178**	**-0.00276**
Benzene	**0.00042**	**0.00016**
Ethanol	**0.00009**	**0.00035**
MTBE	**0.00050**	
1,3-Butadiene	**0.00080**	**0.00130**
MEK		
Acetone		
Formaldehyde	**-0.00057**	**-0.00049**
Acetaldehyde	**0.00385**	**0.00203**
Isoprene	**-0.00026**	
ALK1	**0.01700**	**0.03412**
ALK2	**-0.00676**	**0.01356**
ARO1	**-0.02446**	**-0.02267**
ARO2	**-0.08406**	**-0.12305**
OLE1	**-0.00190**	**-0.00541**
OLE2	**-0.02467**	**0.00484**
OLE3		

* **TOFP** = $\sum_i (OFP_i)(VOC_i^o)$

[a] **Grosjean *et al.* (1998)**

[b] **Grosjean (1999)**

Table 7.7 Contribution From Individual VOCs to PAN Formation* (ppm)

VOCs	South Coast[b] 1968	Los Angeles[c] 1968	Los Angeles LARPP[d] 1973	Los Angeles 8/28/87[a]	SCAQS 8/28/87[a]	Los Angeles 12/3/87[a]	Claremont[f] 9/8/93	Azusa[e] 8/6/97	Los Angeles[e] 10/4/97	Los Angeles[e] 8/22/97
Ethene	0.00263	0.00295		0.00001	0.00048	0.00139	0.00002	0.00006	0.00013	0.00050
Benzene				-0.00009	-0.00003	-0.00007	< 1E-05		-0.00008	0.00001
Ethanol										
MTBE										
1,3-Butadiene		0.00051					< 1E-05			0.00001
MEK				0.00001		0.00019		0.00008	0.00002	< 1E-05
Acetone				0.00002		0.00010		0.00006	0.00003	< 1E-05
Formaldehyde	0.00001	0.00001		-0.00004	-0.00004	-0.00010		-0.00002	-0.00003	< 1E-05
Acetaldehyde	0.00046	0.00055	0.00016	0.00018	0.00021	0.00061		0.00037	0.00015	0.00003
Isoprene			0.00000	0.00003		0.00007		0.00003	0.00004	0.00019
ALK1	0.01394	0.01687	0.00011	-0.00129	0.00430	0.01113	0.00003	-0.00041	0.00044	0.00050
ALK2	0.00305	0.00308	-0.00021	-0.00291	0.00096	0.00142	0.00001	-0.00168	-0.00036	0.00020
ARO1	0.00065	-0.00136	-0.00016	-0.00081	0.00017	0.00043	0.00002	-0.00125	-0.00124	0.00028
ARO2	0.00415	0.00701	0.00034	0.00359	0.00060	0.00127	0.00008	0.00179	0.00089	0.00064
OLE1	0.00178	0.00444	0.00052	0.00229	0.00036	0.01166	0.00002	0.00068	0.00267	0.00031
OLE2		0.00319	0.00048	0.00023		0.00059	0.00002	0.00048	0.00029	0.00016
OLE3							< 1E-05			0.00012

* $\text{TPANFP} = \sum_i (PANFP_i)(VOC_i^o)$

[a]Lawson, 1990, [b]Lonemann, 1968, [c]Kopczynski, 1968, [d]Calvert, 1976, [e]McCauley, 1999, [f]Pasek, 1999

Table 7.8 Contribution From Individual VOCs to PAN Formation* (ppm)

VOCs	Porto Alegre, Brazil 1998[a]	Avenida Brazil, Rio de Janeiro 1999[b]
Ethene	**-0.00004**	**-0.00006**
Benzene	**-0.00011**	**-0.00009**
Ethanol	**0.00009**	**0.00012**
MTBE	**-0.00003**	
1,3-Butadiene	**0.00018**	**0.00014**
MEK		
Acetone		
Formaldehyde	**-0.00002**	**-0.00001**
Acetaldehyde	**0.00077**	**0.00047**
Isoprene	**0.00012**	
ALK1	**-0.00151**	**-0.00419**
ALK2	**-0.00471**	**-0.01112**
ARO1	**-0.00048**	**0.00002**
ARO2	**0.00726**	**0.01781**
OLE1	**0.00149**	**0.00177**
OLE2	**0.00505**	**0.00911**
OLE3		

* $\text{TPANFP} = \sum_i (PANFP_i)(VOC_i^o)$

[a] **Grosjean *et al.*, 1998**

[b] **Grosjean, 1999**

Table 7.9 Contribution From Individual VOCs to PPN Formation[a,b] (ppm)

VOCs	Los Angeles 8/28/87[c]	SCAQS 8/28/87[c]	Los Angeles 12/3/87[c]	Azusa[g] 8/6/97	Los Angeles[g] 10/4/97	Los Angeles[g] 8/22/97	Claremont[h] 9/8/93	South Coast[d] 1968	Los Angeles[e] 1968	Los Angeles LARPP[f] 1973
Ethene	0.00004	0.00003		-0.00008	0.00003	0.00003	< 1E-05	-0.00006	-0.00005	0.00011
Benzene				-0.00003	-0.00001	-0.00003	< 1E-05		-0.00002	< 1E-05
Ethanol										
MTBE										
1,3 Butadiene		0.00015					< 1E-05			< 1E-05
MEK						0.00004		0.00001	< 1E-05	< 1E-05
Acetone						> -1E-05		> -1E-05	> -1E-05	< 1E-05
Formaldehyde	-0.00004	-0.00002		-0.00001	-0.00002	-0.00006		-0.00001	-0.00001	< 1E-05
Acetaldehyde	0.00002	0.00003	0.00002	0.00001	0.00004	0.00004		0.00004	0.00002	< 1E-05
Isoprene				< 1E-05		0.00001		< 1E-05	< 1E-05	0.00004
ALK1	0.00506	0.00608	0.00013	-0.00004	0.00132	0.00380	0.00001	0.00003	0.00035	0.00014
ALK2	0.00156	0.00160	0.00001	0.00015	0.00034	0.00062	< 1E-05	0.00024	0.00049	0.00007
ARO1	-0.00061	-0.00177	-0.00014	-0.00108	-0.00009	-0.00044	< 1E-05	-0.00088	-0.00078	0.00005
ARO2	-0.00103	-0.00138	-0.00002	-0.00038	-0.00004	-0.00022	0.00001	-0.00051	-0.00025	0.00013
OLE1	0.00019	0.00053	0.00005	0.00015	0.00006	0.00139	< 1E-05	0.00004	0.00023	0.00007
OLE2		0.00032	0.00004	< 1E-05		0.00004	< 1E-05	-0.00003	-0.00001	0.00003
OLE3							< 1E-05			0.00003

[a] $\mathrm{TPPNFP} = \sum_i (PPNFP_i)(VOC_i^o)$.

[b] Note that PPN represents peroxypropionyl nitrate and higher molecular weight acyl peroxy nitrates

[c] Lawson, 1990, [d] Lonemann, 1968 [e] Kopczynski, 1968, [f] Calvert, 1976, [g] McCauley, 1999, [h] Pasek, 1999

Table 7.10 Contribution From Individual VOCs to PPN Formation[a,b] (ppm)

VOCs	Porto Alegre, Brazil 1998[c]	Avenida Brazil, Rio de Janeiro 1999[d]
Ethene	-0.00008	-0.00005
Benzene	-0.00003	-0.00002
Ethanol	-0.00002	-0.00004
MTBE	-0.00001	
1,3-Butadiene	0.00013	0.00023
MEK		
Acetone		
Formaldehyde	> -1E-05	< 1E-05
Acetaldehyde	0.00001	0.00001
Isoprene	< 1E-05	
ALK1	-0.00009	-0.00045
ALK2	0.00019	-0.00044
ARO1	-0.00065	-0.00058
ARO2	-0.00128	-0.00193
OLE1	0.00004	0.00019
OLE2	0.00035	0.00107
OLE3		

[a] $\text{TPPNFP} = \sum_i (PPNFP_i)(VOC_i^o)$

[b] Note that PPN represents peroxypropionyl nitrate and higher molecular weight. acyl peroxy nitrates

[c] Grosjean *et al.* (1998)

[d] Grosjean (1999)

Individual reactivities or forming potentials from the results show a variation in estimated values across different scenarios, because a VOC reactivity is dependent upon local ambient conditions, such as VOC/NO_x ratios noted in previous studies (Carter, 1989; Derwent and Jenkin, 1991). A relative scale to each base mixture reactivity may significantly eliminate the variation of individual reactivities over different ambient conditions. However, pursuing a robust regulatory reactivity or forming potential scale is beyond the scope of this study.

B-7.4. Other Study of PAN Formation Potentials

The PAN formation potential results in Table 7.7 and Table 7.8 are in agreement with the results obtained by Bowman and Seinfeld (1994) for the relative contribution of lumped VOC species to PAN formation. From Table 7.11, ALK1, ALK2, ARO2, and OLE1 have large contributions to PAN formation, while acetaldehyde has a low contribution to PAN formation.

Table 7.11 Relative Contribution of Lumped VOC Species to PAN Formation[a]

Species	Description[b]	Initial Concentration[d] (ppbC)	Contribution to PAN[d] (%)
CO	Carbon monoxide	1,500	-
CH4	Methane	1,700	-
HCHO	Formaldehyde	8	-
CCHO	Acetaldehyde	5	2.6
RCHO	Higher molecular weight aldehydes	2	0.5
MEK	Higher molecular weight ketones	16	1.4
ALK1	Low molecular weight alkanes	353	18.6
ALK2	Higher molecular weight alkanes	236	13.5
ARO1	Benzene and toluene	147	9.4
ARO2	Higher molecular weight aromatics (mostly xylenes)	108	15.2
ETHE	Ethylene	75	6.8
OLE1	Low molecular weight, less reactive alkenes	60	14.9
OLE2	Low molecular weight, more reactive alkenes	29	8.9
OLE3	Biogenic compounds (isoprene + terpenes)	62	8.3

[a] Adapted from Bowman and Seinfeld (1994)

[b] SAPRC90 (Carter, 1990)

[c] Using 1987 SCAQS emission inventory as input data

[d] At $VOC/NO_X = 8.2$ ppbC/ppb

B-8. References

ARB (Air Resources Board) (1992) “Technical Guidance Document: Photochemical Modeling,” April (http://www.arb.ca.gov/ccaqs/models/models.htm).

ARB (Air Resources Board) (1999) “EMFAC2000 On-Road Emissions Inventory Estimation Model - Technical Support Document,” November (http://www.arb.ca.gov/msei/pubs/tsd.zip).

Atkinson, R. (1999a) Letter to Bart Croes, November 23.

Atkinson, R. (1999b) Communication to Bart Croes, November 30.

Bowman, F.M. and J.H. Seinfeld (1994) “Ozone Productivity of Atmospheric Organics,” *Journal of Geophysical Research*, **99:** 5309-5324.

Calvert, J.G (1976) “Hydrocarbon Involvement in Photochemical Smog Formation,” *Environmental Science & Technology*, **10:** 256-262.

Carter, W.P.L (1988) “Appendix C: Documentation for the SAPRC Atmospheric Photochemical Mechanism Preparation and Emissions Processing Programs for Implementation in Airshed Models,” Final Report for Air Resources Board. Contract No. A5-122-32, October.

Carter, W.P.L and R. Atkinson (1989) “Computer Modeling Studies of Incremental Hydrocarbon Reactivity,” *Environmental Science & Technology*, **23:** 864-880.

Carter, W.P.L. (1990) “A Detailed Mechanism for the Gas-Phase Atmospheric Reactions of Organic Compounds,” *Atmospheric Environment*, **24A:** 481-518.

Carter, W.P.L, D. Luo, I.L. Malkina, and J.A. Pierce (1993) "An Experimental and Modeling Study of the Photochemical Ozone Reactivity of Acetone," Final Report for Chemical Manufacturers Association Contract No. KET-ACE-CRC.

Carter, W.P.L. (1994) “Development of Ozone Reactivity Scales for Organic Gases,” *Journal of the Air & Waste Management Association*, **44:** 881-899.

Carter, W.P.L. (1995) “Computer Modeling of Environmental Chamber Studies of Maximum Incremental Reactivities of Volatile Organic Compounds,” *Atmospheric Environment*, **29:** 2513-2527.

Carter, W.P.L. (1996) “Condensed Atmospheric Photooxidation Mechanisms for Isoprene,” *Atmospheric Environment*, **30:** 4275-4290.

Carter, W.P.L., D Luo, and I.L. Malkina (1997) “Environmental Chamber Studies for Development of an Updated Photochemical Mechanism for VOC Reactivity Assessment,” Final Report for California Air Resources Board Contract 92-345, Coordinating Research Council Project M-9, and National Renewable Energy Laboratory Contract ZF-2-12252-07, November 26.

Carter, W.P.L (1999a), Personal Communication, Riverside, CA.

Carter, W.P.L (1999b) "Documentation of the SAPRC-99 Chemical Mechanism for VOC Reactivity Assessment," Draft Report to the California Air Resources Board, September 13.

De Haan, *et al.* (1999), *Int. Rev. Phys. Chem*. **18**, 343

Derwent, R.G., Jenkin, M.E. (1991) "Hydrocarbons and the Long-Range Transport of Ozone and PAN Across Europe, *Atmospheric Environment*, **25A:** 1661-1678.

Derwent, R.G., M.E. Jenkin, S.M. Saunders, and M.J. Pilling (1998) "Photochemical Ozone Creation Potentials for Organic Compounds in Northwest Europe Calculated with A Master Chemical Mechanism," *Atmospheric Environment*, **32:** 2429-2441.

Fantechi, G., N.R. Jensen, O. Saastad, J. Hjorth, and J. Peeters (1998) "Reactions of Cl Atoms With Selected VOC: Kinetics, Products and Mechanisms," *Journal of Atmospheric Chemistry*, **31:** 247-267.

Finlayson-Pitts, B.J. and J.N. Pitts, Jr. (1986) *"Atmospheric Chemistry: Fundamentals and Experimental Techniques,"* A Wiley-Interscience Publication, John Wiley & Sons, New York.

Finlyson-Pitts, B.J. (1999), Comments on Draft Report: Air Quality Impacts of the Use of Ethanol in California Reformulated Gasoline, December 6 Letter to Bart Croes, CARB.

Gery, M., G.Z. Whitten, J.P. Killus, and M.C. Dodge (1990) "A Photochemical Kinetics Mechanism for Urban and Regional Scale Computer Modeling," *Journal of Geophysical Research,* **94:** 12,925-12,956.

Grosjean, E., D. Grosjean, and R.A. Rasmussen (1998) "Ambient Concentrations, Sources, Emission Rates and Photochemical Reactivity of C2-C10 Hydrocarbons in Porto Alegre, Brazil," *Environmental Science & Technology*, **32:** 2061-2069.

Grosjean, D. (1999) Personal Communication, Ventura, CA.

Hov, Ö. (1985), The Effects of Chlorine on the Formation of Photochemical Oxidants in Southern Telemark, Norway. *Atmospheric Environment* **19**: 471.

Khan, M., Y.J. Yang, and A.G. Russell (1999), "Photochemical Reactivities of Common Solvents: Comparisons between Urban and Regional Domains," *Atmospheric Environment*, **33:** 1085-1092.

Kopczynski, S.L., W.A. Lonneman, F.D. Sutterfield, and P.E. Darley (1972) "Photochemistry of Atmospheric Samples in Los Angeles," *Environmental Science & Technology,* **6:** 342-347.

Kumar, N., F.W. Lurmann, and W.P.L. Carter (1995) "Development of the Flexible Chemical Mechanism Version of the Urban Airshed Model," Final Report STI-94470-1508-FR. prepared for the California Air Resources Board, August.

Kumar, N., F.W. Lurmann, and W.P.L Carter (1996) "Assessment of Effects of Chemical Uncertainty on Airshed Model Results," Final Report for California Air Resources Board Contract No. 93-716, Statewide Air Pollution Research Center, Riverside, California, June 13.

Lawson, D.R. (1990) "The Southern California Air Quality Study," *Journal of the Air & Waste Management Association* **40:** 156-165.

Lonnemann, W.A., S.L. Kopczynski, P.E. Darley and F.D. Sutterfield (1974) "Hydrocarbon Composition of Urban Air Pollution," *Environmental Science & Technology*, **8:** 229-234.

McCauley, E. (1999) Personal Communication, Sacramento, CA.

Morris, R.E. and T.C. Myers (1990) "User's Guide for the Urban Airshed Model, Volume I: Users Manual for UAM (CB-IV)" Systems Applications, Inc., EPA-450/4-90-007A, June.

Pasek, R. (1999) Personal Communication, Sacramento, CA.

Platt, U. and G. Moortgat (1999) "Heterogeneous and Homogeneous Chemistry of Reactive Halogen Compounds in the Lower Troposphere." *Journal of Atmospheric Chemistry*, **34:** 1-8.

SCAQMD (South Coast Air Quality Management District) (1994) "1994 Air Quality Management Plan," September.

Singer, B.C. and R.A. Harley (2000) "A Fuel-Based Inventory of Motor Vehicle Exhaust Emissions in the Los Angeles Area During Summer 1997," *Atmospheric Environment*, in press.

Stutz, J., K. Hebestreit, B. Alicke, and U. Platt (1999) "Chemistry of Halogen Oxides in the Troposphere: Comparison of Model Calculations with Recent Field Data." *Journal of Atmospheric Chemistry*, **34:** 65-85.

Whitten, G.Z., H. Hogo, and J.P. Killus (1980) "The Carbon-Bond Mechanism: A Condensed Kinetic Mechanism for Photochemical Smog," *Environmental Science & Technology*, **14:** 690-700.

Yang, Y.J., W.R. Stockwell, and J.B. Milford (1995) "Uncertainty in Incremental Reactivities of Volatile Organic Compounds," *Environmental Science & Technology*, **29:** 1336-1345.

Attachment B1 – Listing of SAPRC97 Chemical Mechanism

This attachment provides a listing of the SAPRC97 mechanism. Separate listings are provided for the isoprene reaction mechanism and for other species treated explicitly in Attachments B2 and B3, respectively. Interpretation of reactions rates constants can be found in Kumar *et al.* (1996). Note that this chemical mechanism contains explicit gas-phase reactions for some organic compounds, such as formaldehyde, acetaldehyde, ethylene, and PAN. However, the PPN model species represents higher acyl peroxy nitrates (e.g., CH_3-CH_2-CH_2-CH_2-CO-OO-NO_2), but not alkyl peroxy nitrates such as CH_3-CH_2-CH_2-CH_2-OO-NO_2. The latter are not represented in the model because of their rapid back-decomposition to reactants at ambient temperatures. PPN does not represent the aromatic acyl peroxy nitrates that are represented by the PBZN model species (Carter, 1990 and 1999a). In the newest version of update to the mechanism, SAPRC99, Carter (1999b) uses PAN2 instead of PPN.

A summary of the reaction rate constants used in the mechanism is provided for the benefit of the reader. The default rate parameter, k, input in the mechanism is:

Label) A, E, B ; reaction list

Where

$$k = A(T/T_{REF})^{B}\exp(-E/RT) \qquad \text{(B1-1)}$$

Where A is the Arrhenius pre-exponential factor in $cm^3 molecule^{-1} sec^{-1}$, T_{REF} is a reference temperature (300 K), B is a constant, E is activation energy in kcal/mole, and R is the ideal gas constant in $kcal\, mole^{-1} K^{-1}$ (Kumar *et al.*, 1995). For those reaction rate constants that are temperature and pressure dependent, the Troe falloff expression is used. The default input parameters for the falloff rates constant are:

Label) FALLOFF ; reaction list

A0, E0, B0

A1, E1, B1

F, N

The falloff expression is

$$k = [k0*M/(1+(K0*M/K1))]*F^{Z} \qquad \text{(B1-2)}$$

with

$$Z = 1/[\ 1+\log_{10}(k0*M/k1)/N^2\ ] \qquad \text{(B1-3)}$$

Where

$$k0 = A0*[(T/T_{REF})^{B0}]*\exp(-E0/RT) \qquad \text{(B1-4)}$$

$$k1 = A1*[(T/T_{REF})^{B1}]*\exp(-E1/RT) \qquad \text{(B1-5)}$$

Here, k0 is the low-pressure limiting rate constant, and A0 its value at 300 K, k1 is the high-pressure limiting rate constant, with A1 its value at 300 K. For second-order

reactions, the units of k0, k1, A0, and A1 are in cm^3 $molecule^{-1}sec^{-1}$, while for first-order reaction the units are in sec^{-1}. F is the broadening factor of the falloff curve, M is the total pressure fixed at 1.0 $x10^6$ ppm. The constants E0 and E1 are activation energies in kcal $mole^{-1}$ $^oK^{-1}$, and B0, B1, and N are constants for each reaction (Finlayson-Pitts, 1986; Kumar *et al.*, 1995; Carter, 1990). Finally, photolytic reactions are indicated by the PF= label.

```
1)          PF=NO2                  ;NO2 + HV = NO + O
2) 6.0E-34, 0.0, -2.3               ;O + O2 + M = O3 + M
3A) 6.5E-12,  -0.238                ;O + NO2 = NO + O2
!
3B)         FALLOFF                 ;O + NO2 = NO3 + M
9.0E-32  0.0  -2.0
2.2E-11  0.0   0.0
0.6      1.0
!
4) 2.00E-12,  2.782                 ;O3 + NO = NO2 + O2
5) 1.400E-13,  4.968                ;O3 + NO2 = O2 + NO3
 6) 1.7E-11, -0.298                 ;NO + NO3 = #2 NO2
7) 3.300E-39, -1.05                 ;NO + NO + O2 = #2 NO2
!
 8)         FALLOFF                 ;NO2 + NO3 = N2O5
2.2E-30  0.0  -4.3
1.5E-12  0.0  -0.5
0.6      1.0
!
9) 9.09E+26, 22.26                  ;N2O5 + #RCON8 = NO2 + NO3
10) 1.0E-21 0.0                     ;N2O5 + H2O = #2 HNO3
11) 2.5E-14, 2.44                   ;NO2 + NO3 = NO + NO2 + O2
12A)      PF=NO3NO                  ;NO3 + HV = NO + O2
12B)      PF=NO3NO2                 ;NO3 + HV = NO2 + O
13A)      PF=O3O3P                  ;O3 + HV = O + O2
13B)      PF=O3O1D                  ;O3 + HV = O*1D2 + O2
14) 2.2E-10,         0.0            ;O*1D2 + H2O = #2 HO
15) 1.919E-11,     -0.251           ;O*1D2 + M = O + M
!
16)         FALLOFF                 ;HO  + NO = HONO
7.0E-31  0.0  -2.6
1.5E-11   0.0  -0.5
0.6          1.0
!
 17)        PF=HONO                 ;HONO + HV = HO  + NO
!
 18)        FALLOFF                 ;HO  + NO2 = HNO3
2.6E-30  0.0  -3.2
2.4E-11  0.0  -1.3
0.6         1.0
!
 19) 6.45E-15,      -1.652           ;HO  + HNO3 = H2O + NO3     ! 1 ATM ONLY.
21) 2.4E-13, 0.0                    ;HO  + CO = HO2  + CO2      !1 ATM ONLY
22) 1.600E-12,  1.87                ;HO  + O3 = HO2  + O2
 23) 3.700E-12, -0.48               ;HO2  + NO = HO  + NO2
!
24)         FALLOFF                 ;HO2  + NO2 = HNO4
```

```
1.8E-31  0.0  -3.2
4.7E-12  0.0  -1.4
0.6      1.0
!
25) 4.76E+26, 21.66          ;HNO4 + #RCON24 = HO2  + NO2
 27) 1.3E-12,        -0.755  ;HNO4 + HO  = H2O + NO2 + O2
 28) 1.100E-14,  0.994       ;HO2  + O3 = HO  + #2 O2
 29A) 2.2E-13,   -1.23       ;HO2  + HO2  = H2O2 + O2
 29B) 1.9E-33,      -1.95    ;HO2  + HO2  + M = H2O2 + O2
 29C) 3.1E-34,   -5.60       ;HO2  + HO2  + H2O = H2O2 + O2 + H2O
!29D) 2.7E-54,   -6.32       ;HO2  + HO2  + M + H2O = H2O2 + O2  +H2O
 29D) 6.6E-35,   -6.32       ;HO2  + HO2  + H2O = H2O2 + O2 + H2O  !(1 ATM ONLY)
 30A) 2.2E-13,   -1.23       ;NO3 + HO2  = HNO3 + O2
 30B) 1.9E-33,      -1.95    ;NO3 + HO2  + M = HNO3 + O2
 30C) 3.1E-34,   -5.60       ;NO3 + HO2  + H2O = HNO3 + O2 + H2O
 30D) 6.6E-35,   -6.32       ;NO3 + HO2  + H2O = HNO3 + O2 + H2O
31) PF=H2O2                  ;H2O2 + HV = #2 HO
32) 3.300E-12, 0.397         ;H2O2 + HO  = HO2  + H2O
33) 4.60E-11,  -0.457        ;HO  + HO2  = H2O + O2
B1) 4.200E-12, -0.360        ;RO2  + NO = NO
!
B2)       FALLOFF            ;RCO3  + NO = NO
5.65E-28  0.0  -7.1
2.64E-11  0.0  -0.9
0.27      1.0
!
B4)       FALLOFF            ;RCO3  + NO2 = NO2
2.57E-28  0.0  -7.1
12.0E-12  0.0  -0.9
0.30      1.0
!
B5) 3.40E-13,  -1.590        ;RO2  + HO2  = HO2
B6) 3.40E-13,  -1.590        ;RCO3  + HO2  = HO2
B8)  1.0E-15                 ;RO2  + RO2  =
B9)  1.86E-12, -1.053        ;RO2  + RCO3  =
B10) 2.8E-12, -1.053         ;RCO3  + RCO3  =
B11)      SAMEK B1           ;RO2-R  + NO = NO2 + HO2
B12)      SAMEK B5           ;RO2-R  + HO2  = XOOH
B13)      SAMEK B8           ;RO2-R  + RO2  = RO2  + #.5 HO2
B14)      SAMEK B9           ;RO2-R  + RCO3  = RCO3  + #.5 HO2
B19)      SAMEK B1           ;RO2-N  + NO = RNO3
B20)      SAMEK B5           ;RO2-N  + HO2  = XOOH + MEK  + #1.5 XC
B21)      SAMEK B8           ;RO2-N  + RO2  = RO2  + #.5 HO2  + MEK + #1.5 XC
B22)      SAMEK B9           ;RO2-N  + RCO3  = RCO3  + #.5 HO2  + MEK + #1.5 XC
B15)      SAMEK B1           ;R2O2  + NO = NO2
B16)      SAMEK B5           ;R2O2  + HO2  =
B17)      SAMEK B8           ;R2O2  + RO2  = RO2
B18)      SAMEK B9           ;R2O2  + RCO3  = RCO3
B23)      SAMEK B1           ;RO2-XN  + NO = XN
B24)      SAMEK B5           ;RO2-XN  + HO2  = XOOH
B25)      SAMEK B8           ;RO2-XN  + RO2  = RO2  + #.5 HO2
B26)      SAMEK B9           ;RO2-XN  + RCO3  = RCO3  + HO2
G2)       SAMEK B1           ;RO2-NP  + NO = NPHE
G3)       SAMEK B5           ;RO2-NP  + HO2  = XOOH + #6 XC
G4)       SAMEK B8           ;RO2-NP  + RO2  = RO2  + #.5 HO2  + #6 XC
G5)       SAMEK B9           ;RO2-NP  + RCO3  = RCO3  + HO2  + #6 XC
```

```
B7)       PF=CO2H                ;XOOH + HV = HO2  + HO
B7A) 1.18E-12, -0.254            ;HO  + XOOH = HO
B7B) 1.79E-12, -0.435            ;HO  + XOOH = RO2-R  + RO2
C1)       PF=HCHONEWR            ;HCHO + HV = #2 HO2  + CO
C2)       PF=HCHONEWM            ;HCHO + HV = H2 + CO
C3) 1.125E-12 -1.288 2.0         ;HCHO + HO  = HO2  + CO + H2O
C4)  9.7E-15, -1.242             ;HCHO + HO2  = HOCOO
C4A)  2.4E+12,  13.91            ;HOCOO  = HO2  + HCHO
C4B)      SAMEK B1               ;HOCOO  + NO = XC + NO2 + HO2
C9) 2.8E-12,        5.00         ;HCHO + NO3 = HNO3 + HO2  + CO
C10) 5.55E-12, -0.618            ;CCHO + HO  = CCO-O2  + H2O + RCO3
C11A) PF=CCHOR                   ;CCHO + HV = CO + HO2  + HCHO + RO2-R  + RO2
C12) 1.4E-12,  3.696             ;CCHO + NO3 = HNO3 + CCO-O2  + RCO3
C25) 8.5E-12  -0.50              ;RCHO + HO  = C2CO-O2  + RCO3
C26)      PF=RCHO                ;RCHO + HV = CCHO + RO2-R  + RO2  + CO + HO2
C27)  1.4E-12,  3.696            ;NO3 + RCHO = HNO3 + C2CO-O2  + RCO3
C38) 4.81E-13 0.457 2.0          ;ACET + HO  = R2O2  + HCHO + CCO-O2  + RCO3  + RO2
C39)      PF=ACET-93C            ;ACET + HV = CCO-O2  + HCHO + RO2-R  + RCO3  + RO2
C44) 2.92E-13 -0.823 2.0         ;MEK + HO  = H2O + #.5 "CCHO + HCHO + CCO-O2  + &
                                 C2CO-O2 " + RCO3  + #1.5 "R2O2  + RO2 "
C57)      PF=KETONE              ;MEK + HV + #0.1 = CCO-O2  + CCHO + RO2-R  + RCO3  &
                                 + RO2
C95)  2.191E-11, 1.408           ;RNO3 + HO  = NO2 + #.155 MEK + #1.05 RCHO + &
                                  #.48 CCHO + #.16 HCHO + #.11 XC + #1.39 "R2O2  + RO2 "
C13)      SAMEK B2               ;CCO-O2  + NO = CO2 + NO2 + HCHO + RO2-R  + RO2
C14)      SAMEK B4               ;CCO-O2  + NO2 = PAN
C15)      SAMEK B6               ;CCO-O2  + HO2  = XOOH + CO2 + HCHO
C16)      SAMEK B9               ;CCO-O2  + RO2  = RO2  + #.5 HO2  + CO2 + HCHO
C17)      SAMEK B10              ;CCO-O2  + RCO3  = RCO3  + HO2  + CO2 + HCHO
!
 C18)     FALLOFF                ;PAN = CCO-O2  + NO2 + RCO3
4.90E-03  23.972  0.0
4.00E+16  27.079  0.0
0.30      1.00
!
C28)      SAMEK B2               ;C2CO-O2  + NO = CCHO + RO2-R  + CO2 + NO2 + RO2
C29)  8.4E-12 0.0 0.0            ;C2CO-O2  + NO2 = PPN
C30)      SAMEK B6               ;C2CO-O2  + HO2  = XOOH + CCHO + CO2
C31)      SAMEK B9               ;C2CO-O2  + RO2  = RO2  + #.5 HO2  + CCHO + CO2
C32)      SAMEK B10              ;C2CO-O2  + RCO3  = RCO3  + HO2  + CCHO + CO2
C33) 1.6E+17, 27.966             ;PPN = C2CO-O2  + NO2 + RCO3
TBON)  2.4E-11                   ;C2(C)-O  + NO2 = RNO3 + #-2 XC
TBOD)  7.5E+14, 16.2             ;C2(C)-O  = ACET + HCHO + RO2-R  + RO2
C58A)    PF=GLYOXAL1             ;GLY + HV  = #.8 HO2  + #.45 HCHO + #1.55 CO
C58B)    PF=GLYOXAL2             ;GLY + HV + #0.029 = #.13 HCHO + #1.87 CO
 C59)     1.14E-11               ;GLY + HO  = #.6 HO2  + #1.2 CO + #.4 "HCOCO-O2  + &
                                 RCO3 "
 C60)     SAMEK C12              ;GLY + NO3 = HNO3 + #.6 HO2  + #1.2 CO + &
                                  #.4 "HCOCO-O2  + RCO3 "
 C62)     SAMEK B2               ;HCOCO-O2  + NO = NO2 + CO2 + CO + HO2
 C63)     SAMEK B4               ;HCOCO-O2  + NO2 = GPAN
 C64)     SAMEK C18              ;GPAN = HCOCO-O2  + NO2 + RCO3
 C65)     SAMEK B6               ;HCOCO-O2  + HO2  = XOOH + CO2 + CO
 C66)     SAMEK B9               ;HCOCO-O2  + RO2  = RO2  + #.5 HO2  + CO2 + CO
 C67)     SAMEK B10              ;HCOCO-O2  + RCO3  = RCO3  + HO2  + CO2 + CO
C68A)    PF=MEGLYOX1             ;MGLY + HV = HO2  + CO + CCO-O2  + RCO3
```

```
C68B)   PF=MEGLYOX2          ;MGLY + HV + #.107 = HO2  + CO + CCO-O2  + RCO3
C69)    1.72E-11             ;MGLY + HO  = CO + CCO-O2  + RCO3
C70)    SAMEK C12            ;MGLY + NO3 = HNO3 + CO + CCO-O2  + RCO3
G46)    2.63E-11             ;HO  + PHEN = #.15 RO2-NP  + #.85 RO2-R  + #.2 GLY + &
                             #4.7 XC + RO2
G51)    3.6E-12              ;NO3 + PHEN = HNO3 + BZ-O
G52)    4.2E-11              ;HO  + CRES = #.15 RO2-NP  + #.85 RO2-R  + #.2 MGLY + &
                              #5.5 XC + RO2
G57)    2.1E-11              ;NO3 + CRES = HNO3 + BZ-O  + XC
G30)    1.29E-11             ;BALD + HO  = BZ-CO-O2  + RCO3
G31)    PF=BZCHO             ;BALD + HV + #.05 = #7 XC
G32) 1.4E-12,  3.747         ;BALD + NO3 = HNO3 + BZ-CO-O2
G33)    SAMEK B2             ;BZ-CO-O2  + NO = BZ-O  + CO2 + NO2 + R2O2  + RO2
G34) 8.4E-12 0.0 0.0         ;BZ-CO-O2  + NO2 = PBZN
G36)    SAMEK B6             ;BZ-CO-O2  + HO2  = XOOH + CO2 + PHEN
G37)    SAMEK B9             ;BZ-CO-O2  + RO2  = RO2  + #.5 HO2  + CO2 + PHEN
G38)    SAMEK B10            ;BZ-CO-O2  + RCO3  = RCO3  + HO2  + CO2 + PHEN
G35)  1.6E+15,  25.90        ;PBZN = BZ-CO-O2  + NO2 + RCO3
G43) 1.3E-11, -0.596         ;BZ-O  + NO2 = NPHE
G44)    SAMEK B5             ;BZ-O  + HO2  = PHEN
G45)    1.0E-3               ;BZ-O  = PHEN
G58)    3.6E-12              ;NPHE + NO3 = HNO3 + BZ(NO2)-O
G59)    SAMEK G43            ;BZ(NO2)-O  + NO2 = #2 XN + #6 XC       ! DINITROPHENOL
G60)    SAMEK B5             ;BZ(NO2)-O  + HO2  = NPHE
G61)    SAMEK G45            ;BZ(NO2)-O  = NPHE
G7)     1.14E-11             ;HO  + AFG1 = HCOCO-O2  + RCO3
G8)     PF=ACROLEIN          ;AFG1 + HV + #0.077 = HO2  + HCOCO-O2  + RCO3
U2OH)   1.72E-11             ;HO  + AFG2 = C2CO-O2  + RCO3
U2HV)   PF=ACROLEIN          ;AFG2 + HV = HO2  + CO + CCO-O2  + RCO3
RCH4) 6.255E-13 2.548 2.0    ;CH4 + HO  = HCHO + RO2-R  + RO2
RZ1)    1.0                  ;(HCHO2) = #.7 HCOOH + #.12 "HO  + HO2  + CO" + &
                              #.18 "H2 + CO2"
RZ2)    1.0                  ;(CCHO2) = #.25 CCOOH + #.15 "CH4 + CO2" + #.6 HO  + &
                              #.3 "CCO-O2  + RCO3 " + #.3 "RO2-R  + HCHO + CO + &
                              RO2 "
RZ3)    1.0                  ;(RCHO2) = #.25 CCOOH + #.15 CO2 + #.6 HO  + &
                             #.3 "C2CO-O2  + RCO3 " + #.3 "RO2-R  + CCHO + CO + &
                              RO2 " + #.55 XC
RZ4)    1.0                  ;(C(C)CO2) = HO  + R2O2  + HCHO + CCO-O2  + RCO3  + RO2
RZ5)    1.0                  ;(C(R)CO2) = HO  + CCO-O2  + CCHO + R2O2  + RCO3  + RO2
RZ6)    1.0                  ;(CYCCO2) = #.3 "HO  + C2CO-O2  + R2O2  + RCO3  + &
                              RO2 " + #.3 RCHO + #4.2 XC
RZ7)    1.0                  ;(BZCHO2) = #.5 "BZ-O  + R2O2  + CO + HO "
ETOH)  1.960E-12 -0.870      ;ETHE + HO  = RO2-R  + RO2  + #1.56 HCHO + #.22 CCHO
ETO3)  9.140E-15  5.127      ;ETHE + O3 = HCHO + (HCHO2)
ETN3)  5.430E-12  6.043      ;ETHE + NO3 = R2O2  + RO2  + #2 HCHO + NO2
ETOA)  1.040E-11  1.574      ;ETHE + O = RO2-R  + HO2  + RO2  + HCHO + CO

A1OH)                        ;HO  + ALK1 = #A1OHRR RO2-R  + #A1OHNR RO2-N  + &
                              #A1OHXN RO2-XN  + #A1OHNP RO2-NP  + #A1OHRH HO2  + &
                              #A1OHR2 R2O2  + #A1OHRS RO2  + #A1OHA1 HCHO + &
                              #A1OHA2 CCHO + #A1OHA3 RCHO + #A1OHK3 ACET + &
                              #A1OHK4 MEK + #A1OHCO CO + #A1OHC2 CO2 + &
                              #A1OHPH PHEN + #A1OHCR CRES + #A1OHBZ BALD + &
                              #A1OHGL GLY + #A1OHMG MGLY + #A1OHU1 AFG1 + &
                              #A1OHU2 AFG2 + #A1OHTB C2(C)-O  + #A1OHQ1 CCO-O2  + &
```

```
                    #A1OHQ2 C2CO-O2  + #A1OHQS RCO3  + #A1OHXC XC
!
A2OH)               ;HO  + ALK2 = #A2OHRR RO2-R  + #A2OHNR RO2-N  + &
                    #A2OHXN RO2-XN  + #A2OHNP RO2-NP  + #A2OHRH HO2  + &
                    #A2OHR2 R2O2  + #A2OHRS RO2  + #A2OHA1 HCHO + &
                    #A2OHA2 CCHO + #A2OHA3 RCHO + #A2OHK3 ACET + &
                    #A2OHK4 MEK + #A2OHCO CO + #A2OHC2 CO2 + &
                    #A2OHPH PHEN + #A2OHCR CRES + #A2OHBZ BALD + &
                    #A2OHGL GLY + #A2OHMG MGLY + #A2OHU1 AFG1 + &
                    #A2OHU2 AFG2 + #A2OHTB C2(C)-O  + #A2OHQ1 CCO-O2  + &
                    #A2OHQ2 C2CO-O2  + #A2OHQS RCO3  + #A2OHXC XC
!
B1OH)               ;HO  + ARO1 = #B1OHRR RO2-R  + #B1OHNR RO2-N  + &
                    #B1OHXN RO2-XN  + #B1OHNP RO2-NP  + #B1OHRH HO2  + &
                    #B1OHR2 R2O2  + #B1OHRS RO2  + #B1OHA1 HCHO + &
                    #B1OHA2 CCHO + #B1OHA3 RCHO + #B1OHK3 ACET + &
                    #B1OHK4 MEK + #B1OHCO CO + #B1OHC2 CO2 + &
                    #B1OHPH PHEN + #B1OHCR CRES + #B1OHBZ BALD + &
                    #B1OHGL GLY + #B1OHMG MGLY + #B1OHU1 AFG1 + &
                    #B1OHU2 AFG2 + #B1OHTB C2(C)-O  + #B1OHQ1 CCO-O2  + &
                    #B1OHQ2 C2CO-O2  + #B1OHQS RCO3  + #B1OHXC XC
!
B2OH)               ;HO  + ARO2 = #B2OHRR RO2-R  + #B2OHNR RO2-N  + &
                    #B2OHXN RO2-XN  + #B2OHNP RO2-NP  + #B2OHRH HO2  + &
                    #B2OHR2 R2O2  + #B2OHRS RO2  + #B2OHA1 HCHO + &
                    #B2OHA2 CCHO + #B2OHA3 RCHO + #B2OHK3 ACET + &
                    #B2OHK4 MEK + #B2OHCO CO + #B2OHC2 CO2 + &
                    #B2OHPH PHEN + #B2OHCR CRES + #B2OHBZ BALD + &
                    #B2OHGL GLY + #B2OHMG MGLY + #B2OHU1 AFG1 + &
                    #B2OHU2 AFG2 + #B2OHTB C2(C)-O  + #B2OHQ1 CCO-O2  + &
                    #B2OHQ2 C2CO-O2  + #B2OHQS RCO3  + #B2OHXC XC
!
O1OH)               ;OLE1 + HO  = #O1OHRR RO2-R  + #O1OHRN RO2-N  + &
                    #O1OHRS RO2  + #O1OHA1 HCHO + #O1OHA2 CCHO + &
                    #O1OHA3 RCHO + #O1OHK3 ACET + #O1OHK4 MEK + &
                    #O1OHBZ BALD + #O1OHXC XC
!
O1O3)               ;OLE1 + O3 = #O1O3A1 HCHO + #O1O3A2 CCHO + &
                    #O1O3A3 RCHO + #O1O3K3 ACET + #O1O3K4 MEK + &
                    #O1O3BZ BALD + #O1O3Z1 (HCHO2) + #O1O3Z2 (CCHO2) + &
                    #O1O3Z3 (RCHO2) + #O1O3Z4 (C(C)CO2) + &
                    #O1O3Z5 (C(R)CO2) + #O1O3Z6 (CYCCO2) + &
                    #O1O3Z8 (BZCHO2) + #O1O3OH HO  + #O1O3RR RO2-R  + &
                    #O1O3RN RO2-N  + #O1O3XN RO2-XN  + #O1O3NP RO2-NP  + &
                    #O1O3RH HO2  + #O1O3R2 R2O2  + #O1O3RS RO2  + &
                    #O1O3Q1 CCO-O2  + #O1O3Q2 C2CO-O2  + #O1O3QS RCO3  + &
                    #O1O3XC XC
!
O1OA)               ;OLE1 + O = #O1OARR RO2-R  + #O1OARH HO2  + &
                    #O1OARS RO2  + #O1OAA1 HCHO + #O1OAA3 RCHO + &
                    #O1OAK4 MEK + #O1OACO CO + #O1OAXC XC
!
O1N3)               ;OLE1 + NO3 = #O1N3N2 NO2 + #O1N3N3 HNO3 + &
                    #O1N3RH HO2  + #O1N3RR RO2-R  + #O1N3RN RO2-N  + &
                    #O1N3R2 R2O2  + #O1N3RS RO2  + #O1N3A1 HCHO + &
                    #O1N3A2 CCHO + #O1N3A3 RCHO + #O1N3K3 ACET + &
```

```
                    #O1N3K4 MEK + #O1N3BZ BALD + #O1N3XC XC
!
O2OH)               ;OLE2 + HO  = #O2OHRR RO2-R  + #O2OHRN RO2-N  + &
                    #O2OHRS RO2  + #O2OHA1 HCHO + #O2OHA2 CCHO + &
                    #O2OHA3 RCHO + #O2OHK3 ACET + #O2OHK4 MEK + &
                    #O2OHBZ BALD + #O2OHXC XC
!
O2O3)               ;OLE2 + O3 = #O2O3A1 HCHO + #O2O3A2 CCHO + &
                    #O2O3A3 RCHO + #O2O3K3 ACET + #O2O3K4 MEK + &
                    #O2O3BZ BALD + #O2O3Z1 (HCHO2) + #O2O3Z2 (CCHO2) + &
                    #O2O3Z3 (RCHO2) + #O2O3Z4 (C(C)CO2) + &
                    #O2O3Z5 (C(R)CO2) + #O2O3Z6 (CYCCO2) + &
                    #O2O3Z8 (BZCHO2) + #O2O3OH HO  + #O2O3RR RO2-R  + &
                    #O2O3RN RO2-N  + #O2O3XN RO2-XN  + #O2O3NP RO2-NP  + &
                    #O2O3RH HO2  + #O2O3R2 R2O2  + #O2O3RS RO2  + &
                    #O2O3Q1 CCO-O2  + #O2O3Q2 C2CO-O2  + #O2O3QS RCO3  + &
                    #O2O3XC XC
!
O2OA)               ;OLE2 + O = #O2OARR RO2-R  + #O2OARH HO2  + &
                    #O2OARS RO2  + #O2OAA1 HCHO + #O2OAA3 RCHO + &
                    #O2OAK4 MEK + #O2OACO CO + #O2OAXC XC
!
O2N3)               ;OLE2 + NO3 = #O2N3N2 NO2 + #O2N3N3 HNO3 + &
                    #O2N3RH HO2  + #O2N3RR RO2-R  + #O2N3RN RO2-N  + &
                    #O2N3R2 R2O2  + #O2N3RS RO2  + #O2N3A1 HCHO + &
                    #O2N3A2 CCHO + #O2N3A3 RCHO + #O2N3K3 ACET + &
                    #O2N3K4 MEK + #O2N3BZ BALD + #O2N3XC XC
!
O3OH)               ;OLE3 + HO  = #O3OHRR RO2-R  + #O3OHRN RO2-N  + &
                    #O3OHRS RO2  + #O3OHA1 HCHO + #O3OHA2 CCHO + &
                    #O3OHA3 RCHO + #O3OHK3 ACET + #O3OHK4 MEK + &
                    #O3OHBZ BALD + #O3OHXC XC
!
O3O3)               ;OLE3 + O3 = #O3O3A1 HCHO + #O3O3A2 CCHO + &
                    #O3O3A3 RCHO + #O3O3K3 ACET + #O3O3K4 MEK + &
                    #O3O3BZ BALD + #O3O3Z1 (HCHO2) + #O3O3Z2 (CCHO2) + &
                    #O3O3Z3 (RCHO2) + #O3O3Z4 (C(C)CO2) + &
                    #O3O3Z5 (C(R)CO2) + #O3O3Z6 (CYCCO2) + &
                    #O3O3Z8 (BZCHO2) + #O3O3OH HO  + #O3O3RR RO2-R  + &
                    #O3O3RN RO2-N  + #O3O3XN RO2-XN  + #O3O3NP RO2-NP  + &
                    #O3O3RH HO2  + #O3O3R2 R2O2  + #O3O3RS RO2  + &
                    #O3O3Q1 CCO-O2  + #O3O3Q2 C2CO-O2  + #O3O3QS RCO3  + &
                    #O3O3XC XC
!
O3OA)               ;OLE3 + O = #O3OARR RO2-R  + #O3OARH HO2  + &
                    #O3OARS RO2  + #O3OAA1 HCHO + #O3OAA3 RCHO + &
                    #O3OAK4 MEK + #O3OACO CO + #O3OAXC XC
!
O3N3)               ;OLE3 + NO3 = #O3N3N2 NO2 + #O3N3N3 HNO3 + &
                    #O3N3RH HO2  + #O3N3RR RO2-R  + #O3N3RN RO2-N  + &
                    #O3N3R2 R2O2  + #O3N3RS RO2  + #O3N3A1 HCHO + &
                    #O3N3A2 CCHO + #O3N3A3 RCHO + #O3N3K3 ACET + &
                    #O3N3K4 MEK + #O3N3BZ BALD + #O3N3XC XC
!
!          END OF FILE
```

Attachment B2 – Listing of Reactions of Isoprene (Condensed 1-Product)

```
ISOH) 2.54E-11 -0.81     ;ISOP + HO = #.088 RO2N  + #.912 RO2R  + &
                          #.629 HCHO + #.912 ISPD + #.079 R2O2  + &
                          #1.079 RO2
!                         #1.079 RO2 + #.283 XC
ISO3) 7.86E-15  3.80     ;ISOP + O3 = #.4 HCHO + #.6 ISPD + #.55 BHCHO2 + &
                          #.2 CC3O2 + #.2 CC3HO2
!                         #.2 CC3O2 + #.2 CC3HO2 + #.05 XC
ISOA) 3.60E-11           ;ISOP + O = #.75 ISPD + #.25 "C3O3 + &
                          RCO3 + #2 HCHO + RO2R  + RO2"
!ISOA) 3.60E-11           ;ISOP + O = #.75 "ISPD + XC "+ #.25 "C3O3 + &
!                         RCO3 + #2 HCHO + RO2R  + RO2"
ISN3) 3.03E-12  0.89     ;ISOP + NO3 = #.8 "RCHO + RNO3 + RO2R " + &
                          #.2 "ISPD + R2O2  + NO2" + RO2
!                         #.2 "ISPD + R2O2  + NO2" + RO2 + #-2.2 XC
ISN2) 1.50E-19           ;ISOP + NO2 = #.8 "RCHO + RNO3 + RO2R " + &
                          #.2 "ISPD + R2O2  + NO" + RO2
!                         #.2 "ISPD + R2O2  + NO" + RO2 + #-2.2 XC
!
IPOH) 3.36E-11           ;ISPD + HO = #.293 CO + #.252 CCHO + #.126 HCHO + &
                          #.041 GLY + #.021 RCHO + #.168 MGLY + #.314 MEK + &
                          #.503 RO2R  + #.21 CCO3 + #.288 C3O3 + &
                          #.21 R2O2  + #.713 RO2 + #.498 RCO3
!                         #.21 R2O2  + #.713 RO2 + #.498 RCO3 + #-.112 XC
IPO3) 7.11E-18           ;ISPD + O3 = #.02 CCHO + #.04 HCHO + #.01 GLY + &
                          #.84 MGLY + #.09 MEK + #.66 BHCHO2 + &
                          #.09 HCOCHO2 + #.18 HOCCHO2 + #.06 C2O2CHO + &
                          #.01 COHC2O2
!                         #.01 COHC2O2 + #-.39 XC
IPHV) PF=ACROLEIN        ;ISPD + HV + #.0036 = #.333 CO + #.067 CCHO + &
                          #.9 HCHO + #.033 MEK + #.333 HO2 + #.7 RO2R  + &
                          #.267 CCO3 + #.7 C3O3 + #.7 RO2 + &
                          #.967 RCO3
!                         #.967 RCO3 + #-.133 XC
IPN3) 1.0E-15            ;ISPD + NO3 = #.643 CO + #.282 HCHO + #.85 RNO3 + &
                          #.357 RCHO + #.925 HO2 + #.075 C3O3 + &
                          #.075 R2O2  + #.925 RO2 + #.075 RCO3 + #.075 HNO3
!                         #.075 R2O2  + #.925 RO2 + #.075 RCO3 + #.075 HNO3 + &
!                         #-2.471 XC
ISZ1) 1.0                ;CC3O2 = HO + R2O2  + HCHO + C3O3 + RO2 + &
                          RCO3
ISZ2) 1.0                ;CC3HO2 = #.75 RCHO + #.25 ISPD
!ISZ2) 1.0                ;CC3HO2 = #.75 RCHO + #.25 ISPD + #.5 XC
MAZ1) 1.0                ;C2O2CHO = HO + R2O2  + HCHO + HC2O4 + RO2 + &
                          RCO3
M1Z1) 1.0                ;HOCCHO2 = #.6 HO + #.3 "CCO3 + RCO3" + &
                          #.3 "RO2R  + HCHO + CO + RO2"
!                         #.3 "RO2R  + HCHO + CO + RO2" + #.8 XC
```

```
M2Z1) 1.0                  ;HCOCHO2 = #.12 "HO2 + #2 CO + HO" + &
                            #.51 HCHO
!M2Z1) 1.0                 ;HCOCHO2 = #.12 "HO2 + #2 CO + HO" + #.74 XC + &
!                           #.51 "CO2 + HCHO"
M2Z2) 1.0                  ;COHC2O2 = HO + MGLY + HO2 + R2O2  + RO2
 !         END OF FILE
```

Attachment B3 – Listing of Explicit Reaction Mechanisms for Other VOCs

```
OH001) 2.500E-12  0.397  0.000   ;C6H6 + HO = #.236 PHEN + #.207 GLY &
                                   + #1.44 AFG1 + #.764 RO2-R + #.236 HO2 &
                                  + #1.29 XC + #.764 RO2
!
OH033) 1.480E-11 -0.890  0.000   ;BUTD + HO = RO2-R + RO2 + HCHO + RCHO
!
O3033) 1.340E-14  4.537  0.000   ;BUTD + O3 = #.6 HCHO + RCHO + #-1.2 XC &
                                  + #.4 (HCHO2) + #.6 (CCHO2)
!
N3033) 1.000E-13  0.000  0.000   ;BUTD + NO3 = R2O2 + RO2 + HCHO + RCHO &
                       + NO2
!
OA033) 2.100E-11  0.000  0.000   ;BUTD + O = #.4 HO2 + #.5 RCHO + #.5 MEK &
                       + #.5 XC
!
OH018) 3.840E-13  0.000  0.000   ;PDCB + HO = #.236 PHEN + #.207 GLY &
                                  + #1.44 AFG1 + #.764 RO2-R + #.236 HO2 &
                                  + #1.29 XC + #.764 RO2

OH152) 9.640E-12  2.403  0.000   ;PERC + HO = RO2-R + CCHO + RO2
!
OH086) 6.14E-18  1.987  2.000    ;DICM + HO = RO2-R + HCHO + RO2
!
AS1) 6.14E-25                    ; AS = AS
CR1) 6.14E-25                    ; CRVI = CRVI
!
 C1)       PF=HCHONEWR           ;FORM + HV = #2 HO2  + CO
 C2)       PF=HCHONEWM           ;FORM + HV = H2 + CO
 C3) 1.125E-12 -1.288 2.0        ;FORM + HO  = HO2  + CO + H2O
 C4)  9.7E-15, -1.242            ;FORM + HO2  = HOCOO
 C9) 2.8E-12,       5.00         ;FORM + NO3 = HNO3 + HO2  + CO
!
 C10) 5.55E-12, -0.618           ;ALD + HO  = CCO-O2  + H2O + RCO3
 C11A) PF=CCHOR                  ;ALD + HV = CO + HO2  + HCHO + RO2-R  + RO2
 C12) 1.4E-12,  3.696            ;ALD + NO3 = HNO3 + CCO-O2  + RCO3
!
OH091) 5.560E-13 -1.057  2.000   ;ETOH + HO = #.1 RO2-R + #.9 HO2 &
                                  + #.156 HCHO + #.922 CCHO + #.1 RO2
!
OH108) 6.129E-13 -0.914  2.000   ;MTBE + HO = #.02 RO2-N + #.98 RO2-R &
```

```
                                    + #.37 R2O2 + #.39 HCHO + #.41 MEK + #2.87 XC &
                                    + #1.37 RO2
!           END OF FILE
```